

TOPOLOGY OF GRAPH CONFIGURATION SPACES AND QUANTUM STATISTICS



Adam Sawicki

School of Mathematics

September 2014

A DISSERTATION SUBMITTED TO THE UNIVERSITY OF BRISTOL
IN ACCORDANCE WITH THE REQUIREMENTS OF THE DEGREE
OF DOCTOR OF PHILOSOPHY IN THE FACULTY OF SCIENCE

Abstract

In this thesis we develop a full characterization of abelian quantum statistics on graphs. We explain how the number of anyon phases is related to connectivity. For 2-connected graphs the independence of quantum statistics with respect to the number of particles is proven. For non-planar 3-connected graphs we identify bosons and fermions as the only possible statistics, whereas for planar 3-connected graphs we show that one anyon phase exists. Our approach also yields an alternative proof of the structure theorem for the first homology group of n -particle graph configuration spaces. Finally, we determine the topological gauge potentials for 2-connected graphs. Moreover we present an alternative application of discrete Morse theory for two-particle graph configuration spaces. In contrast to previous constructions, which are based on discrete Morse vector fields, our approach is through Morse functions, which have a nice physical interpretation as two-body potentials constructed from one-body potentials. We also give a brief introduction to discrete Morse theory.

Dedication

I dedicate this thesis to my family and friends.

Acknowledgements

Foremost, I would like to express my sincere gratitude to my advisors Prof. Jon P. Keating and Dr Jonathan M. Robbins for discussions we had, their patience and constant encouragement.

Besides my advisors, I would like to thank my fellow officemates in Mathematics Department: Jo Dwyer, Orestis Georgiou, Jo Hutchinson, Andy Poulton and James Walton (in fact a chemist) for all the fun we have had in the last three years. I hope our friendship will continue! I also wish to thank my friend Rami Band for many stimulating discussions we had on the subject of this thesis and the experience of the 2011 Royal Society Summer Science Exhibition.

Finally, I would like to thank my family, in particular my sister Ania for being so positively crazy!

Author's Declaration

I declare that the work in this dissertation was carried out in accordance with the requirements of the University's Regulations and Code of Practice for Research Degree Programmes and that it has not been submitted for any other academic award. Except where indicated by specific reference in the text, the work is the candidate's own work. Work done in collaboration with, or with the assistance of, others, is indicated as such. Any views expressed in the dissertation are those of the author.

Adam Sawicki

Date: September 2014

Contents

Abstract	i
Dedication	ii
Acknowledgements	iii
Author's Declaration	iv
1 Introduction	1
1.1 Quantum statistics	2
1.1.1 Standard approach to quantum statistics	2
1.1.2 Topological approach to quantum statistics	4
1.2 Aharonov-Bohm Effect as an example of topological phase	6
1.3 Graphs	10
1.3.1 Subgraphs, paths, trees and cycles	10
1.3.2 Connectivity	11
1.3.3 Decomposition of a graph into 3-connected components	13
1.4 The fundamental group	15
1.5 Cell complexes	17
1.6 Homology groups	19
1.7 Structure theorem for finitely generated Abelian groups	22
1.7.1 Finitely generated Abelian groups	22
1.8 Topology of configuration spaces and quantum statistics	24
1.8.1 Quantum statistics for $C_n(\mathbb{R}^m)$	25

1.9	Graph configuration spaces	26
1.10	Quantum graphs	29
1.10.1	Topological gauge potential	30
2	Quantum Statistics on graphs	32
2.1	Quantum statistics on graphs	34
2.1.1	3-connected graphs	35
2.1.2	2-connected graphs	36
2.1.3	1-connected graphs	37
2.1.4	Aharonov-Bohm phases	38
2.2	Graph configuration spaces	38
2.3	Two-particle quantum statistics	41
2.3.1	A spanning set of $H_1(\mathcal{D}^2(\Gamma))$	43
2.3.2	3-connected graphs	45
2.3.3	2-connected graphs	51
2.3.4	1-connected graphs	56
2.4	n -particle statistics for 2-connected graphs	59
2.4.1	A spanning set of $H_1(\mathcal{D}^n(\Gamma))$	60
2.5	n -particle statistics on 1-connected graphs	63
2.5.1	Star graphs	64
2.5.2	The fan graphs	69
2.6	Gauge potentials for 2-connected graphs	71
2.7	Morse theory argument	77
3	Discrete Morse functions for graph configuration spaces	82
3.1	Introduction	82
3.2	Morse theory in the nutshell	84
3.2.1	Classical Morse theory	84
3.2.2	Discrete Morse function	86
3.2.3	Discrete Morse vector field	88
3.2.4	The Morse complex	90

3.3	A perfect Morse function on Γ and its discrete vector field.	91
3.4	The main examples	93
3.5	Discrete Morse theory and topological gauge potentials	97
3.6	General consideration for two particles	99
3.7	Summary	104
3.8	Proofs	105
4	Summary and outlook	112
	Bibliography	116

List of Figures

1.1	(a) The contractible loop in \mathbb{R}^2 (b) the non-contractible loop in $\mathbb{R}^2 - D(0, \rho)$	9
1.2	The magnetic flux through a disk in $M = \mathbb{R}^2 - D(0, \rho)$	9
1.3	The dashed edges represent examples of (a) a path, (b) a cycle, (c) a spanning tree, of graph Γ	12
1.4	(a) A graph Γ , (b) Components of Γ , (c) Topological components of Γ	12
1.5	Example of two independent paths between vertices v_1 and v_2 , dashed and dotted subgraphs of Γ	14
1.6	(a) A graph, (b) Its topological components resulting from v_1 -cut, (c) The full block decomposition.	15
1.7	(a) A 2-connected graph, (b) Components resulting from $\{v_1, v_2\}$ -cut, (c) Marked components resulting from $\{v_1, v_2\}$ -cut.	16
1.8	Examples of (a) an irregular cell complex. $\alpha^{(1)}$ is an irregular 1-cell and $\beta^{(0)}$ is an irregular face of $\alpha^{(1)}$, $\tau^{(2)}$ is a regular 2-cell. (b) A regular cell complex.	18
1.9	The cell complex X_T of the 2-torus T^2	21
1.10	(a) The star graph Γ , (b) the two-particle configuration space $C_2(\Gamma)$, (c) the two-particle discrete configuration space $\mathcal{D}^2(\Gamma)$	28
2.1	The large almost planar 3-connected graph.	36
2.2	The graph G (without the edge e) is planar 3-connected. With e , the graph is K_5	36

2.3	Linear chain of 3-connected nonplanar components with alternating Bose and Fermi statistics.	37
2.4	The Aharonov-Bohm phase for the equatorial cycle depends on whether the second particle is at the north or south pole.	38
2.5	(a) The triangle graph Γ (b) The 2-particle configuration space $\mathcal{D}^2(\Gamma)$	42
2.6	(a) The Y-graph Γ . (b) The 2-particle combinatorial configuration space $\mathcal{D}^2(\Gamma)$. (c) The 2-particle configuration space $C_2(\Gamma)$; dashed lines and open vertices denote configurations where the particles are coincident. Such configurations are excluded from $C_2(\Gamma)$	43
2.7	(a) The lasso graph Γ (b) The 2-particle configuration space $\mathcal{D}^2(\Gamma)$	44
2.8	The dependence of the AB-phase for cycle c on the position of the second particle when (a) there is a path between v_1 and v_2 disjoint with c , (b) every path joining v_1 and v_2 passes through c	45
2.9	Wheel graphs. (a) Dashed lines denote a pair of Y subgraphs Y_{v_1} and Y_{v_2} centered at adjacent vertices v_1 and v_2 on the rim. The three shared edges of the Y subgraphs (long dashes) form a cycle C . (b) The Y subgraph Y_h (edges are dashed) has three outer vertices b_1 , v_1 and v_2 . Two of the edges of Y_h together with a path on the rim joining v_1 and v_2 form a cycle C (long dashes). A second Y-graph Y_{v_2} (edges are dashed) shares two edges of C	48
2.10	(a) Adding an edge (b) Expanding at the vertex.	50
2.11	(a) An example of a 2-connected graph, (b) the components of the 2-cut $\{x, y\}$, (c) the marked components.	51
2.12	(a) 2-vertex cut of Γ . The γ_i 's are the interiors of the connected components Γ_i . (b) Y_x with two edges connected to γ_2 (c) two Y-cycles with three edges in three different components (d) the equality of ϕ_{Y_x} and ϕ_{Y_y}	55

2.13 (a) The Y -graphs Y_1 and Y_2 have central vertex v and two common edges (long dashes) with vertices in $\Gamma_{v,3}$, but different edges (short dashes) with different vertices α_1 and α_2 in $\Gamma_{1,v}$. Their exchange phases are the same. (b) Each edge of the Y -graph is attached to a different component. (c) Y -graphs with two edges in the same component (d) Two Y -graphs centered at v with external vertices $\{1, 3, 4\}$ and $\{1', 3, 4\}$ respectively. (e) The relevant part of 2-particle configuration space of (d). 57

2.14 The subdivided lasso for (a) 3 particles, (b) 4 particles. 61

2.15 Subgraphs of the configurations spaces for the lasso graphs with (a) 3 particles: $\phi_{C,3} = \phi_{C,2}^2 + \phi_Y^5$, (b) 4 particles: $\phi_{C,4} = \phi_{C,3}^3 + \phi_Y^{6,7}$. . . 61

2.16 (a) The relation between AB-phases, (b) the stabilization of the first homology group. 63

2.17 (a) The star graph with E arms and n particles. Each arm has n vertices. The exchange zone S'_E can accommodate $2, 3, \dots, E - 1$ particles. (b) The fan graph F 69

2.18 The Y subgraphs (a) Y_1 and (b) Y_2 70

2.19 A sufficiently subdivided graph for 3 particles, edges in a maximal spanning tree are shown with solid lines and edges omitted to obtain the tree are shown with dashed lines. Vertices are labeled following the boundary of the tree clockwise from the root vertex 1. 78

2.20 An exchange cycle starting from the root configuration $\{1, 2, 3\}$ and using a single 1-cell (c) that does not respect the flow at the non-trivial vertex 3. Large bold nodes indicate the initial positions of particles and light nodes their final positions. In paths (a),(b),(d) and (e) particles move according to the vector field. 80

2.21 Examples of paths that form Y -cycles in the over-complete spanning set; large bold nodes indicate the initial positions of particles on the path and light nodes the final position a particle moves to. (a),(b) and (c) together form a Y -cycle, exchanging two particles at the non-trivial vertex 3, similarly (c),(d) and (e) also form a Y -cycle. Paths (a) through (e) together in order is a cycle homotopic to the exchange cycle starting from the root configuration shown in figure 2.20. 81

3.1 Examples of (a) an irregular cell complex. $\alpha^{(1)}$ is an irregular 1 - cell and $\beta^{(0)}$ is an irregular face of $\alpha^{(1)}$. (b) A regular cell complex with $\tau^{(2)} \supset \alpha^{(1)} \supset \beta^{(0)}$ 87

3.2 Examples of (a) a Morse function, and (b) a non-Morse function, since the 2-cell has value 5 and there are two 1-cells in its boundary with higher values assigned (6, 7). 88

3.3 Examples of (a) a correct and (b) an incorrect discrete gradient vector fields; the 2-cell is the head of two arrows and the 1-cell is the head and tail of one arrow. 90

3.4 (a) The perfect discrete Morse function f_1 on the graph Γ and its discrete gradient vector field. (b) The Morse complex $M(f_1)$ 92

3.5 (a) One particle on lasso, (b) The perfect discrete Morse function f_1 93

3.6 (a) The two particles on lasso, $\mathcal{D}^2(\Gamma_1)$, (b) the discrete Morse function and its gradient vector field (c) the Morse complex (d) the topological gauge potential Ω 94

3.7 (a) One particle on bow-tie (b) Perfect discrete Morse function . . . 95

3.8 (a) Two particles on bow-tie (b) the discrete Morse function and its gradient vector field, (c) the Morse complex $M(f_2)$ 97

3.9 The critical cell $e_1 \times e_2$ where both e_1 and e_2 do not belong to T . . 105

3.10 (a) $e(v) \cap e = \emptyset$ and $e \notin T$, (b) The noncritical cells $v \times e$ and $e(v) \times e$ 106

List of Figures

3.11 (a) Two edges of T with $e(v) \cap e(u) = \emptyset$, (b) The problem of 2-cell
 $e(v) \times e(u)$ (c),(d) two possible fixings of \tilde{f}_2 107

3.12 $e(v) \cap e(u) \neq \emptyset$ and $\tau(v) = u$ 110

3.13 (a) Two edges of T with $e(v) \cap e(u) \neq \emptyset$, (b) The problem of 1-cells
 $v \times (u, \tau(u))$ and $u \times (v, \tau(v))$ (c),(d) The two possible fixings of \bar{f}_2 111

Chapter 1

Introduction

This thesis concerns the characterization of quantum statistics on graphs. Naturally, one should first explain what it means. As with many problems in mathematical physics it is hard to do it in a one sentence. However, in the subsequent sections of the introduction it is done. The subject, as I see it, is inevitably connected to some basic concepts in algebraic topology and graph theory. The main purpose of this, rather short, introduction is to persuade the reader that quantum statistics and the first homology group of an appropriate configuration space are one and the same thing. I knowingly avoid using the full formalism of quantum mechanics on non-simply connected spaces. This can be found in many textbooks and in my opinion is not relevant to understand the problem and the main results of the thesis. Writing this text I tried to minimize the number of irrelevant details so that the key ideas and concepts were clearly visible. Therefore, for example, I do not prove theorems whose proofs do not contribute to the understanding of the main flow of the text. The interested reader is asked to consult the cited references. On the other hand, in order to make the manuscript available to a reader not familiar with homology groups and graph theory I include a basic discussion of the relevant facts. Although one can find it unnecessary, from time to time, I repeat definitions and key properties of some important objects. I believe that it is better to do this rather than to send the reader to a distant page where they were discussed for the first time.

The chapter is organized as follows: In section 1.1 I shortly explain the concept

of quantum statistics describing two approaches. The first one is standard and the second topological. Then in section 1.2 the Aharonov-Bohm effect is discussed as an example of a topological phase. The subsequent five sections contain the discussion of basic properties of graphs, cell complexes and their homotopy and homology groups. Next, in section 1.8 I define the many-particle configuration space and explain that its first homology group encodes the information about quantum statistics. The calculation for the case of particles living in \mathbb{R}^2 and \mathbb{R}^n , where $n \geq 3$ is included. Then in section 1.9 I generalize the above concept to graphs and introduce the basic mathematical object of this thesis, i.e. the discrete configuration space of n -particles, $\mathcal{D}^n(\Gamma)$. This space has the structure of a cell complex and is topologically equivalent to the configuration space of n -particles on a graph, $C_n(\Gamma)$. In the last section of this chapter I discuss the tight-binding model of n -particles on a graph, define the topological gauge potentials and explain the connection between them, the first homology and quantum statistics. The background material of the introduction is mostly based on [38] and [45].

1.1 Quantum statistics

In this section I describe two approaches to quantum statistics. The first one introduces it as an additional postulate of quantum mechanics. The second, which I will follow throughout the thesis, is topological in its nature.

1.1.1 Standard approach to quantum statistics

In quantum mechanics any quantum system is described by its underlying Hilbert space. Let us denote by \mathcal{H}_1 the one-particle Hilbert space, i.e. the Hilbert space of a single particle. By one of the postulates of quantum mechanics the Hilbert space of n distinguishable particles, \mathcal{H}_n , is the tensor product of the Hilbert spaces of the

constituents, i.e.

$$\mathcal{H}_n = \underbrace{\mathcal{H}_1 \otimes \dots \otimes \mathcal{H}_1}_n.$$

If we want to treat particles as indistinguishable some additional modifications of \mathcal{H}_n are required. First, the indistinguishability implies that all observables need to commute with permutations of the particle labels. Therefore, one decomposes \mathcal{H}_n into irreducible representations of the permutation group S_n :

$$\mathcal{H} = \bigoplus_{\lambda} \mathcal{H}_{\lambda},$$

where λ labels those representations. The components \mathcal{H}_{λ} represent essentially different permutation symmetries. Note that *a priori* all components \mathcal{H}_{λ} are equally good, i.e. none of them is distinguished in any way. The distinction between them is due to symmetrization postulates of quantum mechanics, i.e. physically realizable components \mathcal{H}_{λ} are only

1. symmetric tensors : $\mathcal{H}_{\lambda} = S^n \mathcal{H}_1$,
2. antisymmetric tensors : $\mathcal{H}_{\lambda} = \bigwedge^n \mathcal{H}_1$,

which are trivial and sign representations of the permutation group S_n , respectively. The first one corresponds to bosons and the second to fermions. Other components or equivalently other representations of S_n are physically excluded. In order to decide if the considered particles obey Bose or Fermi statistics one looks at the spin. The spin-statistics theorem [40] says that particles with integer spin are bosons and with half-integer, fermions. It is worth mentioning that at the level of non-relativistic quantum mechanics the spin-statistics theorem is actually a postulate as it is proved only in the framework of quantum field theory. Nevertheless, there were attempts to deduce it on the level of QM (see for example [12]). The antisymmetric property of fermionic states is also known as the Pauli exclusion principle which says that no two identical fermions may occupy the same quantum state simultaneously. Finally, let us mention that symmetrization postulate has an important consequences if one looks at the energy distribution of many non-interacting

particles. More precisely, assume that we have a collection of non-interacting indistinguishable particles and ask how they occupy a set of available discrete energy states. Then the expected number of particles in the i -th energy state is given by:

$$n_i = \frac{g_i}{e^{(E_i - \mu)/kT} - 1}, \quad \text{for bosons,}$$

$$n_i = \frac{g_i}{e^{(E_i - \mu)/kT} + 1}, \quad \text{for fermions,}$$

where, T is temperature, k is Boltzmann constant and g_i is the degeneracy of the E_i energy state.

1.1.2 Topological approach to quantum statistics

After discussing the standard way of introducing quantum statistics we switch to the topological approach. Interestingly, it is based on the topological properties of the classical configuration space.

In classical mechanics, particles are considered distinguishable. Therefore, the n -particle configuration space is the Cartesian product, $M^{\times n}$, where M is the one-particle configuration space. By contrast, in quantum mechanics elementary particles may be considered indistinguishable. This conceptual difference in the description of many-body systems prompted Leinaas and Myrheim [36] (see also [44, 46]) to study classical configuration spaces of indistinguishable particles, $C_n(M)$ which led to the discovery of anyon statistics. We first briefly describe the work of Leinaas and Myrheim.

As noted by the authors of [36] indistinguishability of classical particles places constraints on the usual configuration space, $M^{\times n}$. Configurations that differ by particle exchange must be identified. One also assumes that two classical particles cannot occupy the same configuration. Consequently, the classical configuration space of n indistinguishable particles is the orbit space

$$C_n(M) = (M^{\times n} - \Delta)/S_n,$$

where Δ corresponds to the configurations for which at least two particles are at the same point in M , and S_n is the permutation group. Significantly, the space

$C_n(M)$ may have non-trivial topology. As permuted configurations are identified in $C_n(M)$ any closed curve in $C_n(M)$ corresponds to a process in which particles start at some configuration and then return to the same configuration modulo they might have been exchanged. Some of these curves are non-contractible and therefore the space $C_n(M)$ has nontrivial fundamental group $\pi_1(C_n(M))$.

Quantum mechanics on non-simply connected configuration spaces For many (or just one particle) whose classical configuration space \mathcal{C} is non-simply connected quantum mechanics allows an additional freedom stemming from the non-triviality of the fundamental group $\pi_1(\mathcal{C})$. In order to describe this freedom we assume in the following that all particles are free, i.e. there are no external fields and on the classical level they do not interact. In the subsequent section we discuss in details the Aharonov-Bohm effect which is an example of the general concept we describe here.

Let A be a connection 1-form of a d -dimensional vector bundle over \mathcal{C} with the structure group $U(d)$ (see [38] for more details). As we do not want to affect classical mechanics, we assume that the curvature 2-form $F = DA$ vanishes. In the following we will need the notion of the holonomy group. Let $\gamma : [0, 1] \rightarrow \mathcal{C}$ be a closed curve. As we consider d -dimensional vector bundle, over any point of γ there is a d -dimensional vector space V_d . For any vector v_0 over the point $\gamma(0)$ we consider the parallel transport through γ . The result of this process is vector v_1 . Notably v_0 and v_1 need not to be the same. Therefore to each loop one can assign a matrix M_γ which depends only on the loop and

$$v_1 = M_\gamma v_0, \quad \forall v_0 \in V_d.$$

The collection of all matrices M_γ for all loops based at some fixed point $p \in \mathcal{C}$ is called the holonomy group. Moreover, when $F = 0$, M_γ depends only on the homotopy type of the loop. Therefore holonomy group is a d -dimensional representation of the fundamental group (see section 1.4 for definition of fundamental group). When $d = 1$ this representation is abelian and assigns phase factors to non-contractible loops in \mathcal{C} . When $d > 1$ it assigns in general non-commuting unitary

matrices to non-contractible loops in \mathcal{C} . Finally, these matrices act on d -component wavefunction.

Classical configuration spaces and quantum statistics In 1977 Leinaas and Myrheim [36] considered the classical configuration space of n indistinguishable particles, $C_n(M)$ in the above described context. Their work showed that the representations of the fundamental group $\pi_1(C_n(M))$ determine all possible quantum statistics. In particular they described in details the cases when $M = \mathbb{R}^2$ and $M = \mathbb{R}^k$, where $k \geq 3$. Notably for $M = \mathbb{R}^2$ they found that the fundamental group is the braid group which led to the discovery of anyon statistics. Similar results were obtained by Laidlaw and DeWitt [35] who considered the problem of quantum statistics using the language of path integrals. As clearly pointed out by Dowker [17] when one is interested in the abelian quantum statistics only, determination of the fundamental group is not actually necessary. Instead, the first homology group which is the abelianized version of $\pi_1(C_n(M))$ plays the major role. In this thesis we determine it for graph configuration spaces.

1.2 Aharonov-Bohm Effect as an example of topological phase

In this section we discuss the Aharonov-Bohm effect. In particular we explain the topological nature of the phase gained by the wavefunction when it goes around the magnetic flux. Our exposition mainly follows [13].

In non-relativistic quantum mechanics the canonical commutation relations for a free particle living in n -dimensional space M are given by:

$$[x_i, x_j] = 0 = [p_i, p_j], \quad [x_i, p_j] = i\delta_{ij}, \quad (1.2.1)$$

where $i, j \in \{1, \dots, n\}$. The standard representation of position and momenta

operators satisfying (1.2.1) is given by:

$$(x_i \Psi)(x) = x_i f(x), \quad (p_i \Psi)(x) = -i \frac{\partial}{\partial x_i} f(x). \quad (1.2.2)$$

It was perhaps first noticed¹ by Dirac [16], that operators:

$$p_i^\omega = -i \frac{\partial}{\partial x_i} + \omega_i(x), \quad (1.2.3)$$

where

$$\omega = \sum_i \omega_i dx^i, \quad d\omega = 0, \quad (1.2.4)$$

satisfy the canonical commutation relations, i.e.

$$[x_i, x_j] = 0 = [p_i^\omega, p_j^\omega], \quad [x_i, p_j^\omega] = \delta_{ij}, \quad (1.2.5)$$

as well. When the configuration space M has the trivial topology, e.g. $M = \mathbb{R}^n$

$$d\omega = 0 \Rightarrow \exists f \ \omega = df. \quad (1.2.6)$$

Therefore, using gauge freedom, i.e. $\Psi'(x) = e^{-if(x)} \Psi(x)$ it is possible to remove ω from p_i . To this end, note that

$$\begin{aligned} p_i^\omega \Psi'(x) &= \left(-i \frac{\partial}{\partial x_i} + \omega_i(x) \right) e^{-if(x)} \Psi(x) = \\ &= -ie^{-if(x)} \frac{\partial}{\partial x_i} \Psi(x) - \frac{\partial}{\partial x_i} f(x) e^{-if(x)} \Psi(x) + \omega_i e^{-if(x)} \Psi(x) = \\ &= -ie^{-if(x)} \frac{\partial}{\partial x_i} \Psi(x) = e^{-if(x)} p_i \Psi(x). \end{aligned}$$

On the other hand, when configuration space has a non-trivial topology the implication given by (1.2.6) does not hold and it is not possible to use the above argument. Before discussing the Aharonov-Bohm effect which is, in some sense, a manifestation of this phenomenon we first focus on a more general situation. The operators p_i are generators of translation and when $\omega = 0$ one has

$$(e^{\epsilon^i p_i} \Psi)(x) = \Psi(x + \epsilon). \quad (1.2.7)$$

¹According to authors of [13].

It is easy to verify that when transporting the state vector Ψ along curve $C : [0, T] \rightarrow M$ we get

$$(e^{i \int_C dx^i p_i^{\omega}} \Psi)(x) = \Psi(x + \Delta x) e^{\int_C \omega}. \quad (1.2.8)$$

Therefore for a closed loop C

$$(e^{i \int_C dx^i p_i} \Psi)(x) = \Psi(x) e^{\oint_C \omega}. \quad (1.2.9)$$

Let us consider two situations when $M = \mathbb{R}^2$ and when $M = \mathbb{R}^2 - D(0, \rho)$, where $D(0, \rho)$ is a disk of radius ρ (see figures 1.1(a) and 1.1(b), respectively). For the first case the loop C is contractible and we have

$$\oint_C \omega = \int_S d\omega = 0. \quad (1.2.10)$$

For figure 1.1(b), that is, when the disk $D(0, \rho)$ is removed from the domain contained inside the loop C , i.e. when $M = \mathbb{R}^2 - D(0, \rho)$ we have

$$0 = \int_S d\omega = \oint_C \omega - \oint_{\partial D} \omega \Rightarrow \oint_C \omega = \oint_{\partial D} \omega, \quad (1.2.11)$$

and hence the phase $\phi = \oint_C \omega$ in equation (1.2.9) might be non-zero. For a general loop C which goes around the disk D clockwise n_+ times and anticlockwise n_- times one gets

$$\oint_C \omega = (n_+ - n_-) \oint_{\partial D} \omega = (n_+ - n_-) \phi. \quad (1.2.12)$$

As a conclusion we see that in certain topologies it does matter which definition of momentum operators (1.2.2) or (1.2.3) we use. On the other hand, it is also clear that the differential 1-form ω should be taken into account only if it has some physical meaning. From a physics perspective the simplest example of such physical realization is the magnetic field whose potential A is a connection 1-form. Recall, that by the minimal coupling principle, in the presence of a magnetic field $B = dA$ all derivatives in all equations of physics should be substituted by covariant derivatives. Thus

$$p_i \rightarrow p_i - eA_i, \quad B = dA.$$

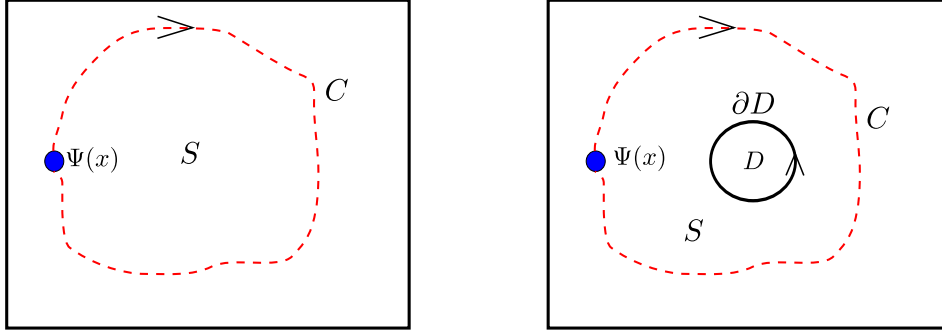


Figure 1.1: (a) The contractible loop in \mathbb{R}^2 (b) the non-contractible loop in $\mathbb{R}^2 - D(0, \rho)$

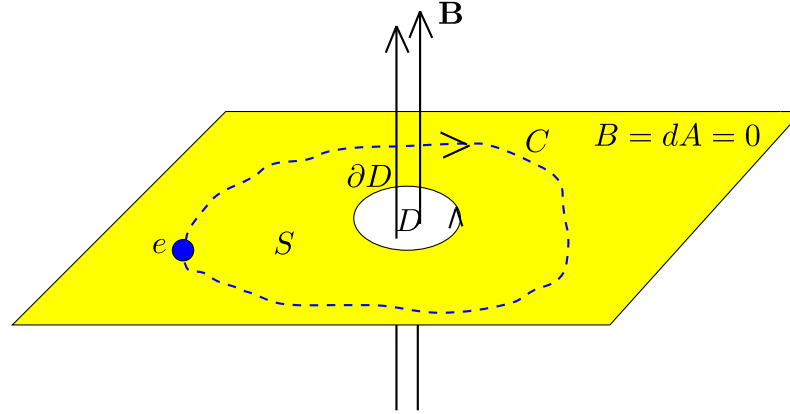


Figure 1.2: The magnetic flux through a disk in $M = \mathbb{R}^2 - D(0, \rho)$

Therefore the magnetic potential eA plays the role of ω from the previous considerations. Let us next consider the situation shown in figure 1.2. We assume

$$dA(x) = 0 \text{ if } x \in M.$$

The phase $\phi = \oint_C eA$ is called the Aharonov-Bohm phase and is given by

$$\begin{aligned} \oint_C eA &= (n_+ - n_-) \oint_{\partial D} eA = (n_+ - n_-)e \int_D dA = (n_+ - n_-)e \int_D B = \\ &= (n_+ - n_-)e\phi_B, \end{aligned}$$

i.e. it is proportional to the flux $\phi_B = \int_D B$ of the magnetic field B through the disk D . The existence of this phase was experimentally verified in 1960 [15] by measuring the shift in the interference pattern of the electrons in the geometry which is

almost identical with the one shown in figure 1.2. Finally, let us note that the existence of the Aharonov-Bohm phase is inevitably related to the non-contractibility of the loop through which electrons travel. Thus for graphs, we will call the phase gained by a particle going around the cycle an Aharonov-Bohm phase (see chapter 2 for more details).

1.3 Graphs

In this section we introduce the notion of graphs and discuss their basic properties. A graph $\Gamma = (E, V)$, where V and E are finite sets, is a collection of $|V|$ points called vertices and $|E|$ edges which connect some of the vertices. We will write $v_1 \sim v_2$ ($v_1 \not\sim v_2$) if two vertices $v_1, v_2 \in V$ are connected (not connected) by an edge, respectively. An undirected edge between v_1 and v_2 will be denoted by $e = v_1 \leftrightarrow v_2$. Similarly a directed edge from v_1 to v_2 (v_2 to v_1) will be denoted by $v_1 \rightarrow v_2$ ($v_2 \rightarrow v_1$). In the following we will consider only simple graphs, i.e. graphs for which any pair of vertices is connected by at most one edge (there are no multiple edges) and each edge is connected to exactly two different vertices (there are no loops). A typical way to encode the information about connections between vertices of Γ is by means of the so-called adjacency matrix. The adjacency matrix of Γ is a $|V| \times |V|$ matrix such that

$$A_{i,j} := A_{v_i,v_j} = 1 \text{ if } v_i \sim v_j \in E, \quad (1.3.1)$$

and $A_{ij} = 0$ otherwise. If vertices v_i and v_j are connected by an edge, i.e. if $A_{ij} \neq 0$, we say they are adjacent. It is straightforward to see that $|E| = \frac{1}{2} \sum_{jk} A_{jk}$.

1.3.1 Subgraphs, paths, trees and cycles

Here we assume that $\Gamma = (V, E)$ is a simple connected graph. A subgraph $\Gamma' = (V', E')$ of the graph Γ is a graph such that $V' \subset V$, $E' \subset E$ and edges from E' connect vertices from V' . There are two elementary methods for constructing a subgraph out of the given graph. For $e \in E$ one can consider a graph with $|E| - 1$

edges obtained from Γ by deletion of the edge e . It will be denoted by $\Gamma \setminus e$. Similarly for a vertex $v \in V$ one defines graph $\Gamma \setminus v$ which is a result of deleting vertex v together with all the edges connected to v . The generalization of these procedures to many edges or vertices is straightforward.

We proceed with definitions of other important subgraphs: paths, cycles and trees.

Definition 1.3.1. A path $P = (v_1, v_2, \dots, v_k)$ on Γ is a subgraph of Γ such that $v_i \sim v_{i+1}$.

We will call the vertices v_2, \dots, v_{k-1} of path $P = (v_1, v_2, \dots, v_k)$ the internal vertices. A path $P = (v_1, v_2, \dots, v_k)$ will be called a *simple path* if $v_i \neq v_j$ for any $i, j \in \{1, \dots, k\}$.

Definition 1.3.2. A cycle $C = (v_1, v_2, \dots, v_k)$ on Γ is a subgraph of Γ such that $v_i \sim v_{i+1}$ and $v_k = v_1$.

Definition 1.3.3. A tree T of Γ is a subgraph of Γ such that any pair of vertices is connected by exactly one path.

Equivalently, $T \subset \Gamma$ is a tree if it contains no cycles. Among all trees of Γ we distinguish the so-called *spanning trees*. A spanning tree $T = \{V_T, E_T\}$ of Γ is a tree such that its set of vertices is exactly the set of vertices of Γ , i.e. $V_T = V$. Therefore, a spanning tree is a maximal subgraph of Γ without cycles. In order to calculate the number of cycles of a given graph $\Gamma = \{V, E\}$ we note that any spanning tree of Γ has $|V| - 1$ edges. Therefore, the number of cycles is

$$\beta_1(\Gamma) = |E| - (|V| - 1) = |E| - |V| + 1. \quad (1.3.2)$$

This number, which is called the first Betti number, will play a major role in the next chapters.

1.3.2 Connectivity

In this section we discuss the notion of connectivity of a graph. We start with the definition of a connected graph.

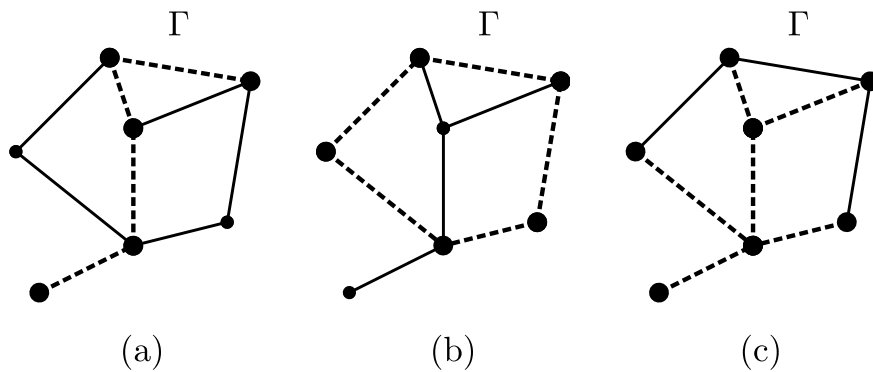


Figure 1.3: The dashed edges represent examples of (a) a path, (b) a cycle, (c) a spanning tree, of graph Γ .

Definition 1.3.4. A graph is connected, if any pair of its vertices is connected by a path.

In the following we will need the notion of k -connected graphs. Note at the beginning that after the removal of a vertex (or vertices) from Γ , the graph Γ can split into several disjoint connected components (see figure 1.4 (b)). The topological closures of connected components of $\Gamma \setminus X$ will be called topological components or, if it does not cause ambiguity, just components (see figure 1.4 (c) for an intuitive definition of the topological closure). The definition of k -connected graph is closely

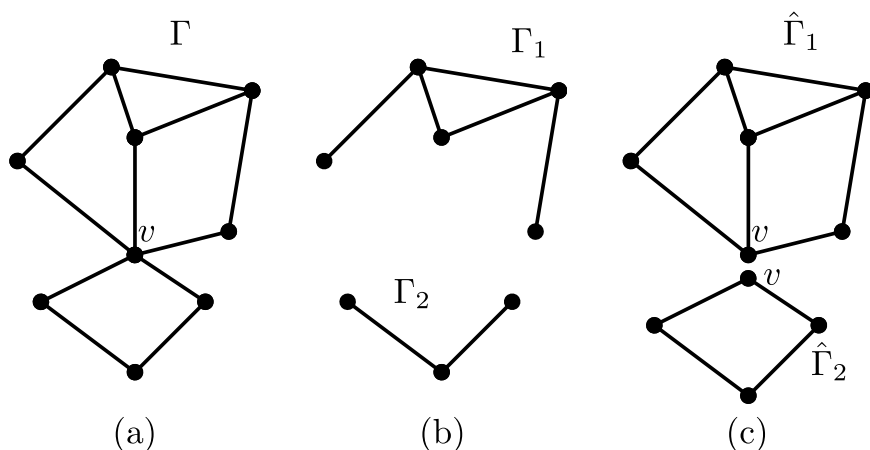


Figure 1.4: (a) A graph Γ , (b) Components of Γ , (c) Topological components of Γ .

related to this notion, i.e.

Definition 1.3.5. A graph $\Gamma = \{V, E\}$ is k -connected, where $k \in \mathbb{N}$, if $|V| > k$ and $\Gamma \setminus X$ is connected for any set $X \subset V$ with $|X| < k$.

In definition 1.3.5 the graph $\Gamma \setminus X$ should be understood as a graph obtained from Γ by removal of vertices X as explained in section 1.3.1. Moreover, we assume that every graph is 0-connected. Note also that by definition 1.3.5 all connected graphs are 1-connected. We next define the connectivity of a graph.

Definition 1.3.6. The connectivity of Γ , $\kappa(\Gamma)$, is the greatest integer k such that Γ is k -connected.

Note that the definition of k -connected graph is phrased in terms of vertex removals rather than in terms of paths joining pairs of vertices. In order to link it with paths we first define independent paths between pairs of vertices.

Definition 1.3.7. Two (or more) paths between vertices v_1 and v_2 of Γ are independent if they do not have common inner vertices (see figure 1.5).

The following Menger's theorem [45] gives the characterization of k -connected graphs in terms of independent paths.

Theorem 1.3.8. A graph is k -connected if and only if there are k independent paths between any two of its vertices.

1.3.3 Decomposition of a graph into 3-connected components

As we will see in the next sections, the characterisation of quantum statistics on graphs requires an understanding of the decomposition of a graph into 3-connected components. We start with the definition of a cut.

Definition 1.3.9. A cut X of a graph Γ is a set of vertices such that $\Gamma \setminus X$ is disconnected, that is, it consists of at least two components.

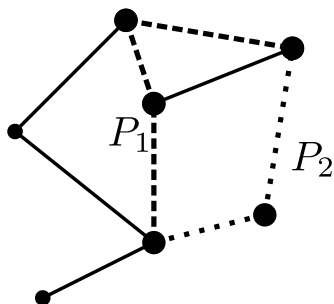


Figure 1.5: Example of two independent paths between vertices v_1 and v_2 , dashed and dotted subgraphs of Γ .

We will say that X is an n -cut if $|X| = n$. We next introduce the notion of a block of the graph.

Definition 1.3.10. *A block is a maximal connected subgraph without a 1-cut.*

Note that by definition 1.3.10 any block is either a maximal 2-connected subgraph or a single edge. For example, if Γ is a tree then its blocks are precisely the edges. Having a 1-connected simple graph one can consider the set of its 1-cuts. For each 1-cut we can further consider its topological components. Next for each component, if possible we apply the remaining 1-cuts. Repeating this process iteratively we arrive with topological components which are either 2-connected or given by edges. This way we decompose a 1-connected graph into the set of 2-connected components and edges, which are in fact the blocks of the considered graph (see figure 1.6 for an example of this kind of decomposition). It can be shown that the decomposition is unique [45]. If the 2-connected components obtained from the above decomposition are not 3-connected they can be further decomposed into the set of 3-connected components and perhaps cycles. This is done by considering the set of 2-cuts. For each 2-cut $\{x, y\} \subset V$ we take all its topological components. In order to ensure that these components are 2-connected we add an additional edge between vertices $\{x, y\}$ and call them the *marked components*. Repeating this process iteratively we arrive at marked components which are either 3-connected or topological cycles (see figure 1.7 for an example of this kind of decomposition). Although the final

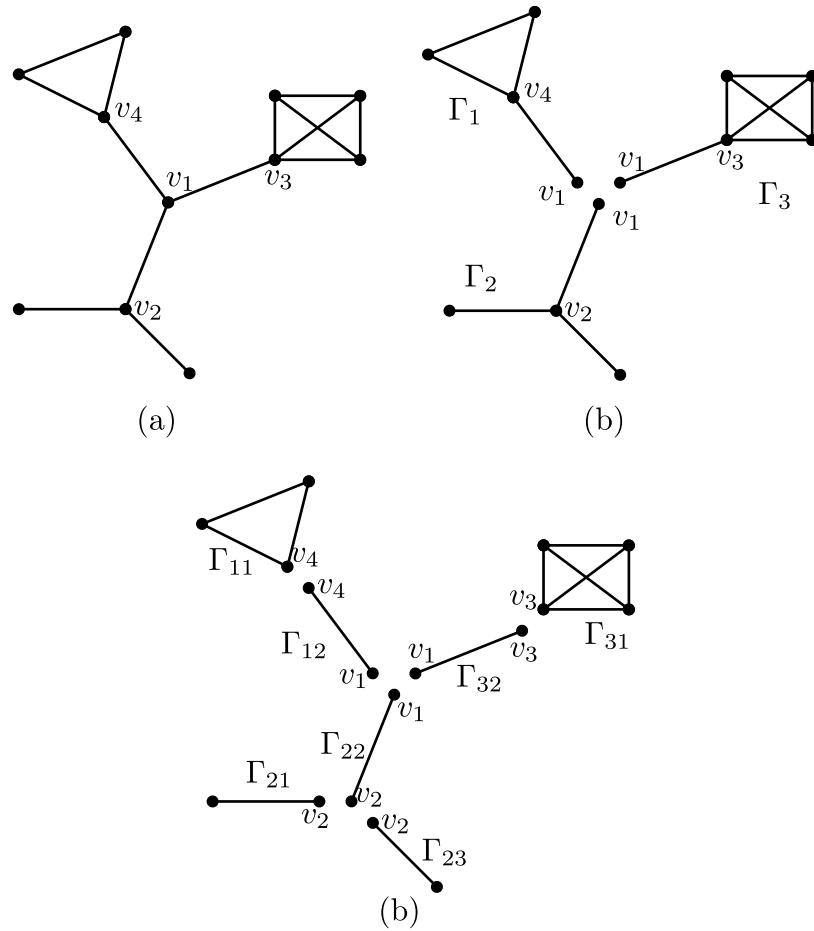


Figure 1.6: (a) A graph, (b) Its topological components resulting from v_1 -cut, (c) The full block decomposition.

set of marked components is typically not unique, one can show that the numbers of 3-connected components and cycles do not depend on the order in which one applies 2-cuts.

1.4 The fundamental group

In this section we introduce the fundamental group of a topological space. As we will see, up to continuous deformations, the elements of this group are loops of the considered space.

Let X be a topological space. A path in X is a continuous map $f : [0, 1] \rightarrow X$.

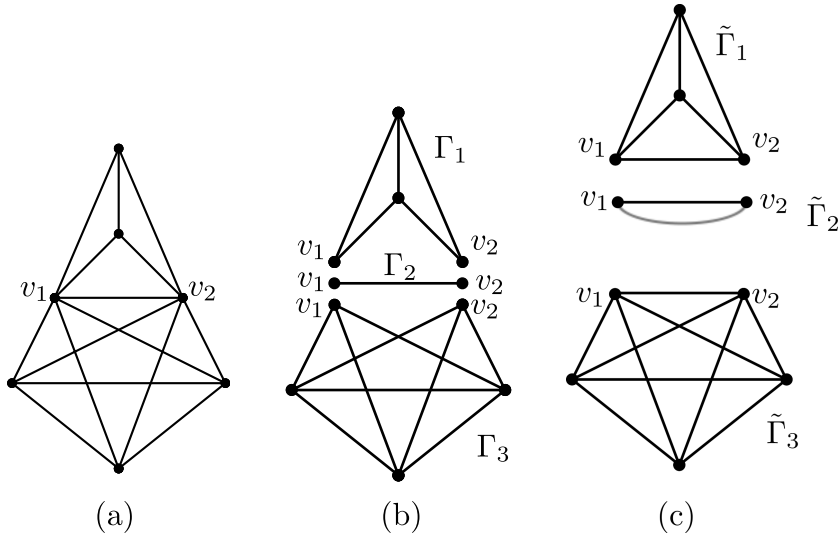


Figure 1.7: (a) A 2-connected graph, (b) Components resulting from $\{v_1, v_2\}$ -cut, (c) Marked components resulting from $\{v_1, v_2\}$ -cut.

Consider the family of paths $f_t : [0, 1] \rightarrow X$, where $t \in [0, 1]$ and:

- the endpoints $f_t(0) = x_0$ and $f_t(1) = x_1$ are fixed, i.e. do not depend on t ,
- the map $F(s, t) := f_t(s)$, that is the map $F : [0, 1] \times [0, 1] \rightarrow X$ is continuous.

The family satisfying these conditions is called a *homotopy of paths* in X .

Definition 1.4.1. Two paths f_0 and f_1 with fixed endpoints, i.e. $f_0(0) = f_1(0)$ and $f_0(1) = f_1(1)$, are homotopic if they can be connected by a homotopy of paths.

The homotopy equivalent paths will be denoted by $f_0 \simeq f_1$. One can show that the relation of homotopy of paths with fixed points, i.e. \simeq is an equivalence relation and therefore divides paths into disjoint classes. We next define the product of two paths.

Definition 1.4.2. Let $f, g : [0, 1] \rightarrow X$ be such that $f(1) = g(0)$. The product path $f \cdot g$ is the path given by

$$f \cdot g(t) = \begin{cases} f(2t) & 0 \leq t \leq \frac{1}{2}, \\ g(2t - 1) & \frac{1}{2} \leq t \leq 1. \end{cases}$$

It is easy to see that the product of paths behaves well with respect to homotopy classes of paths, i.e. if $f_0 \simeq f_1$ and $g_0 \simeq g_1$ then $f_0 \cdot g_0 \simeq f_1 \cdot g_1$.

Let us next consider loops, that is paths whose starting and ending points are the same (we call it basepoint). We denote by $\pi_1(X, x_0)$ the set of all homotopy classes of loops with basepoint x_0 . One can show that $\pi_1(X, x_0)$ is a group with respect to the product of homotopy classes of loops defined by $[f][g] = [f \cdot g]$ called *the fundamental group* of X at the basepoint x_0 . Moreover, if two basepoints x_0 and x_1 lie in the same path-component of X the groups $\pi_1(X, x_0)$ and $\pi_1(X, x_1)$ are isomorphic. Therefore for path-connected spaces we often write $\pi_1(X)$ instead of $\pi_1(X, x_0)$.

We next describe the fundamental group of a simple connected graph². Let $T \subset \Gamma$ be a spanning tree of Γ . Choose v_0 to be any vertex of Γ (hence of T). Each edge e_i of $\Gamma \setminus T$, which we will call a deleted edge, defines a loop in Γ . To see this note that there is a unique simple path joining v_0 with each of the endpoints of e_i . The announced loop, which we denote by e_i , starts from v_0 goes through the path in T to one of the endpoints of e_i , then through e_i and then returns to v_0 across the path in T . The homotopy classes of these loops generate $\pi_1(\Gamma)$. More precisely:

Theorem 1.4.3. *Let Γ be a connected simple graph and T its spanning tree. Then the fundamental group $\pi_1(\Gamma)$ is a free group whose basis is given by classes $[e_i]$ corresponding to deleted edges $e_i \in \Gamma \setminus T$.*

1.5 Cell complexes

An example of a topological space is a cell complex which we discuss in the following.

Let $B_n = \{x \in \mathbb{R}^n : \|x\| \leq 1\}$ be the standard unit-ball. The boundary of B_n is the unit-sphere $S^{n-1} = \{x \in \mathbb{R}^n : \|x\| = 1\}$. A cell complex X is a nested

²The topology we use is a topology of a cell complex which is defined in section 1.5

sequence of topological spaces

$$X^0 \subseteq X^1 \subseteq \dots \subseteq X^n, \quad (1.5.1)$$

where the X^k 's are the so-called k - skeletons defined as follows:

- The 0 - skeleton X^0 is a discrete set of points.
- For $\mathbb{N} \ni k > 0$, the k - skeleton X^k is the result of attaching k - dimensional balls B_k to X^{k-1} by gluing maps

$$\sigma : S^{k-1} \rightarrow X^{k-1}. \quad (1.5.2)$$

By k -cell $\alpha^{(k)}$ we understand the interior of the ball B_k attached to the $(k - 1)$ -skeleton X^{k-1} . We will denote by $\bar{\alpha}^{(k)}$ the cell $\alpha^{(k)}$ together with its boundary. The k -cell is regular if its gluing map is an embedding (i.e., a homeomorphism onto its image). Finally we say that X is n -dimensional if n is the highest dimension of the cells in X .

Notice that every simple graph Γ can be treated as a regular cell complex with vertices as 0-cells and edges as 1-cells. If a graph contains loops, these loops are irregular 1-cells (the two points that comprise the boundary of B_1 are attached to a single vertex of the 0-skeleton). The product $\Gamma^{\times n}$ inherits a cell-complex structure; its cells are cartesian products of cells of Γ .

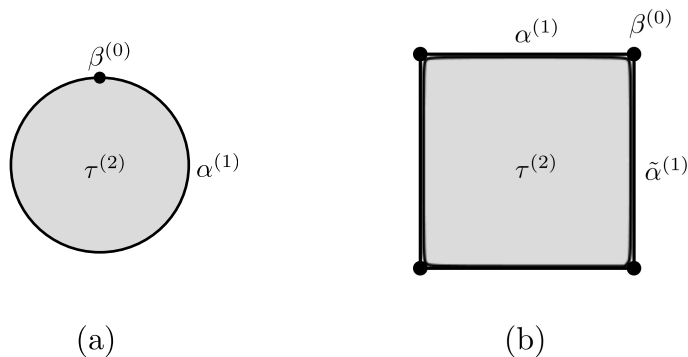


Figure 1.8: Examples of (a) an irregular cell complex. $\alpha^{(1)}$ is an irregular 1-cell and $\beta^{(0)}$ is an irregular face of $\alpha^{(1)}$, $\tau^{(2)}$ is a regular 2-cell. (b) A regular cell complex.

1.6 Homology groups

In this section we define homology groups, $H_k(X, \mathbb{Z})$ over the integers of the n -dimensional cell complex X . As we will always speak about integer homology we will often write $H_k(X)$ instead of $H_k(X, \mathbb{Z})$.

The construction of homology groups goes in several steps which we now describe. First, we assign an arbitrary orientation on the cells of X . Let m_p be the number of p -cells in X . The oriented p -cells will be denoted by $\{e_1^{(p)}, e_2^{(p)} \dots e_{m_p}^{(p)}\}$. The p -chain is a formal linear combination

$$c = a_1 e_1^{(p)} + a_2 e_2^{(p)} + \dots + a_{m_p} e_{m_p}^{(p)}, \quad (1.6.1)$$

where coefficients a_i are integers. We denote by $C_p(X)$ the set of all p -chains. This set can be given the structure of an abelian group. The addition in this group is defined by

$$\begin{aligned} c_1 &= a_1 e_1^{(p)} + a_2 e_2^{(p)} + \dots + a_{m_p} e_{m_p}^{(p)}, \\ c_2 &= b_1 e_1^{(p)} + b_2 e_2^{(p)} + \dots + b_{m_p} e_{m_p}^{(p)}, \\ c_1 + c_2 &= (a_1 + b_1) e_1^{(p)} + a_2 e_2^{(p)} + \dots + (a_{m_p} + b_{m_p}) e_{m_p}^{(p)}. \end{aligned}$$

In fact $C_p(X)$ is isomorphic to the direct sum of m_p copies of \mathbb{Z} , i.e. $C_p(X) \simeq \mathbb{Z}^{m_p}$.

We next consider the boundary map

$$\partial_p : C_p(X) \rightarrow C_{p-1}(X), \quad (1.6.2)$$

which assigns to an oriented p -cell e_i^p its boundary (see [25] for a discussion on boundary maps). The boundary map satisfies $\partial_{p-1} \partial_p = 0$, that is the boundary of the boundary is zero. This way we arrive at the *chain complex* $(C(X)_\bullet, \partial_\bullet)$, that is a sequence of abelian groups $C_n(X), \dots, C_0(X)$ connected by boundary homomorphisms $\partial_p : C_p(X) \rightarrow C_{p-1}(x)$, such that that composition of any two consecutive maps is zero $\partial_{p-1} \partial_p = 0$. The standard way to denote a chain complex is the following:

$$C_n(X) \xrightarrow{\partial_n} C_{n-1} \xrightarrow{\partial_{n-1}} \dots C_2(X) \xrightarrow{\partial_2} C_1(X) \xrightarrow{\partial_1} C_0(X) \xrightarrow{\partial_0} 0. \quad (1.6.3)$$

Let us denote by $\text{Ker}(\partial_p)$ and $\text{Im}(\partial_p)$ the kernel and the image of the boundary map ∂_p . The elements of $\text{Ker}(\partial_p)$ are called p -cycles and the elements of $\text{Im}(\partial_p)$ are called p -boundaries. The p -th homology group is defined as

$$H_p(X) = \text{Ker}(\partial_p)/\text{Im}(\partial_{p+1}), \quad (1.6.4)$$

so it is a quotient space of p -cycles by p -boundaries.

We next present an example of a calculation of homology groups, i.e. we calculate the first homology group of the 2-torus, T^2 . To this end we consider the cell complex X_T shown in figure 1.9. In fact, this is the simplest triangularization of T^2 . The cell complex X_T consists of two 2-cells, three 1-cells and one 0-cell, i.e.

$$\begin{aligned} C_2(X_T) &= \text{Span}_{\mathbb{Z}}\{f_1, f_2\}, \\ C_1(X_T) &= \text{Span}_{\mathbb{Z}}\{e_1, e_2, e_3\}, \\ C_0(X_T) &= \text{Span}_{\mathbb{Z}}\{v\}. \end{aligned} \quad (1.6.5)$$

Therefore we have the following chain complex

$$C_2(X_T) \xrightarrow{\partial_2} C_1(X) \xrightarrow{\partial_1} C_0(X) \xrightarrow{\partial_0} 0. \quad (1.6.6)$$

In order to calculate $H_1(X_T, \mathbb{Z})$ we need to calculate the kernel and the image of boundary maps ∂_1 and ∂_2 respectively. Taking into account the orientation denoted in figure 1.9 we have

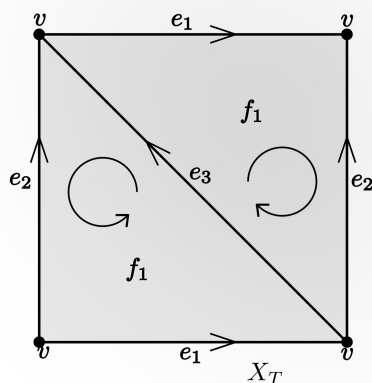
$$\begin{aligned} \partial_1 e_1 &= \partial_1 e_2 = \partial_1 e_3 = v - v = 0, \\ \partial_2 f_1 &= \partial_2 f_2 = e_1 - e_2 + e_3. \end{aligned} \quad (1.6.7)$$

Therefore

$$\begin{aligned} \text{Ker}\partial_1 &= \text{Span}_{\mathbb{Z}}\{e_1, e_2, e_3\} = \text{Span}_{\mathbb{Z}}\{e_1, e_2, e_1 - e_2 + e_3\}, \\ \text{Im}\partial_2 &= \text{Span}_{\mathbb{Z}}\{e_1 - e_2 + e_3\}. \end{aligned} \quad (1.6.8)$$

Using (1.6.4) one easily sees that

$$H_1(X_T, \mathbb{Z}) = \text{Ker}(\partial_1)/\text{Im}(\partial_2) = \text{Span}_{\mathbb{Z}}\{[e_1], [e_2]\} \simeq \mathbb{Z} \oplus \mathbb{Z}. \quad (1.6.9)$$

Figure 1.9: The cell complex X_T of the 2-torus T^2

We finish this section by making a statement about the connection between the first homology group $H_1(X)$ and the fundamental group $\pi_1(X)$. This connection is based on the fact that the map $f : [0, 1] \rightarrow X$ can be viewed as either a path or a 1-cell. Moreover if f represents a loop the considered 1-cell is a cycle. We need to first define the commutator subgroup of $\pi_1(X)$.

Let G be a group and denote by e its identity element. The commutator of two elements $g, h \in G$ is defined as

$$[g, h] = g^{-1}h^{-1}gh. \quad (1.6.10)$$

Note that $[g, h] = e$ if and only if $gh = hg$. The subgroup generated by all commutators of G , which we denote by $[G, G]$, is a normal subgroup of G . To see this note

that if $u \in [G, G]$ and $g \in G$ then $g^{-1}ug = u(u^{-1}g^{-1}ug) = u[u, g]$. By normality of $[G, G]$ the quotient $G/[G, G]$ is a group. This group is called *abelianization* of G as it is necessarily abelian. In fact if group G is abelian itself then $G/[G, G] = G$.

The following theorem relates $H_1(X)$ to $\pi_1(X)$

Theorem 1.6.1. *The first homology group $H_1(X)$ is the abelianization of the fundamental group $\pi_1(X)$*

By theorem 1.4.3 the fundamental group of a connected graph Γ is a free group generated by loops through the deleted edges. Combining this result with theorem 1.6.1 one easily obtains

Theorem 1.6.2. *The first homology group $H_1(X)$ of a graph Γ is $H_1(\Gamma, \mathbb{Z}) = \mathbb{Z}^{\beta_1(\Gamma)}$, where $\beta_1(\Gamma)$ is the number of independent cycles of Γ given by formula 1.3.2.*

1.7 Structure theorem for finitely generated Abelian groups

Homology groups of a finite cell complex X are finitely generated Abelian groups. Therefore, in this section we discuss the structure theorem for these kind of groups.

1.7.1 Finitely generated Abelian groups

Let $\{G, +\}$ be an Abelian group. We put 0 as the neutral element of G and $-x$ denotes the inverse of x . For $x \in G$ and $n \in \mathbb{Z}$ we put

$$nx = \begin{cases} \underbrace{x + \dots + x}_n & n > 0, \\ \underbrace{-x + \dots + (-x)}_n & n < 0, \\ nx = 0 & n = 0. \end{cases}$$

It is easy to see that for any chosen $x_1, \dots, x_k \in G$ the set of elements

$$\{n_1x_1 + \dots + n_kx_k : \forall i n_i \in \mathbb{Z}\}, \quad (1.7.1)$$

is the subgroup of G generated by $x_1, \dots, x_k \in G$. We say that $x_1, \dots, x_k \in G$ are linearly independent if $n_1x_1 + \dots + n_kx_k = 0$ if and only if $\forall i n_i = 0$.

Definition 1.7.1. A group G is a finitely generated Abelian group if and only if there are elements $x_1, \dots, x_k \in G$ such that $G = \{n_1x_1 + \dots + n_kx_k : \forall i n_i \in \mathbb{Z}\}$. Moreover, if the generating elements can be chosen to be linearly independent the group G is a finitely generated free abelian group isomorphic to

$$G \simeq \underbrace{\mathbb{Z} \oplus \dots \oplus \mathbb{Z}}_k = \mathbb{Z}^k. \quad (1.7.2)$$

The number k is called the rank of G .

For a finitely generated Abelian group which is not free there are some relations between generating elements. In order to describe these relations we will need the following

Theorem 1.7.2. Let G be a finitely generated free abelian group of rank p and H a subgroup. There always exists choice of generators x_1, \dots, x_l , $l \leq p$ in G such that $H = k_1x_1 + \dots + k_lx_l$, i.e. H can be expressed in the form:

$$H = k_1\mathbb{Z} \oplus \dots \oplus k_l\mathbb{Z}, \quad (1.7.3)$$

where $k_i\mathbb{Z} = \{x \in \mathbb{Z} : k_i|x\}$ and $\forall i k_i|k_{i+1}$ and $l \leq p$.

The structure theorem of an arbitrary finitely generated Abelian group reads:

Theorem 1.7.3. Let G be a finitely generated Abelian group. Then

$$G \simeq \underbrace{\mathbb{Z} \oplus \dots \oplus \mathbb{Z}}_k \oplus \mathbb{Z}_{k_1} \oplus \dots \oplus \mathbb{Z}_{k_l} = \mathbb{Z}^k \oplus \mathbb{Z}_{k_1} \oplus \dots \oplus \mathbb{Z}_{k_l}, \quad (1.7.4)$$

where $k_i|k_{i+1}$ for all $i \in \{1, \dots, l\}$.

Proof. Let x_1, \dots, x_p be generating elements of G . The map

$$f : \underbrace{\mathbb{Z} \oplus \dots \oplus \mathbb{Z}}_p \rightarrow G \quad (1.7.5)$$

$$f(n_1, \dots, n_p) = n_1x_1 + \dots + n_px_p, \quad (1.7.6)$$

is a surjective homomorphism between Abelian groups and therefore by the first isomorphism theorem $G = \underbrace{\mathbb{Z} \oplus \dots \oplus \mathbb{Z}}_p / \text{Ker}(f)$. But the kernel of f is a subgroup of $\underbrace{\mathbb{Z} \oplus \dots \oplus \mathbb{Z}}_p$. By theorem 1.7.2

$$\text{Ker}(f) = k_1\mathbb{Z} \oplus \dots \oplus k_l\mathbb{Z}, \quad (1.7.7)$$

for some $l \leq p$. Hence,

$$G = \underbrace{\mathbb{Z} \oplus \dots \oplus \mathbb{Z}}_p / k_1\mathbb{Z} \oplus \dots \oplus k_l\mathbb{Z} = \quad (1.7.8)$$

$$\underbrace{\mathbb{Z} \oplus \dots \oplus \mathbb{Z}}_k \oplus \mathbb{Z}_{k_1} \oplus \dots \oplus \mathbb{Z}_{k_l} = \quad (1.7.9)$$

$$\mathbb{Z}^k \oplus \mathbb{Z}_{k_1} \oplus \dots \oplus \mathbb{Z}_{k_l}, \quad (1.7.10)$$

where $k = p - l$. □

1.8 Topology of configuration spaces and quantum statistics

In this section we define configuration spaces, discuss their basic properties and relate them to quantum statistics.

Let us denote by M the one-particle classical configuration space (e.g., an m -dimensional manifold) and by

$$F_n(M) = \{(x_1, x_2, \dots, x_n) : x_i \in X, x_i \neq x_j\}, \quad (1.8.1)$$

the space of n distinct points in M . The n -particle configuration space is defined as an orbit space

$$C_n(M) = F_n(M)/S_n, \quad (1.8.2)$$

where S_n is the permutation group of n elements and the action of S_n on $F_n(M)$ is given by

$$\sigma(x_1, \dots, x_n) = (x_{\sigma^{-1}(1)}, \dots, x_{\sigma^{-1}(n)}), \quad \forall \sigma \in S_n. \quad (1.8.3)$$

Any closed loop in $C_n(M)$ represents a process in which particles start at some particular configuration and end up in the same configuration modulo that they might have been exchanged. As explained in section 1.4 the space of all loops up to continuous deformations equipped with loop composition is the fundamental group $\pi_1(C_n(M))$.

The abelianization of the fundamental group is the first homology group $H_1(C_n(M))$, and its structure plays an important role in the characterization of quantum statistics. In order to clarify this idea we will first consider the well-known problem of quantum statistics of many particles in \mathbb{R}^m , $m \geq 2$. We will describe fully both the fundamental and homology groups of $C_n(\mathbb{R}^m)$ for $m \geq 2$, showing that for $m \geq 3$, the only possible statistics are bosonic and fermionic, while for $m = 2$ anyon statistics emerges.

1.8.1 Quantum statistics for $C_n(\mathbb{R}^m)$

The case $M = \mathbb{R}^m$ and $m \geq 3$. When $M = \mathbb{R}^m$ and $m \geq 3$ the fundamental group $\pi_1(F_n(\mathbb{R}^m))$ is trivial, since there are enough degrees of freedom to avoid coincident configurations during the continuous contraction of any loop. Let us recall that we have a natural action of the permutation group S_n on $F_n(\mathbb{R}^m)$ which is free³. In such a situation the following theorem holds [25].

Theorem 1.8.1. *If an action of a finite group G on a space Y is free then G is isomorphic to $\pi_1(Y/G)/p_*(\pi_1(Y))$, where $p : Y \rightarrow Y/G$ is the natural projection and $p_* : \pi_1(Y) \rightarrow \pi_1(Y/G)$ is the induced map of fundamental groups.*

Notice that in particular if $\pi_1(Y)$ is trivial we get $G = \pi_1(Y/G)$. In our setting $Y = F_n(\mathbb{R}^m)$ and $G = S_n$. The triviality of $\pi_1(F_n(\mathbb{R}^m))$ implies that the fundamental group of $C_n(\mathbb{R}^m)$ is given by

$$\pi_1(F_n(\mathbb{R}^m)/S_n) = \pi_1(C_n(\mathbb{R}^m)) = S_n. \quad (1.8.4)$$

³The action of a group G on X is free iff the stabilizer of any $x \in X$ is the neutral element of G .

The homology group $H_1(C_n(\mathbb{R}^m), \mathbb{Z})$ is the abelianization of $\pi_1(C_n(\mathbb{R}^m))$. Hence,

$$H_1(C_n(\mathbb{R}^m), \mathbb{Z}) = \mathbb{Z}_2. \quad (1.8.5)$$

Notice that $H_1(C_n(\mathbb{R}^m), \mathbb{Z})$ might also be represented as $(\{1, e^{i\pi}\}, \cdot)$. This result can explain why we have only bosons and fermions in \mathbb{R}^m when $m \geq 3$ (see, e.g. [17] for a detailed discussion).

The case $M = \mathbb{R}^2$. The case of $M = \mathbb{R}^2$ is different as $\pi_1(F_n(\mathbb{R}^m))$ is no longer trivial and it is hard to use Theorem 1 directly. In fact it can be shown (see [22]) that for $M = \mathbb{R}^2$ the fundamental group $\pi_1(C_n(\mathbb{R}^2))$ is an Artin braid group $\text{Br}_n(\mathbb{R}^2)$

$$\text{Br}_n(\mathbb{R}^2) = \langle \sigma_1, \sigma_2, \dots, \sigma_{n-1} \mid \sigma_i \sigma_{i+1} \sigma_i = \sigma_{i+1} \sigma_i \sigma_{i+1}, \sigma_i \sigma_j = \sigma_j \sigma_i \rangle, \quad (1.8.6)$$

where in the first group of relations we take $1 \leq i \leq n - 2$, and in the second, we take $|i - j| \geq 2$. Although this group has a complicated structure, it is easy to see that its abelianization is

$$H_1(C_n(\mathbb{R}^2), \mathbb{Z}) = \mathbb{Z}. \quad (1.8.7)$$

This simple fact gives rise to a phenomena called anyon statistics [36, 46], i.e., particles in \mathbb{R}^2 are no longer fermions or bosons but instead any phase $e^{i\phi}$ can be gained when they are exchanged [17].

1.9 Graph configuration spaces

Here we consider the main problem of this thesis, namely $M = \Gamma$ is a graph. We describe the combinatorial structure of $C_n(\Gamma)$.

Let $\Gamma = (V, E)$ be a metric⁴ connected simple graph on $|V|$ vertices and $|E|$ edges. Similarly to the previous cases we define

$$F_n(\Gamma) = \{(x_1, x_2, \dots, x_n) : x_i \in \Gamma, x_i \neq x_j\}, \quad (1.9.1)$$

⁴A graph is metric if its edges have assign lengths.

and

$$C_n(\Gamma) = F_n(\Gamma)/S_n, \quad (1.9.2)$$

where S_n is the permutation group of n elements. Notice also that the group S_n acts freely on $F_n(\Gamma)$, which means that $F_n(\Gamma)$ is the covering space of $C_n(\Gamma)$. It seems *a priori* a difficult task to compute $H_1(C_n(\Gamma))$. Fortunately, this problem can be reduced to the computation of the first homology group of a cell complex, which we define now.

Following [24] we define the n -particle combinatorial configuration space as

$$\mathcal{D}^n(\Gamma) = (\Gamma^{\times n} - \tilde{\Delta})/S_n, \quad (1.9.3)$$

where $\tilde{\Delta}$ denotes all cells whose closure intersects with Δ . The space $\mathcal{D}^n(\Gamma)$ possesses a natural cell - complex structure with vertices as 0-cells, edges as 1-cells, 2-cells corresponding to moving two particles along two disjoint edges in Γ , and k - cells defined analogously. The existence of a cell - complex structure happens to be very helpful for investigating the homotopy structure of the underlying space. Namely, we have the following theorem:

Theorem 1.9.1. [1, 41](Abrams) *For any graph Γ with at least n vertices, the inclusion $\mathcal{D}^n(\Gamma) \hookrightarrow C_n(\Gamma)$ is a homotopy equivalence iff the following hold:*

1. *Each path between distinct vertices of valence not equal to two passes through at least $n - 1$ edges.*
2. *Each closed path in Γ passes through at least $n + 1$ edges.*

For $n = 2$ these conditions are automatically satisfied (provided Γ is simple). Intuitively, they can be understood as follows:

1. In order to have homotopy equivalence between $\mathcal{D}^n(\Gamma)$ and $C_n(\Gamma)$, we need to be able to accommodate n particles on every edge of graph Γ .
2. For every cycle there is at least one free (not occupied) vertex which enables the exchange of particles along this cycle.

Using Theorem 1.9.1, the problem of finding $H_1(C_n(\Gamma))$ is reduced to the problem of computing $H_1(\mathcal{D}^n(\Gamma))$. In the following two chapters of the thesis we will discuss how to determine $H_1(\mathcal{D}^n(\Gamma))$. Meanwhile, to clarify the idea behind theorem 1.9.1 let us consider the following example.

Example 1.9.2. Let Γ be a star graph on four vertices (see figure 1.10(a)). The two-particle configuration spaces $C_2(\Gamma)$ and $\mathcal{D}^2(\Gamma)$ are shown in figures 1.10(b),(c). Notice that $C_2(\Gamma)$ consists of six 2 - cells (three are interiors of triangles and the other three are interiors of squares), eleven 1 - cells and six 0 - cells. Vertices $(1, 1)$, $(2, 2)$, $(3, 3)$ and $(4, 4)$ do not belong to $C_2(\Gamma)$. Similarly dashed edges, i.e. $(1, 1) - (2, 2)$, $(2, 2) - (4, 4)$, $(2, 2) - (3, 3)$ do not belong to $C_2(\Gamma)$. This is why $C_2(\Gamma)$ is not a cell complex - not every cell has its boundary in $C_2(\Gamma)$. Notice that cells of $C_2(\Gamma)$ whose closures intersect Δ (denoted by dashed lines and diamond points) do not influence the homotopy type of $C_2(\Gamma)$ (see figures 1.10(b),(c)). Hence, the space $\mathcal{D}^2(\Gamma)$ has the same homotopy type as $C_2(\Gamma)$, but consists of six 1 - cells and six 0 - cells. $\mathcal{D}^2(\Gamma)$ is subspace of $C_2(\Gamma)$ denoted by dotted lines in figure 1.10(b). In particular, one can also easily calculate that $H_1(C_2(\Gamma)) = H_1(\mathcal{D}^2(\Gamma))$.

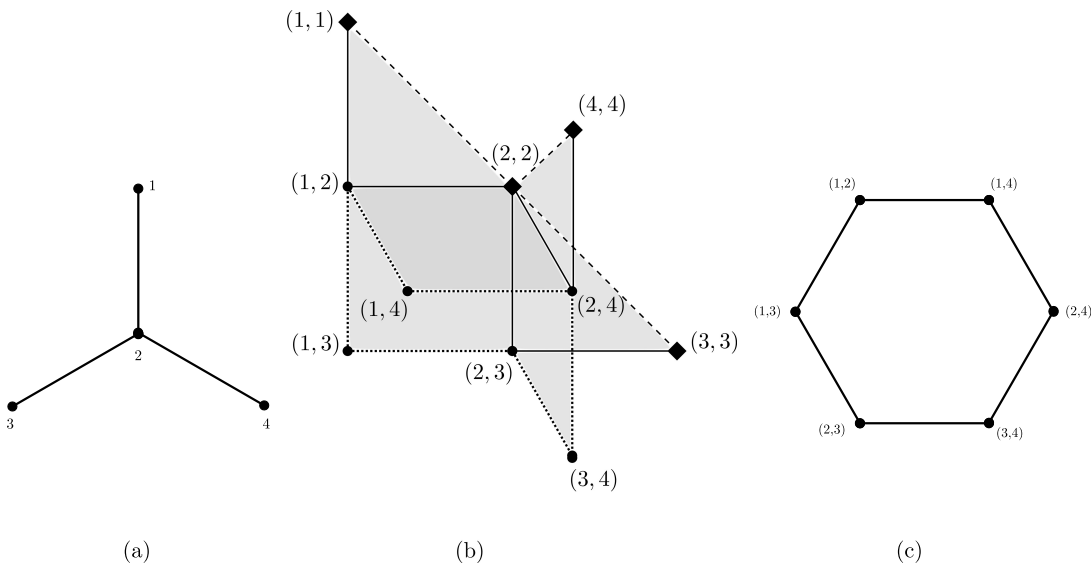


Figure 1.10: (a) The star graph Γ , (b) the two-particle configuration space $C_2(\Gamma)$, (c) the two-particle discrete configuration space $\mathcal{D}^2(\Gamma)$.

1.10 Quantum graphs

The main attraction of quantum graphs is that they are simple models to study complicated phenomena. A metric graph $\Gamma = (V, E)$ is a graph whose edges have assigned lengths. One can consider single-particle quantum mechanics on a metric graph. A particle is described by a collection of wavefunctions, $\{\Psi_e\}_{e \in E}$, living on the edges of Γ . On each edge a Hamiltonian, H_e , is defined. Typically it is of the form:

$$H_e = \frac{1}{2} \left(-i \frac{d}{dx} - A_e(x_e) \right)^2 + V_e(x_e). \quad (1.10.1)$$

In order to ensure selfadjointness of the Hamiltonian, boundary conditions at the vertices are introduced. For a free particle, i.e when $H_e = -\frac{1}{2} \frac{d^2}{dx^2}$ an example is Neumann boundary conditions:

1. Wavefunctions are continuous at vertices.
2. The sum of outgoing derivatives vanishes at each vertex.

The full characterization of boundary conditions for a free particle on a quantum graph was given in [31] and is expressed in terms of Lagrangian planes of a certain complex symplectic form. Quantum mechanics of a single particle on a quantum graph is rather well understood. It has been recently extensively investigated from various angles, e.g. superconductivity [23] quantum chaos [32] or Anderson localization [3].

For understanding quantum statistics on a metric graph Γ , which is a topological property of the underlying configuration space $C_n(\Gamma)$, it is irrelevant to know the lengths of the edges of Γ . That is why in the following we will always treat Γ as a 1-dimensional cell complex. Using the fact that spaces $C_n(\Gamma)$ and $\mathcal{D}^n(\Gamma)$ are homotopic and by definition of the first homology group we need to only study the 2-skeleton of $\mathcal{D}^n(\Gamma)$. In order to provide some physical intuition we will now describe the following model.

1.10.1 Topological gauge potential

Assume that Γ is, as explained in section 1.9, sufficiently subdivided. Note that 0-skeleton of $\mathcal{D}^n(\Gamma)$ consists of unordered collections of n distinct vertices of Γ , $\{v_{i_1}, \dots, v_{i_n}\}$. The connections between 0-cells are described by 1-cells of $\mathcal{D}^n(\Gamma)$. Two 0-cells are connected by an edge iff they have $n - 1$ vertices in common and the remaining two vertices are connected by an edge in Γ . In other words 1-cells of $\mathcal{D}^n(\Gamma)$ are of the form $v_1 \times \dots \times v_{n-1} \times e$ up to permutations, where v_j are vertices of Γ and $e = j \rightarrow k$ is an edge of Γ whose endpoints are not $\{v_1, \dots, v_{n-1}\}$. For simplicity we will use the following notation

$$\{v_1, \dots, v_{n-1}, j \rightarrow k\} := v_1 \times \dots \times v_{n-1} \times e.$$

An n -particle gauge potential is a function $\Omega^{(n)}$ defined on the directed edges of $\mathcal{D}^n(\Gamma)$ with the values in \mathbb{R} modulo 2π such that

$$\Omega^{(n)}(\{v_1, \dots, v_{n-1}, k \rightarrow j\}) = -\Omega^{(n)}(\{v_1, \dots, v_{n-1}, j \rightarrow k\}). \quad (1.10.2)$$

In order to define Ω on linear combinations of directed edges we extend (1.10.2) by linearity.

For a given gauge potential, $\Omega^{(n)}$ the sum of its values calculated on the directed edges of an oriented cycle C will be called the flux of Ω through C and denoted $\Omega(C)$. Two gauge potentials $\Omega_1^{(n)}$ and $\Omega_2^{(n)}$ are called equivalent if for any oriented cycle C the fluxes $\Omega_1^{(n)}(C)$ and $\Omega_2^{(n)}(C)$ are equal modulo 2π .

The n -particle gauge potential $\Omega^{(n)}$ is called a *topological gauge potential* if for any contractible oriented cycle C in $\mathcal{D}^n(\Gamma)$ the flux $\Omega^{(n)}(C) = 0 \pmod{2\pi}$. It is thus clear that equivalence classes of topological gauge potentials are in 1-1 correspondence with the equivalence classes in $H_1(\mathcal{D}^n(\Gamma))$. Therefore, characterization of quantum statistics is characterization of all possible topological gauge potentials. These potentials can be incorporated into the Hamiltonian of a so-called tight-binding model. In short, it is a model whose underlying Hilbert space is spanned by elements of the 0-skeleton of $\mathcal{D}^n(\Gamma)$ and the Hamiltonian is given by the adjacency matrix of the 1-skeleton of $\mathcal{D}^n(\Gamma)$. As $\Omega^{(n)}$ is defined on the edges

of $\mathcal{D}^n(\Gamma)$ it can be added to the Hamiltonian by changing: $H_{\{v_1, \dots, v_{n-1}, k \rightarrow j\}} \rightarrow H_{\{v_1, \dots, v_{n-1}, k \rightarrow j\}} e^{i\Omega^{(n)}(\{v_1, \dots, v_{n-1}, k \rightarrow j\})}$ (see [26] for more detailed discussion in case of two particles).

Chapter 2

Quantum Statistics on graphs

In this chapter we raise the question of what quantum statistics are possible on quantum graphs. In particular we develop a full characterization of abelian quantum statistics on graphs. We explain how the number of anyon phases is related to connectivity. For 2-connected graphs the independence of quantum statistics with respect to the number of particles is proven. For non-planar 3-connected graphs we identify bosons and fermions as the only possible statistics, whereas for planar 3-connected graphs we show that one anyon phase exists. Our approach also yields an alternative proof of the structure theorem for the first homology group of n -particle graph configuration spaces. Finally, we determine the topological gauge potentials for 2-connected graphs.

In order to explore how the quantum statistics picture depends on topology, the case of two indistinguishable particles on a graph was studied in [26] (see also [10]). Recall that a graph Γ is a network consisting of vertices (or nodes) connected by edges. Quantum mechanically, one can either consider the one-dimensional Schrödinger operator acting on the edges, with matching conditions for the wavefunctions at the vertices, or a discrete Schrödinger operator acting on connected vertices (i.e. a tight-binding model on the graph). Such systems are of considerable independent interest and their single-particle quantum mechanics has been studied extensively in recent years [11]. The extension of this theory to many-particle quantum graphs was another motivation for [26] (see also [14]). The discrete case turns

out to be significantly easier to analyse, and in this situation it was found that a rich array of anyon statistics are kinematically possible. Specifically, certain graphs were found to support anyons while others can only support fermions or bosons. This was demonstrated by analysing the topology of the corresponding configuration graphs $C_2(\Gamma) = (\Gamma^{\times 2} - \Delta)/S_2$ in various examples. It opens up the problem of determining general relations between the quantum statistics of a graph and its topology.

As explained in the previous section, mathematically the determination of quantum statistics reduces to finding the first homology group H_1 of the appropriate classical configuration space, $C_n(M)$. Although the calculation for $C_n(\mathbb{R}^N)$ is relatively elementary, it becomes a non-trivial task when \mathbb{R}^N is replaced by a general graph Γ . One possible route is to use discrete Morse theory, as developed by Forman [18]. This is a combinatorial counterpart of classical Morse theory, which applies to cell complexes. In essence, it reduces the problem of finding $H_1(M)$, where M is a cell complex, to the construction of certain discrete Morse functions, or equivalently discrete gradient vector fields. Following this line of reasoning Farley and Sabalka [19] defined the appropriate discrete vector fields and gave a formula for the first homology groups of tree graphs. Recently, making extensive use of discrete Morse theory and some graph invariants, Ko and Park [30] extended the results of [19] to an arbitrary graph Γ . However, their approach relies on a suite of relatively elaborate techniques – mostly connected to a proper ordering of vertices and choices of trees to reduce the number of critical cells – and the relationship to, and consequences for, the physics of quantum statistics are not easily identified.

In this chapter we give a full characterization of all possible abelian quantum statistics on graphs. In order to achieve this we develop a new set of ideas and methods which lead to an alternative proof of the structure theorem for the first homology group of the n -particle configuration space obtained by Ko and Park [30]. Our reasoning, which is more elementary in that it makes minimal use of discrete Morse theory, is based on a set of simple combinatorial relations which stem from the analysis of some canonical small graphs. The advantage for us of this approach is that it

is explicit and direct. This makes the essential physical ideas much more transparent and so enables us to identify the key topological determinants of the quantum statistics. It also enables us to develop some further physical consequences. In particular we give a full characterization of the topological gauge potentials on 2-connected graphs, and identify some examples of particular physical interest, in which the quantum statistics have features that are subtle.

The chapter is organized as follows. We start with a discussion, in section 2.1, of some physically interesting examples of quantum statistics on graphs, in order to motivate the general theory that follows. In section 2.2 we define some basic properties of graph configuration spaces. In section 2.3 we develop a full characterization of the first homology group for 2-particle graph configuration spaces. In section 2.4 we give a simple argument for the stabilization of quantum statistics with respect to the number of particles for 2-connected graphs. Using this we obtain the desired result for n -particle graph configuration spaces when Γ is 2-connected. In order to generalize the result to 1-connected graphs we consider star and fan graphs. The main result is obtained at the end of section 2.5. The first homology group $H_1(C_n(\Gamma))$ is given by the direct sum of a free component, which corresponds to anyon phases and Aharonov-Bohm phases, and a torsion component, which is restricted to be a direct sum of copies of \mathbb{Z}_2 . The last part of the chapter is devoted to the characterization of topological gauge potentials for 2-connected graphs.

2.1 Quantum statistics on graphs

In this section we discuss several examples which illustrate some interesting and surprising aspects of quantum statistics on graphs. A determining factor turns out to be the *connectivity* of a graph. We recall (cf [45]) that a graph is *k-connected* if it remains connected after removing any $k-1$ vertices. (Note that a k -connected graph is also j -connected for any $j < k$.) According to Menger's theorem [45], a graph is k -connected if and only if every pair of distinct vertices can be joined by at least k disjoint paths. A k -connected graph can be decomposed into $(k+1)$ -connected

components, unless it is complete [27]. Thus, a graph may be regarded as being built out of more highly connected components. Quantum statistics, as we shall see, depends on k -connectedness up to $k = 3$. (Remark: in this thesis, quantum statistics refers specifically to phases involving cycles of two or more particles; phases associated with single-particle cycles, called Aharonov-Bohm phases, are introduced in Section 2.4 below).

2.1.1 3-connected graphs

Quantum statistics for any number of particles on a 3-connected graph depends only on whether the graph is planar, and not on any additional structure. We recall that a graph is planar if it can be drawn in the plane without crossings. For planar 3-connected graphs we will show that the statistics is characterised by a single anyon phase associated with cycles in which a pair of particles exchange positions. For non-planar 3-connected graphs, the statistics is either Bose or Fermi – in effect, the anyon phase is restricted to be 0 and π . Thus, as far as quantum statistics is concerned, three- and higher-connected graphs behave like \mathbb{R}^2 in the planar case and \mathbb{R}^d , $d > 2$, in the nonplanar case. A new aspect for graphs is the possibility of combining planar and nonplanar components. The graph shown in figure 2.1 consists of a large square lattice in which four cells have been replaced by a defect in the form of a K_5 subgraph, the (nonplanar) fully connected graph on five vertices. This local substitution makes the full graph nonplanar, thereby excluding anyon statistics.

One of the simplest examples of this phenomenon is provided by the graph G shown in figure 2.2. G is planar 3-connected, and therefore supports an anyon phase. However, if an additional edge e is added, the resulting graph is K_5 , and therefore supports only Bose or Fermi statistics. One can continuously interpolate from a quantum Hamiltonian defined on K_5 to one defined by G by introducing an amplitude coefficient ϵ for transitions along e . For $\epsilon = 0$, the edge e is effectively absent, and the resulting Hamiltonian is defined on G . This situation might appear

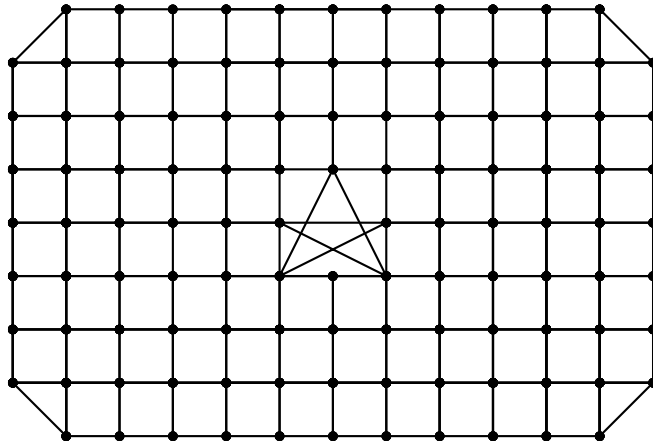


Figure 2.1: The large almost planar 3-connected graph.

to be paradoxical; how could anyon statistics, well defined for $\epsilon = 0$, suddenly disappear for $\epsilon \neq 0$? The resolution lies in the fact that an anyon phase defined for $\epsilon = 0$ introduces, for $\epsilon \neq 0$, physical effects that cannot be attributed to quantum statistics (unless the phase is 0 or π). The transition between planar and nonplanar geometries, which is easily effected with quantum graphs, merits further study.

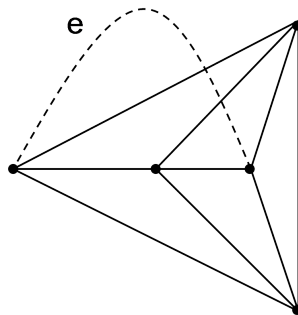


Figure 2.2: The graph G (without the edge e) is planar 3-connected. With e , the graph is K_5 .

2.1.2 2-connected graphs

Quantum statistics on 2-connected graphs is more complex, and depends on the decomposition of individual graphs into cycles and 3-connected components (see

Section 2.3.3). There may be multiple anyon and \mathbb{Z}_2 (or Bose/Fermi alternative) phases. But 2-connected graphs share the following important property: their quantum statistics do not depend on the number of particles, and therefore can be regarded as a characteristic of the particle species. This property is important physically; it means that there is a building-up principle for increasing the number of particles in the system. This is described in detail in Section 2.6, where we show how to construct an n -particle Hamiltonian from a two-particle Hamiltonian. Interesting examples are also obtained by building 2-connected graphs out of higher-connected components. Figure 2.3 shows a chain of identical non-planar 3-connected components. The links between components, represented by lines in figure 2.3, consist of at least two edges, so that resulting graph is 2-connected. In this case, the quantum statistics is in fact independent of the number of particles, and may be determined by specifying exchange phases (0 or π) for each component in the chain. Thus, particles can act as bosons or fermions in different parts of the graph.

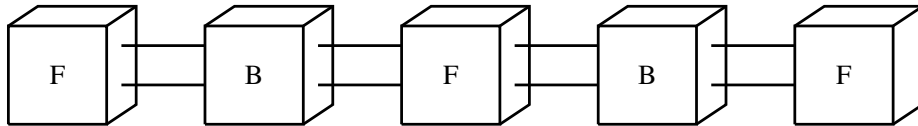


Figure 2.3: Linear chain of 3-connected nonplanar components with alternating Bose and Fermi statistics.

2.1.3 1-connected graphs

Quantum statistics on graphs achieves its full complexity for 1-connected graphs, in which case it also depends on the number of particles n . A representative example, treated in detail in Section 2.5.1, is a star graph with E edges, for which the number of anyon phases is given by

$$\beta_n^E = \binom{n + E - 2}{E - 1} (E - 2) - \binom{n + E - 2}{E - 2} + 1,$$

and therefore depends on both E and n .

2.1.4 Aharonov-Bohm phases

Configuration-space cycles on which one particle moves around a circuit C while the others remain stationary play an important role in the analysis of quantum statistics which follows. We call these Aharonov-Bohm cycles, and the corresponding phases Aharonov-Bohm phases, because they correspond physically to magnetic fluxes threading C . In many-body systems, Aharonov-Bohm phases and quantum statistics phases can interact in interesting ways. In particular, Aharonov-Bohm phases can depend on the positions of the stationary particles. An example is shown in the two-particle octahedron graph (see figure 2.4), in which the Aharonov-Bohm phase associated with one particle going around the equator depends on whether the second particle is at the north or south pole. For 3-connected non-planar graphs, it can be shown that Aharonov-Bohm phases are independent of the positions of the stationary particles. (The octahedron graph, despite appearances, is planar.)

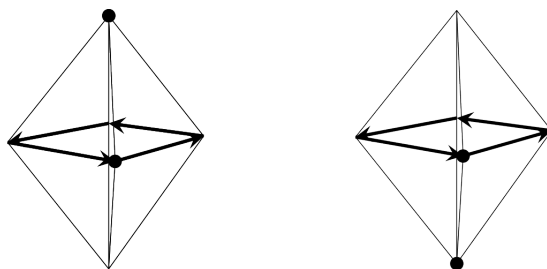


Figure 2.4: The Aharonov-Bohm phase for the equatorial cycle depends on whether the second particle is at the north or south pole.

2.2 Graph configuration spaces

In this section we repeat some definitions and theorems proved in the introduction. They will play a basic role in the current chapter. Let Γ be a metric connected simple graph with V vertices and E edges. In a metric graph edges correspond to finite closed intervals of \mathbb{R} . However, as we will be interested in the topology of the graph, the length of the edges will not play a role in the discussion. As explained in

the introduction an undirected edge between vertices v_1 and v_2 will be denoted by $v_1 \leftrightarrow v_2$. It will also be convenient to be able to label directed edges, so $v_1 \rightarrow v_2$ and $v_2 \rightarrow v_1$ will denote the directed edges associated with $v_1 \leftrightarrow v_2$. A path joining two vertices v_1 and v_m is then specified by a sequence of $m - 1$ directed edges, written $v_1 \rightarrow v_2 \rightarrow \cdots \rightarrow v_m$.

We define the n -particle configuration space as the quotient space

$$C_n(\Gamma) = (\Gamma^{\times n} - \Delta) / S_n, \quad (2.2.1)$$

where S_n is the permutation group of n elements and

$$\Delta = \{(x_1, x_2, \dots, x_n) : \exists_{i,j} x_i = x_j\}, \quad (2.2.2)$$

is the set of coincident configurations. We are interested in the calculation of the first homology group, $H_1(C_n(\Gamma))$ of $C_n(\Gamma)$. The space $C_n(\Gamma)$ is not a cell complex. However, it is homotopy equivalent to the space $\mathcal{D}^n(\Gamma)$, which is a cell complex, defined below.

Recall that a cell complex X is a nested sequence of topological spaces

$$X^0 \subseteq X^1 \subseteq \cdots \subseteq X^n, \quad (2.2.3)$$

where the X^k 's are the so-called k -skeletons defined as follows:

- The 0 - skeleton X^0 is a finite set of points.
- For $\mathbb{N} \ni k > 0$, the k - skeleton X^k is the result of attaching k - dimensional balls $B_k = \{x \in \mathbb{R}^k : \|x\| \leq 1\}$ to X^{k-1} by gluing maps

$$\sigma : S^{k-1} \rightarrow X^{k-1}, \quad (2.2.4)$$

where S^{k-1} is the unit-sphere $S^{k-1} = \{x \in \mathbb{R}^k : \|x\| = 1\}$.

A k -cell is the interior of the ball B_k attached to the $(k - 1)$ -skeleton X^{k-1} .

Every simple graph Γ is naturally a cell complex; the vertices are 0-cells (points) and edges are 1-cells (1-dimensional balls whose boundaries are the 0-cells). The product $\Gamma^{\times n}$ then naturally inherits a cell complex structure. The cells of $\Gamma^{\times n}$ are

Cartesian products of cells of Γ . It is clear that the space $C_n(\Gamma)$ is not a cell complex as points belonging to Δ have been deleted. Following [1] we define an *n-particle combinatorial configuration space* as

$$\mathcal{D}^n(\Gamma) = (\Gamma^{\times n} - \tilde{\Delta})/S_n, \quad (2.2.5)$$

where $\tilde{\Delta}$ denotes all cells whose closure intersects with Δ . The space $\mathcal{D}^n(\Gamma)$ possesses a natural cell complex structure. Moreover,

Theorem 2.2.1. [1] *For any graph Γ with at least n vertices, the inclusion $\mathcal{D}^n(\Gamma) \hookrightarrow C_n(\Gamma)$ is a homotopy equivalence iff the following hold:*

1. *Each path between distinct vertices of valence not equal to two passes through at least $n - 1$ edges.*
2. *Each closed path in Γ passes through at least $n + 1$ edges.*

Following [1, 19] we refer to a graph Γ with properties 1 and 2 as *sufficiently subdivided*. For $n = 2$ these conditions are automatically satisfied (provided Γ is simple). Intuitively, they can be understood as follows:

1. In order to have homotopy equivalence between $\mathcal{D}^n(\Gamma)$ and $C_n(\Gamma)$, we need to be able to accommodate n particles on every edge of graph Γ . This is done by introducing $n - 2$ trivial vertices of degree 2 to make a line subgraph between every adjacent pair of non-trivial vertices in the original graph Γ .
2. For every cycle there is at least one free (not occupied) vertex which enables the exchange of particles around this cycle.

For a sufficiently subdivided graph Γ we can now effectively treat Γ as a combinatorial graph where particles are accommodated at vertices and hop between adjacent unoccupied vertices along edges of Γ . See Figure 2.6 for a comparison of the configuration spaces $C_2(\Gamma)$ and $\mathcal{D}^2(\Gamma)$ of a Y-graph.

Using Theorem 2.2.1, the problem of finding $H_1(C_n(\Gamma))$ is reduced to the problem of computing $H_1(\mathcal{D}^n(\Gamma))$. In the next sections we show how to determine

$H_1(\mathcal{D}^n(\Gamma))$ for an arbitrary simple graph Γ . Note, however, that by the structure theorem for finitely generated modules [38]

$$H_1(\mathcal{D}^n(\Gamma)) = \mathbb{Z}^k \oplus T_l \quad (2.2.6)$$

where T_l is the torsion, i.e.

$$T_l = \mathbb{Z}_{n_1} \oplus \dots \oplus \mathbb{Z}_{n_l}, \quad (2.2.7)$$

and $n_i | n_{i+1}$. In other words $H_1(\mathcal{D}^n(\Gamma))$ is determined by k free parameters $\{\phi_1, \dots, \phi_k\}$ and l discrete parameters $\{\psi_1, \dots, \psi_l\}$ such that for each $i \in \{1, \dots, l\}$

$$n_i \psi_i = 0 \pmod{2\pi}, \quad n_i \in \mathbb{N} \quad \text{and} \quad n_i | n_{i+1}. \quad (2.2.8)$$

Taking into account their physical interpretation we will call the parameters ϕ and ψ continuous and discrete phases respectively.

2.3 Two-particle quantum statistics

In this section we fully describe the first homology group $H_1(\mathcal{D}^2(\Gamma))$ for an arbitrary connected simple graph Γ . We start with three simple examples: a cycle, a Y-graph and a lasso. The 2-particle discrete configuration space of the lasso reveals an important relation between the exchange phase on the Y-graph and on the cycle. Combining this relation with an ansatz for a perhaps over-complete spanning set of the cycle space of $\mathcal{D}^2(\Gamma)$ and some combinatorial properties of k -connected graphs, we give a formula for $H_1(\mathcal{D}^2(\Gamma))$. Our argument is divided into three parts; corresponding to 3-, 2- and 1-connected graphs respectively.

Three examples

- Let Γ be a triangle graph shown in figure 2.5(a). Its combinatorial configuration space $\mathcal{D}^2(\Gamma)$ is shown in figure 1(b). The cycle $(1, 2) \rightarrow (1, 3) \rightarrow$



Figure 2.5: (a) The triangle graph Γ (b) The 2-particle configuration space $\mathcal{D}^2(\Gamma)$.

$(2, 3) \rightarrow (1, 2)$ is not contractible and hence $H_1(\mathcal{D}^2(\Gamma)) = \mathbb{Z}$. In other words we have one free phase ϕ_c and no torsion.

- Let Γ be a Y-graph shown in figure 2.6(a). Its combinatorial configuration space $\mathcal{D}^2(\Gamma)$ is shown in figure 2.6(b). The cycle $(1, 2) \rightarrow (1, 3) \rightarrow (2, 3) \rightarrow (3, 4) \rightarrow (2, 4) \rightarrow (1, 4) \rightarrow (1, 2)$ is not contractible and $H_1(\mathcal{D}^2(\Gamma)) = \mathbb{Z}$. Hence we have one free phase ϕ_Y and no torsion. For comparison the configuration space $C_2(\Gamma)$ is shown in figure 2.6(c). Contracting the triangular planes onto the hexagon and then contracting the surface of the hexagon to the boundary (expanding the empty vertex in the center) one obtains the combinatorial configuration space shown in figure 2.6(b).
- Let Γ be a lasso graph shown in figure 2.7(a). It is a combination of Y and triangle graphs. Its combinatorial configuration space $\mathcal{D}^2(\Gamma)$ is shown in figure 3(b). The shaded rectangle is a 2-cell and hence the cycle $(1, 3) \rightarrow (2, 3) \rightarrow (2, 4) \rightarrow (1, 4) \rightarrow (1, 3)$ is contractible. The cycle $(1, 2) \rightarrow (1, 4) \rightarrow (1, 3) \rightarrow (1, 2)$ corresponds to the situation when one particle is sitting at the vertex 1 and the other moves along the cycle $c = 2 \rightarrow 4 \rightarrow 3 \rightarrow 2$ of Γ . We will call this cycle an Aharonov-Bohm cycle (AB-cycle) and denote its phase $\phi_{c,1}^1$ (the subscript $c, 1$ indicates that c is traversed by just 1 particle, and the superscript 1 indicates the position of the stationary particle). The cycle $(2, 3) \rightarrow (3, 4) \rightarrow (2, 4) \rightarrow (2, 3)$ represents the exchange of two particles around c . The corresponding phase will be denoted by $\phi_{c,2}$. Finally, for the cycle $(1, 2) \rightarrow (1, 3) \rightarrow (2, 3) \rightarrow (3, 4) \rightarrow (2, 4) \rightarrow (1, 4) \rightarrow (1, 2)$, corre-

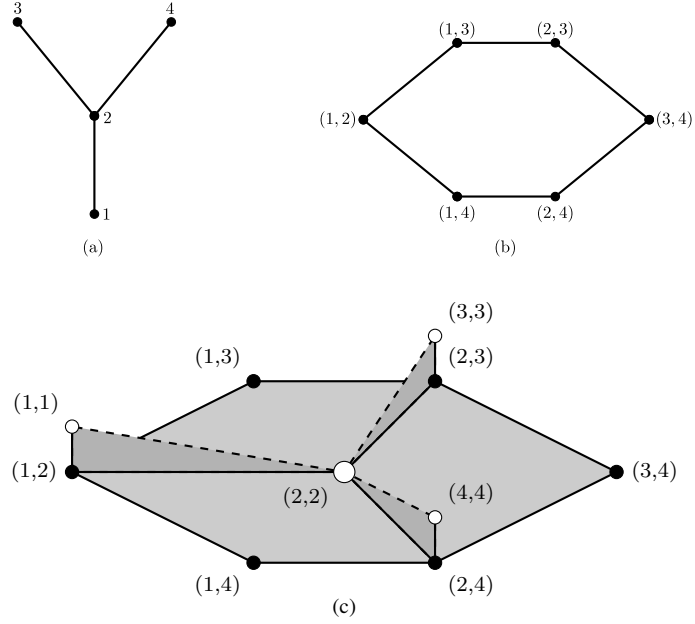


Figure 2.6: (a) The Y-graph Γ . (b) The 2-particle combinatorial configuration space $\mathcal{D}^2(\Gamma)$. (c) The 2-particle configuration space $C_2(\Gamma)$; dashed lines and open vertices denote configurations where the particles are coincident. Such configurations are excluded from $C_2(\Gamma)$.

sponding to exchange of two particles along a Y-graph, the phase is denoted ϕ_Y . There is no torsion in $H_1(\mathcal{D}^2(\Gamma))$. Moreover,

$$\phi_{c,2} = \phi_{c,1}^1 + \phi_Y. \quad (2.3.1)$$

Thus, the Y-phase ϕ_Y and the AB-phase $\phi_{c,1}^1$ determine $\phi_{c,2}$.

Remark 2.3.1. Any relation between cycles on a graph G holds between the corresponding cycles on a graph F containing G as a subgraph or a subgraph homotopic to G . It is for this reason that (2.3.1) will play a key role in relating Y-phases and AB-phases for general graphs.

2.3.1 A spanning set of $H_1(\mathcal{D}^2(\Gamma))$

In order to proceed with the calculation of $H_1(\mathcal{D}^2(\Gamma))$ for arbitrary Γ we need a spanning set of $H_1(\mathcal{D}^2(\Gamma))$. Before we give one, let us discuss the dependence of

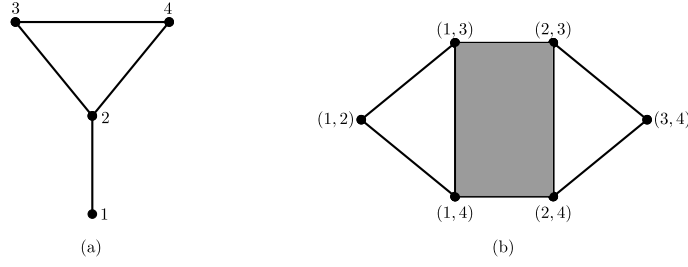


Figure 2.7: (a) The lasso graph Γ (b) The 2-particle configuration space $\mathcal{D}^2(\Gamma)$.

the AB-phase on the position of the second particle. Suppose there is a cycle c in Γ with two vertices v_1 and v_2 not on the cycle. We want to know the relation between $\phi_{c,1}^{v_1}$ and $\phi_{c,1}^{v_2}$. There are two possibilities to consider. The first is shown in figure 2.8(a) and represents the situation when there is a path P_{v_1,v_2} which joins v_1 and v_2 and is disjoint with c . In this case both AB-cycles are homotopy equivalent as they belong to the cylinder $c \times P_{v_1,v_2}$. Therefore,

Fact 1. *Assume there is a cycle c in Γ with two vertices v_1 and v_2 not on the cycle. Suppose there is a path P_{v_1,v_2} which joins v_1 and v_2 and is disjoint with c . Then $\phi_{c,1}^{v_1} = \phi_{c,1}^{v_2}$.*

Assume now that every path joining v_1 and v_2 passes through the cycle c (see figure 2.8(b)). Noting that the graph contains two subgraphs homotopic to the lasso which in turn both contain c , and making use of Remark 2.3.1, we can repeat the argument leading to relation (2.3.1) for each lasso. We obtain,

$$\phi_{c,2} = \phi_{c,1}^{v_1} + \phi_{Y_1}, \quad \phi_{c,2} = \phi_{c,1}^{v_2} + \phi_{Y_2}, \quad (2.3.2)$$

and hence

$$\phi_{c,1}^{v_1} - \phi_{c,1}^{v_2} = \phi_{Y_2} - \phi_{Y_1}. \quad (2.3.3)$$

Thus, for a fixed one-particle cycle c in Γ , the difference between any two AB-phases (corresponding to two different positions of the stationary particle) may be expressed in terms of the Y-phases.

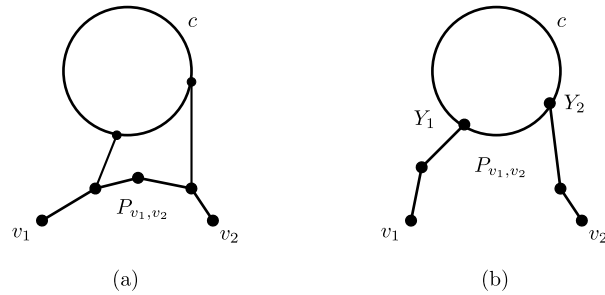


Figure 2.8: The dependence of the AB-phase for cycle c on the position of the second particle when (a) there is a path between v_1 and v_2 disjoint with c , (b) every path joining v_1 and v_2 passes through c .

As we show in section 2.7, a spanning set of $H_1(\mathcal{D}^2(\Gamma))$ is given by all Y and AB-cycles. Note that from relations (2.3.1) and (2.3.3), we can restrict the set of AB-cycles to belong to a basis for $H_1(\Gamma)$ (since all other AB-cycles can be expressed in terms of these and Y-cycles). By Euler's formula, the dimension of $H_1(\Gamma)$ is given by the first Betti number,

$$\beta_1(\Gamma) = E - V + 1, \quad (2.3.4)$$

As a result, we will use a spanning set (which in general is over-complete) containing the following:

1. All 2-particle cycles corresponding to the exchanges on Y subgraphs of Γ .
There may be relations between these cycles.
2. A set of $\beta_1(\Gamma)$ AB-cycles, one for each independent cycle in a basis for $H_1(\Gamma)$.

Thus, $H_1(\mathcal{D}^2(\Gamma)) = \mathbb{Z}^{\beta_1(\Gamma)} \oplus A$, where A is determined by Y-cycles. Consequently, in order to determine $H_1(\mathcal{D}^2(\Gamma))$ one has to study the relations between Y-cycles.

2.3.2 3-connected graphs

In this section we determine $H_1(\mathcal{D}^2(\Gamma))$ for 3-connected graphs. Let Γ be a connected graph. We define an m -separation of Γ [45], where m is a positive integer, as an ordered pair (Γ_1, Γ_2) of subgraphs of Γ such that

1. The union $\Gamma_1 \cup \Gamma_2 = \Gamma$.
2. Γ_1 and Γ_2 are edge-disjoint and have exactly m common vertices, $V_m = \{v_1, \dots, v_m\}$.
3. Γ_1 and Γ_2 have each a vertex not belonging to the other.

It is customary to say that the V_m separates vertices of Γ_1 and Γ_2 different from V_m .

Definition 2.3.2. *A connected graph Γ is n -connected iff it has no m -separation for any $m < n$.*

The following theorem of Menger [45] gives an additional insight into graph connectivity:

Theorem 2.3.3. *For an n -connected graph Γ there are at least n internally disjoint paths between any pair of vertices.*

The basic example of 3-connected graphs are wheel graphs. A wheel graph W^n of order n consists of a cycle with n vertices and a single additional vertex which is connected to each vertex of the cycle by an edge. Following Tutte [45] we denote the middle vertex by h and call it the hub, and the cycle that does not include h by R and call it the rim. The edges connecting the hub to the rim will be called spokes. The importance of wheels in the theory of 3-connected graphs follows from the following theorem:

Theorem 2.3.4. *(Wheel theorem [45]) Let Γ be a simple 3-connected graph different from a wheel. Then for some edge $e \in E(\Gamma)$, either $\Gamma \setminus e$ or Γ/e is simple and 3-connected.*

Here $\Gamma \setminus e$ is constructed from Γ by removing the edge e , and Γ/e is obtained by contracting edge e and identifying its vertices. These two operations will be called edge removal and edge contraction. The inverses will be called edge addition and vertex expansion. Note that vertex expansion requires specifying which edges are connected to which vertices after expansion. As we deal with 3-connected graphs

we will apply the vertex expansion only to vertices of degree at least four and split the edges between new vertices in a such way that they are at least 3-valent.

As a direct corollary of Theorem 2.3.4 any simple 3-connected graph can be constructed in a finite number of steps starting from a wheel graph W^k , for some k ; that is, there exists a sequence of simple 3-connected graphs

$$W_k = \Gamma_0 \mapsto \Gamma_1 \mapsto \dots \mapsto \Gamma_{n-1} \mapsto \Gamma_n = \Gamma,$$

where Γ_i is constructed from Γ_{i-1} by either

1. adding an edge between non-adjacent vertices, or
2. expanding at a vertex of valency at least four.

Therefore, in order to prove inductively some property of a 3-connected graph, it is enough to show that the property holds for an arbitrary wheel graph and that it persists under operations 1. and 2. above.

Lemma 2.3.5. *For wheel graphs W^n all phases ϕ_Y are equal up to a sign.*

Proof. The Y subgraphs of W^n can be divided into two groups: (i) the center vertex of Y is on the rim, and (ii) the center vertex of Y is the hub. For (i) let v_1 and v_2 be two adjacent vertices belonging to the rim, R . Let Y_{v_1} and Y_{v_2} be the corresponding Y-graphs whose central vertices are v_1 and v_2 respectively. Evidently, the two edges of Y_{v_1} and Y_{v_2} which are spokes belong to the same triangle cycle, C , i.e the cycle with vertices v_1 , v_2 and h (see figure 2.9(a)). Moreover, b_1 is connected to b_2 by a path which is disjoint with C . Using Fact 2, we have that $\phi_{c,1}^{b_1} = \phi_{c,1}^{b_2}$. From this and relation (2.3.3), it follows that $\phi_{Y_{v_1}} = \phi_{Y_{v_2}}$. Repeating this reasoning we obtain that all $\phi_{Y_{v_i}}$, with v_i belonging to the rim are equal (perhaps up to a sign). We are left with the Y-graphs whose central vertex is the hub. Similarly (see figure 2.9(b)) we take a cycle, C , with two edges belonging to the chosen Y. Then there is always a Y-graph with two edges belonging to C and center on the rim. Therefore, by Fact 2 and relation (2.3.3) the phase on a Y subgraph whose center vertex is the hub is the same as on the Y subgraphs whose center vertex is on the rim. \square

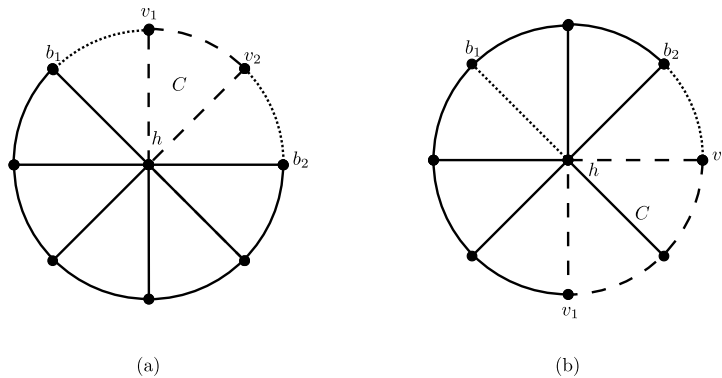


Figure 2.9: Wheel graphs. (a) Dashed lines denote a pair of Y subgraphs Y_{v_1} and Y_{v_2} centered at adjacent vertices v_1 and v_2 on the rim. The three shared edges of the Y subgraphs (long dashes) form a cycle C . (b) The Y subgraph Y_h (edges are dashed) has three outer vertices b_1 , v_1 and v_2 . Two of the edges of Y_h together with a path on the rim joining v_1 and v_2 form a cycle C (long dashes). A second Y-graph Y_{v_2} (edges are dashed) shares two edges of C .

Lemma 2.3.6. *For 3-connected simple graphs all phases ϕ_Y are equal up to a sign.*

Proof. We prove by induction. By Lemma 1 the statement is true for all wheel graphs.

1. Adding an edge: Assume that v_1 and v_2 are non-adjacent vertices of the 3-connected graph Γ . Suppose that the relations on Γ determine that all its ϕ_Y phases are equal (up to a sign). These relations remain if we add an edge e between the vertices v_1 and v_2 . Therefore, on $\Gamma \cup e$, the phases ϕ_Y belonging to Γ must still be equal.

However, the graph $\Gamma \cup e$ contains new Y-graphs, whose central vertices are v_1 or v_2 and one of the edges is e . We need to show that the phase ϕ_Y on these new Y's is the same as on the old ones. Let $\{e, f_1, f_2\}$ be such a Y-graph (see figure 2.10(a)). Let α_1 and α_2 be endpoints of f_1 and f_2 . By 3-connectedness, there is a path between α_1 and α_2 which does not contain v_1 or v_2 . In this way we obtain a cycle C , as shown in figure 2.10(a). Again by 3-connectedness, there is a path P from v_2 to a vertex β in C which does not contain α_1 and α_2 . Let Y' be the Y-graph

with β as its center and edges along C and P , as shown in figure 2.10(a). Then Y' belongs to Γ . Applying Fact 2 and relation (2.3.3) (cf. the proof of Lemma 1) to the cycle C and the two Y-graphs discussed, the result follows.

2. Vertex expansion: Let Γ be a 3-connected simple graph and let v be a vertex of degree at least four. Let $\tilde{\Gamma}$ be a graph derived from Γ by expanding at the vertex v , and assume that the new vertices, v_1 and v_2 , are at least 3-valent. These assumptions are necessary for $\tilde{\Gamma}$ to be 3-connected [45]. Note that Γ and $\tilde{\Gamma}$ have the same number of independent cycles. Moreover, by splitting at the vertex v we do not change the relations between the ϕ_Y phases of Γ . This is simply because if the equality of some of the ϕ_Y phases required a cycle passing through v , one can now use the cycle with one more edge passing through v_1 and v_2 in $\tilde{\Gamma}$. The graph $\tilde{\Gamma}$ contains new Y-graphs, whose central vertices are v_1 or v_2 and one of the edges is $e = v_1 \leftrightarrow v_2$. We need to show that the phase ϕ_Y on these new Ys is the same as on the old ones. Let $\{e, f_1, f_2\}$ be such a graph and let α_1 and α_2 be endpoints of f_1 and f_2 . By 3-connectedness, there is a path between α_1 and α_2 which does not contain v_1 or v_2 . In this way we obtain a cycle C , as shown in figure 2.10(b). Again by 3-connectedness, there is a path P from v_2 to a vertex β in C which does not contain α_1 and α_2 . Let Y' be the Y-graph with β as its center and edges along C and P , as shown in figure 2.10(b). Then Y' belongs to Γ . Applying Fact 2 and relation (2.3.3) to the cycle C and the two Y-graphs discussed, the result follows. \square

Theorem 2.3.7. *For a 3-connected simple graph, $H_1(\mathcal{D}^2(\Gamma)) = \mathbb{Z}^{\beta_1(\Gamma)} \oplus A$, where $A = \mathbb{Z}_2$ for non-planar graphs and $A = \mathbb{Z}$ for planar graphs.*

Proof. By Lemmas 1 and 2 we only need to determine the phase ϕ_Y . Using the construction in [26], it can be shown by elementary calculations that for the graphs K_5 and $K_{3,3}$, $H_1(\mathcal{D}^2(\Gamma)) = \mathbb{Z}^{\beta_1(\Gamma)} \oplus \mathbb{Z}_2$ (shorter calculations using discrete Morse theory are given in [30]). Therefore the phase $\phi_Y = 0$ or π . By Kuratowski's theorem [33] every non-planar graph contains a subgraph which is isomorphic to K_5 or $K_{3,3}$. This proves the statement for non-planar graphs.

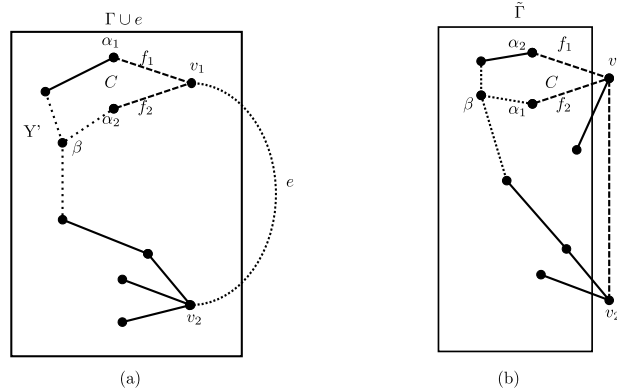


Figure 2.10: (a) Adding an edge (b) Expanding at the vertex.

If Γ is planar, then any phase ϕ_Y can be realised. This can be demonstrated explicitly by appealing to the well-known anyon gauge potential for two particles in the plane,

$$\mathbf{A}(\mathbf{r}) = \frac{\alpha}{2\pi} \hat{\mathbf{z}} \times \frac{\mathbf{r}}{|\mathbf{r}|^2}.$$

The line integral of the one-form

$$\omega = \mathbf{A}(\mathbf{r}_2 - \mathbf{r}_1) \cdot d\mathbf{r}_1 + \mathbf{A}(\mathbf{r}_1 - \mathbf{r}_2) \cdot d\mathbf{r}_2$$

around a primitive cycle in which the two particles are exchanged yields the anyon phase α . If Γ is drawn in the plane and each edge of $\mathcal{D}^2(\Gamma)$ is assigned the phase given by the line integral of ω , then the phase associated with exchanging the particles on a Y -subgraph is given by α .

□

For a given cycle on a 3-connected graph, it follows from Theorem 2.3.7 and relation (2.3.3) that the difference between AB-phases (corresponding to different positions of the stationary particle) is either 0 or $2\phi_Y$. If the graph is nonplanar, we have that $2\phi_Y = 0 \pmod{2\pi}$, so that the AB-phases are independent of the position of stationary particle.

2.3.3 2-connected graphs

In this subsection we discuss 2-connected graphs. First, by considering a simple example we show that in contrast to 3-connected graphs it is possible to have more than one ϕ_Y phase. Using a decomposition procedure of a 2-connected graph into 3-connected graphs and topological cycles we provide the formula for $H_1(\mathcal{D}^2(\Gamma))$.

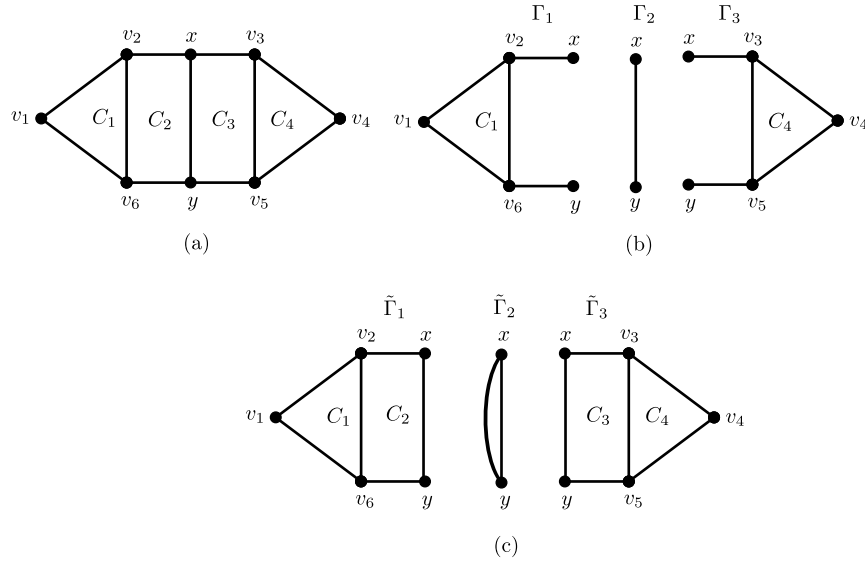


Figure 2.11: (a) An example of a 2-connected graph, (b) the components of the 2-cut $\{x, y\}$, (c) the marked components.

Example 2.3.8. Let us consider graph Γ shown in figure 2.11(a). Since vertices v_1 and v_4 are 2-valent, Γ is not 3-connected. It is however 2-connected. Note that $\beta_1(\Gamma) = 4$ and that there are six Y -graphs, with central vertices v_2, v_3, v_5, v_6, x and y respectively. Using Fact 2 and relation (2.3.3) we verify that

$$\phi_{Y_{v_2}} = \phi_{Y_{v_6}}, \quad \phi_{Y_{v_3}} = \phi_{Y_{v_5}}, \quad \phi_{Y_x} = \phi_{Y_y}. \quad (2.3.5)$$

One can also show that the phases $\phi_{Y_{v_2}}, \phi_{Y_{v_3}}$ and ϕ_{Y_x} are independent.

(For completeness, we give an explicit argument, showing that each one of the phases $\phi_{Y_{v_2}}, \phi_{Y_{v_3}}, \phi_{Y_x}$ can be made to be nonzero while the other two are made to be zero. Following the procedure of [26], we can assign an arbitrary phase α to

the edge $(v_4, v_5) \leftrightarrow (v_3, v_4)$ of $\mathcal{D}^2(\Gamma)$, and zero phase to all its other edges. This is because $(v_4, v_5) \leftrightarrow (v_3, v_4)$ does not belong to a contractible square in $\mathcal{D}^2(\Gamma)$ (no edge of Γ disjoint from $v_3 \leftrightarrow v_5$ has v_4 as a vertex). Since $(v_4, v_5) \leftrightarrow (v_3, v_4)$ uses the edge $v_3 \leftrightarrow v_5$ in Γ , which belongs to Y_{v_3} but not to Y_x or Y_{v_2} , the phase $\phi_{Y_{v_3}}$ associated with particle exchange on Y_{v_3} is given by α (up to a sign) while $\phi_{Y_{v_2}} = \phi_{Y_y} = 0$. A similar argument, based on the fact that the edge $(v_1, v_2) \leftrightarrow (v_1, v_6)$ also does not belong to a contractible square in $\mathcal{D}^2(\Gamma)$, leads to an assignment of phases with $\phi_{Y_{v_2}}$ arbitrary, $\phi_{Y_{v_3}} = \phi_{Y_y} = 0$. Finally, one can assign edge phases in $\mathcal{D}^2(\Gamma)$ so that ϕ_{Y_y} is arbitrary. Adjusting the phases of the edges $(v_4, v_5) \leftrightarrow (v_3, v_4)$ and $(v_1, v_2) \leftrightarrow (v_1, v_6)$ so that $\phi_{Y_{v_2}} = \phi_{Y_{v_3}} = 0$ (which doesn't affect ϕ_{Y_x}), we obtain an assignment of phases with ϕ_{Y_x} arbitrary and $\phi_{Y_{v_3}} = \phi_{Y_{v_2}} = 0$. Thus, $\phi_{Y_{v_2}}$, $\phi_{Y_{v_3}}$ and ϕ_{Y_x} are linearly independent.)

Therefore we have three independent ϕ_Y phases and four AB-phases, and so

$$H_1(\mathcal{D}^2(\Gamma)) = \mathbb{Z}^7. \quad (2.3.6)$$

Vertices $\{x, y\}$ constitute a 2-vertex cut of Γ , i.e. after their deletion Γ splits into three connected components $\Gamma_1, \Gamma_2, \Gamma_3$ (see figure 2.11(b)). They are no longer 2-connected. Moreover, for example, the two Y-subgraphs Y_{v_2} and Y_{v_6} for which $\phi_{Y_{v_2}} = \phi_{Y_{v_6}}$ in Γ no longer satisfy this condition in Γ_1 , i.e. $\phi_{Y_{v_2}} \neq \phi_{Y_{v_6}}$ in Γ_1 . This is because the AB-phases $\phi_{C_{1,1}}^x$ and $\phi_{C_{1,1}}^y$ are not necessarily equal. (This can be readily seen by constructing the two-particle configuration space $\mathcal{D}^2(\Gamma_1)$, an extension of the lasso in Figure 2.7(b), and recognising that the corresponding AB cycles are independent.)

To make components Γ_i 2-connected and at the same time keep the correct relations between the $\phi_{Y_{v_i}}$'s, it is enough to add to each component Γ_i an additional edge between vertices x and y (see figure 2.11(c)). The resulting graphs, which we call the marked components and denote by $\tilde{\Gamma}_i$ [30], are 2-connected. Moreover, the relations between the Y-graphs in each $\tilde{\Gamma}_i$ are the same as in Γ . The union of the three marked components has, however, $\beta_1(\Gamma) + 1$ independent cycles. On the other hand, by splitting Γ into marked components, the Y-cycles Y_x and Y_y have

been lost. Since $\phi_{Y_x} = \phi_{Y_y}$ we have lost one ϕ_Y phase. Summing up we can write $H_1(\mathcal{D}^2(\Gamma)) \oplus \mathbb{Z} = \left[\bigoplus_{i=1}^3 H_1(\mathcal{D}^2(\tilde{\Gamma}_i)) \right] \oplus \mathbb{Z}$.

2-vertex cut for an arbitrary 2-connected graph Γ In figure 2.12(a) a more general 2-vertex cut is shown together with components Γ_i red (note that Γ_i consists of an interior γ_i , the edges connecting γ_i to vertices x and y , and x and y themselves). It is easy to see that the marked components $\tilde{\Gamma}_i$ are 2-connected and the relations between the ϕ_Y phases in each $\tilde{\Gamma}_i$ are the same as in Γ . Let $\mu(x, y)$ be the number of $\tilde{\Gamma}_i$ components into which Γ splits after removal of vertices x and y . By Euler's formula the union $\{\tilde{\Gamma}_i\}_{i=1}^{\mu(x, y)}$ of $\mu(x, y)$ marked components has

$$\begin{aligned} \beta &= \#\text{edges} - \#\text{vertices} + \mu(x, y) \\ &= E(\Gamma) + \mu(x, y) - (V(\Gamma) + 2(\mu(x, y) - 1)) + \mu(x, y) \\ &= E(\Gamma) - V(\Gamma) + 2 = \beta_1(\Gamma) + 1, \end{aligned} \tag{2.3.7}$$

independent cycles. By splitting Γ into the marked components we possibly lose ϕ_Y phases corresponding to the Y-graphs with the central vertex x or y . However

1. If three edges of a Y-graph are connected to the same component we do not lose ϕ_Y .
2. If two edges of a Y-graph are connected to the same component, we do not lose ϕ_Y . The argument is as follows, referring to Figure 2.12(b): Let Y_x denote a Y-graph centered at x with vertices u and v in the interior γ_2 of the component Γ_2 . Since γ_2 is 1-connected, there is a path P in γ_2 from u to v (short dashes in Figure 2.12(b)). Together with the edges from x to u and v , P forms a cycle C in Γ_2 containing two edges of Y_x . In addition, there is a path Q in Γ_2 from u to y . Let w denote the last vertex on Q which belongs to C (w might coincide with u or v , but need not). Let Y_w denote the Y-graph centred at w with two edges along C and one edge along Q . Then Y_w is contained in Γ_2 , and by relation (2.3.3), $\phi_{Y_x} = \phi_{Y_w}$. Therefore, ϕ_{Y_x} is not lost under splitting.

Hence the ϕ_Y phases we lose correspond to the Y-graphs for which each edge is connected to a different component. First we want to show that any two Y-graphs with the central vertex x (or y) whose edges are connected to three fixed components have the same phase. It is enough to show this for Y-graphs which share the same center and two edges. Let us consider two such Y-graphs (see figure 2.12(c) – the dashed edges are common to both Y-graphs; the distinct edges are dotted and dotted-dashed). Let a_1, a_2 and b_1, b_2 be the endpoints of the two shared edges, and α_1, α_2 the endpoints of the two distinct edges. As the γ_i 's are connected, there are paths $P_{a_1, a_2}, P_{b_1, b_2}$ and P_{α_1, α_2} in γ_1, γ_3 and γ_2 respectively. Therefore, we can apply Fact 2 and relation (2.3.3) to the cycle $x \rightarrow a_1 \cup P_{a_1, a_2} \cup a_2 \rightarrow y \rightarrow b_2 \cup P_{b_1, b_2} \cup b_1 \rightarrow x$ and the two considered Y-graphs to conclude that their ϕ_Y phases are the same. Therefore, for each choice of three distinct components, there is just one ϕ_Y phase. Moreover, for a given choice of distinct components, the phase for the Y-graph with central vertex x is the same as for the Y-graph with central vertex y (see figure 2.12(d) where the considered Y-graphs are denoted by dashed and dotted lines). This is once again due to Fact 2 and relation (2.3.3) applied to the cycle $x \rightarrow a_1 \cup P_{a_1, a_2} \cup a_2 \rightarrow y \rightarrow \alpha_2 \cup P_{\alpha_1, \alpha_2} \cup \alpha_1 \rightarrow x$ and the two considered Y-graphs.

Summing up, the number of phases we lose when splitting Γ into $\mu(x, y)$ marked components, $N_2(x, y)$, is equal to the number of independent Y-graphs in the star graph with $\mu(x, y)$ edges. This can be calculated (see for example [26]) to be $N_2(x, y) = \frac{1}{2} (\mu(x, y) - 2) (\mu(x, y) - 1)$. Hence

$$H_1(\mathcal{D}^2(\Gamma)) = \left[\bigoplus_{i=1}^{\mu(x, y)} H_1(\mathcal{D}^2(\tilde{\Gamma}_i)) \right] \oplus \mathbb{Z}^{N_2(x, y) - 1}. \quad (2.3.8)$$

Note that the -1 in the exponent here is to get rid of the additional AB-phase stemming from the calculation (2.3.7). Also, it is straightforward to see that although introducing an additional edge to a marked component may give rise to a new Y-graph, the associated Y-phase is not new, and is equal to a Y-phase of Y-graph inside the component. Finally, it is known in graph theory that by the repeated application of the above decomposition procedure the resulting marked components are either topological cycles or 3-connected graphs [45]. Let n be the number of 2-

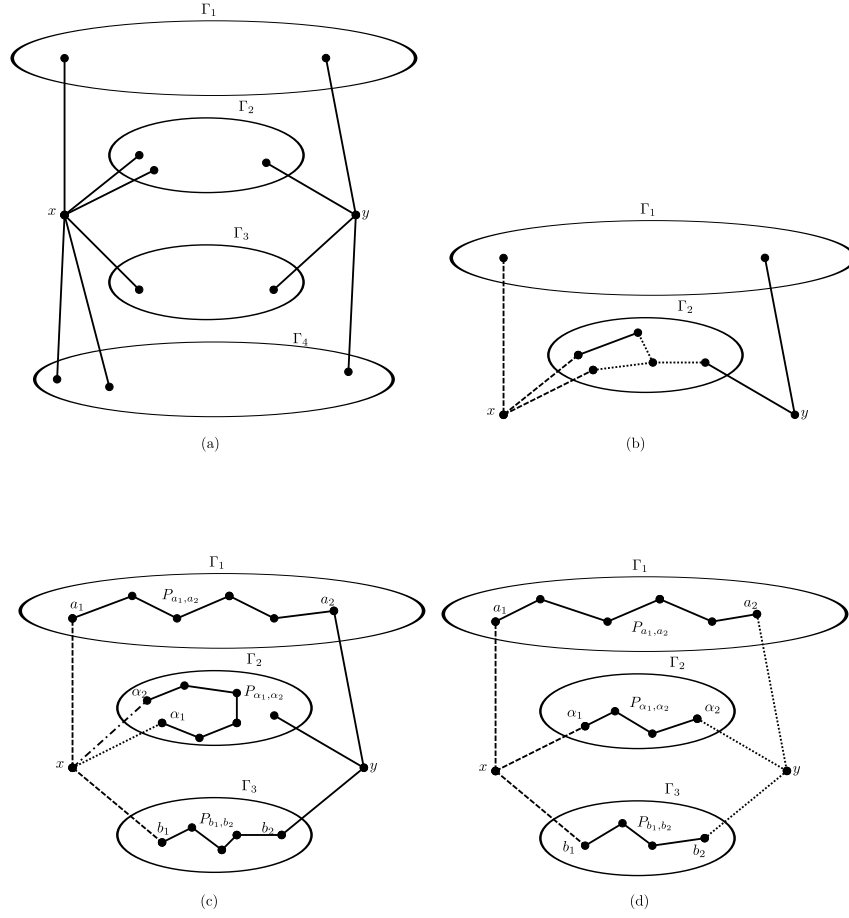


Figure 2.12: (a) 2-vertex cut of Γ . The γ_i 's are the interiors of the connected components Γ_i . (b) Y_x with two edges connected to γ_2 (c) two Y-cycles with three edges in three different components (d) the equality of ϕ_{Y_x} and ϕ_{Y_y} .

vertex cuts which is needed to get such a decomposition, $N_2 = \sum_{\{x_i, y_i\}} N_2(x_i, y_i)$, N_3 the number of planar 3-connected components, N'_3 the number of non-planar 3-connected components and N''_3 the number of the topological cycles. Let $\mu = N_3 + N'_3 + N''_3$. Then

$$H_1(\mathcal{D}^2(\Gamma)) = \left[\bigoplus_{i=1}^{\mu} H_1(\mathcal{D}^2(\tilde{\Gamma}_i)) \right] \oplus \mathbb{Z}^{N_2-n}, \quad (2.3.9)$$

where

$$\begin{aligned}
 H_1(\mathcal{D}^2(\tilde{\Gamma}_i)) &= \mathbb{Z}^{\beta_1(\tilde{\Gamma}_i)} \oplus \mathbb{Z}, \quad \tilde{\Gamma}_i - \text{planar} & (2.3.10) \\
 H_1(\mathcal{D}^2(\tilde{\Gamma}_i)) &= \mathbb{Z}^{\beta_1(\tilde{\Gamma}_i)} \oplus \mathbb{Z}_2, \quad \tilde{\Gamma}_i - \text{nonplanar} \\
 H_1(\mathcal{D}^2(\tilde{\Gamma}_i)) &= \mathbb{Z}, \quad \tilde{\Gamma}_i - \text{topological cycle}
 \end{aligned}$$

Note that $\sum_i \beta_1(\tilde{\Gamma}_i) + N_3'' = \beta_1(\Gamma) + n$ and therefore

$$H_1(\mathcal{D}^2(\Gamma)) = \mathbb{Z}^{\beta_1(\Gamma) + N_2 + N_3} \oplus \mathbb{Z}_2^{N_3'}.$$
 (2.3.11)

2.3.4 1-connected graphs

In this subsection we focus on 1-connected graphs. Assume that Γ is 1-connected but not 2-connected. There exists a vertex $v \in V(\Gamma)$ such that after its deletion Γ splits into at least two connected components. Denote these components by $\Gamma_1, \dots, \Gamma_{\mu(v)}$. It is to be understood that each component Γ_i contains the edges which connect it to v , along with a copy of the vertex v itself. Let E_i denote the number of edges at v which belong to Γ_i . By Euler's formula the union of components $\{\Gamma_i\}_{i=1}^{\mu(v)}$ has

$$E(\Gamma) - (V(\Gamma) + \mu(v) - 1) + \mu(v) = \beta_1(\Gamma)$$
 (2.3.12)

independent cycles, hence the number of independent cycles does not change compared to Γ . Moreover, the phases ϕ_Y inside each of the components are the same as in Γ . Note, however, that by splitting we lose Y-graphs whose three edges do not belong to one fixed component Γ_i . Consequently, there are two cases to consider:

1. Two edges of the Y-graph are attached to one component, for example $\Gamma_{v,3}$, while the third one is attached to another component, $\Gamma_{v,1}$. We claim that the phase ϕ_Y does not depend on the choice of the third edge, provided it is attached to $\Gamma_{v,1}$. To see this consider two Y-graphs, Y_1 and Y_2 shown in figure 2.13(a). Since vertices α_1 and α_2 are connected by a path, by Fact 2

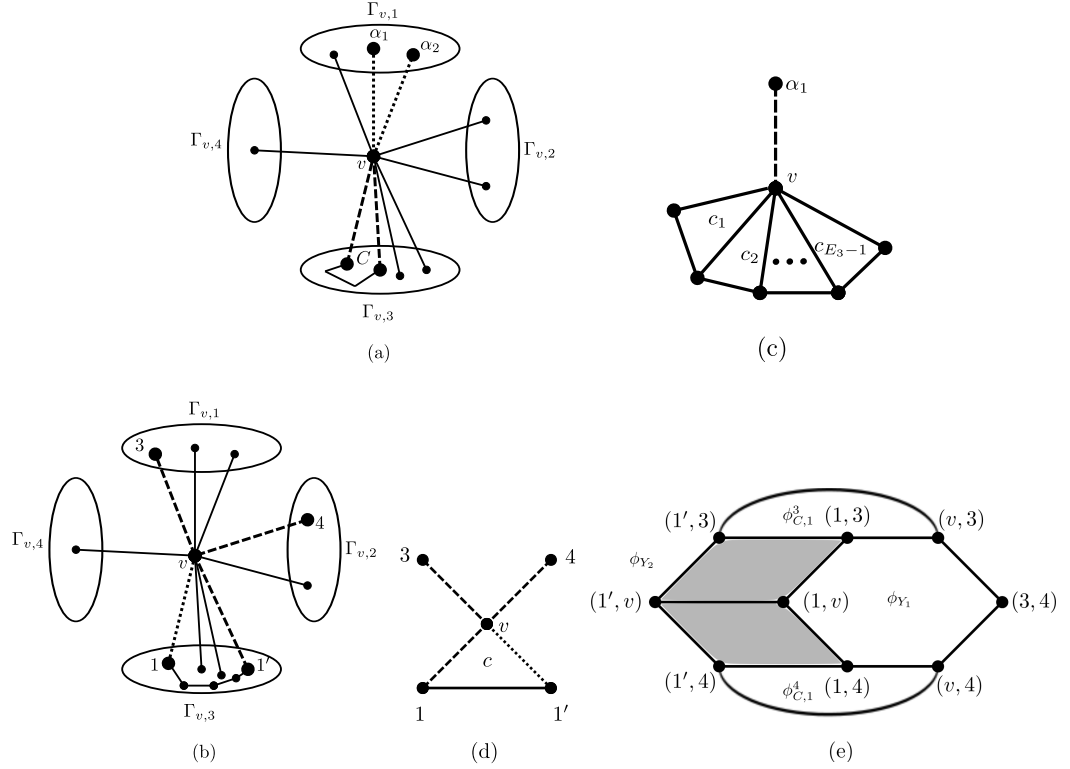


Figure 2.13: (a) The Y-graphs Y_1 and Y_2 have central vertex v and two common edges (long dashes) with vertices in $\Gamma_{v,3}$, but different edges (short dashes) with different vertices α_1 and α_2 in $\Gamma_{1,v}$. Their exchange phases are the same. (b) Each edge of the Y-graph is attached to a different component. (c) Y-graphs with two edges in the same component (d) Two Y-graphs centered at v with external vertices $\{1, 3, 4\}$ and $\{1', 3, 4\}$ respectively. (e) The relevant part of 2-particle configuration space of (d).

$\phi_{C,1}^{\alpha_1} = \phi_{C,1}^{\alpha_2}$. Next, relation (2.3.3) applied to cycle C and the two considered Y graphs gives $\phi_{Y_1} = \phi_{Y_2}$.

After choosing one edge of Y in component $\Gamma_{v,1}$ (by the above argument it does not matter which), we can choose the two other edges in $\Gamma_{v,3}$ in $\binom{E_3}{2}$ ways. Therefore, *a priori*, we have $\binom{E_3}{2}$ Y-graphs to consider. There are, however, relations between them. In order to find the relevant relations consider the graph shown in figure 2.13(c). We are interested in Y-graphs with one edge given by $\alpha_1 \leftrightarrow v$ (dashed line) and two edges joining v to vertices in

$\Gamma_{v,3}$, say j and k . Each such Y -graph determines a cycle c in $\Gamma_{v,3}$ containing vertices v, j and k (since $\Gamma_{v,3}$ is connected). We have that

$$\phi_{c,2} = \phi_{c,1}^{\alpha_1} + \phi_Y. \quad (2.3.13)$$

Therefore, the $\binom{E_3}{2}$ Y -phases under consideration are determined by the AB- and two-particle phases, $\phi_{c,2}$ and $\phi_{c,1}^{\alpha_1}$, of the associated cycles c . These cycles may be expressed as linear combinations of a basis of $E_3 - 1$ cycles, denoted c_1, \dots, c_{E_3-1} , as in figure 2.13(c). It is clear that if $c = \sum_{i=1}^{E_3} r_i c_i$, then

$$\phi_{c,1}^{\alpha_1} = \sum_{i=1}^{E_3-1} r_i \phi_{c_i,1}^{\alpha_1}, \quad \phi_{c,2} = \sum_{i=1}^{E_3-1} r_i \phi_{c_i,2}. \quad (2.3.14)$$

Thus, the Y -phases under consideration may be expressed in terms of the $2(E_3 - 1)$ phases $\phi_{c_i,2}$ and $\phi_{c_i,1}^{\alpha_1}$.

Let Y_i be the Y -graph which determines the cycle c_i . We may turn the preceding argument around; from (2.3.13), the AB-phase $\phi_{c_i,1}^{\alpha_1}$ can be expressed in terms of ϕ_{Y_i} and $\phi_{c_i,2}$. Combining the preceding observations, we deduce that the $\binom{E_3}{2}$ Y -phases lost when the vertex v is removed may be expressed in terms of the phases $\phi_{c_i,2}$ and ϕ_{Y_i} . The phases $\phi_{c_i,2}$ remain when v is removed. It follows that phases ϕ_{Y_i} suffice to determine all of the lost phases, so that the number of independent Y -phases lost is $E_3 - 1$. Repeating this argument for each component, the total number of Y -phases lost is $\sum_{i=1}^{\mu(v)} (E_i - 1)(\mu(v) - 1) = (\mu(v) - 1)(\nu(v) - \mu(v))$, where $\nu(v) = \sum_i E_i$ is the valency of v .

2. Each edge of the Y -graph is attached to a different component. We will show now that once three different components have been chosen it does not matter which of the edges attaching $\Gamma_{v,i}$ to v we choose. It suffices to consider the case where the edges differ for only one component. Let us consider the two Y -graphs shown in figure 2.13(b). The first one consists of the three dashed

edges and the second of two dashed edges attached to $\Gamma_{v,1}$ and $\Gamma_{v,2}$ respectively and the dotted edge attached to $\Gamma_{v,3}$. The two Y-graphs are shown on their own in figure 2.13(d); we let Y_1 and Y_2 denote the Y-graphs with vertices $\{1, 3, 4, v\}$ and $\{1', 3, 4, v\}$ respectively. A subgraph of the corresponding 2-particle configuration space is shown in figure 2.13(e). There we see that

$$\phi_{Y_2} = \phi_{Y_1} + \phi_{c,1}^3 + \phi_{c,1}^4. \quad (2.3.15)$$

In Step 1 above, we showed that the AB phases $\phi_{c,1}^3$ and $\phi_{c,1}^4$ can be expressed in terms of $\phi_{c,2}$ and Y-phases already accounted for in Step 1. Thus, the number of the independent Y-phases we lose is equal to the number of independent Y-cycles in the two-particle configuration space of the star graph with $\mu(v)$ edges, that is, $(\mu(v) - 1)(\mu(v) - 2)/2$.

Summing up we can write

$$H_1(\mathcal{D}^2(\Gamma)) = \left[\bigoplus_{i=1}^{\mu(v)} H_1(\mathcal{D}^2(\Gamma_{v,i})) \right] \oplus \mathbb{Z}^{N_1(v)}, \quad (2.3.16)$$

where $N_1(v) = (\mu(v) - 1)(\mu(v) - 2)/2 + (\mu(v) - 1)(\nu(v) - \mu(v))$. It is known in graph theory [45] that by the repeated application of the above decomposition procedure the resulting components become finally 2-connected graphs. Let v_1, \dots, v_l be the set of cut vertices such that components $\Gamma_{v_i,k}$ are 2-connected. Making use of formula (2.3.11) we can write

$$H_1(\mathcal{D}^2(\Gamma)) = \mathbb{Z}^{\beta(\Gamma) + N_1 + N_2 + N_3} \oplus \mathbb{Z}_2^{N'_3}, \quad (2.3.17)$$

where $N_1 = \sum_i N_1(v_i)$.

2.4 n -particle statistics for 2-connected graphs

Having discussed 2-particle configuration spaces, we switch to the n -particle case, $\mathcal{D}^n(\Gamma)$, where $n > 2$. We proceed in a similar manner to the previous section. First

we give a spanning set of $H_1(\mathcal{D}^n(\Gamma))$. Next we show that if Γ is 2-connected the first homology group stabilizes with respect to n , that is, $H_1(\mathcal{D}^n(\Gamma)) = H_1(\mathcal{D}^2(\Gamma))$. Making use of formula (2.3.11)

$$H_1(\mathcal{D}^n(\Gamma)) = \mathbb{Z}^{\beta(\Gamma)+N_2+N_3} \oplus \mathbb{Z}_2^{N'_3}.$$

2.4.1 A spanning set of $H_1(\mathcal{D}^n(\Gamma))$

In order to calculate $H_1(\mathcal{D}^n(\Gamma))$ we first need to subdivide the edges of Γ appropriately. By Theorem 2.2.1 each edge of Γ must be able to accommodate n particles and each cycle needs to have at least $n+1$ vertices, that is, Γ needs to be sufficiently subdivided. Before we specify a spanning set of $H_1(\mathcal{D}^n(\Gamma))$ we first discuss two interesting aspects of this space. The first one concerns the relation between the exchange phase of k particles, $k \leq n$ on the cycle C of the lasso graph and its ϕ_Y phases (see Lemma 2.4.1). The second gives the relation between the AB-phases for fixed cycle c of Γ and the different possible positions of the $n-1$ stationary particles.

Lemma 2.4.1. *The exchange phase, $\phi_{C,n}$, of n particles on the cycle c of the lasso graph is the sum of the exchange phase, $\phi_{C,n-1}^1$, of $n-1$ particles on the cycle C with the last particle sitting at the vertex not belonging to C , e.g. vertex 1, and the phase ϕ_Y associated with the exchange of two particles on the Y subgraph with $n-2$ particles placed in the vertices v_1, \dots, v_{n-2} of C not belonging to the Y*

$$\phi_{C,n} = \phi_{C,n-1}^1 + \phi_Y^{v_1, \dots, v_{n-2}}.$$

Proof. By (2.3.1), the lemma is true for $n=2$. The proof for $n=3$ particles is shown in figure 2.15(a), and contains the essence of the argument for general n . Indeed, the way to incorporate additional particles is illustrated by the $n=4$ case, shown in figure 2.15(b). Note that figure 2.15 shows only the small portion of the $n=3$ and $n=4$ configuration spaces required to establish the lemma. These configuration spaces are derived from the 1-particle lasso graphs shown in figures

2.14(a) and 2.14(b) respectively; it is easy to see that these are indeed sufficiently subdivided. The Y-graphs we consider for $n = 3$ and $n = 4$ are $\{2 \leftrightarrow 3, 3 \leftrightarrow 4, 3 \leftrightarrow 6\}$ and $\{3 \leftrightarrow 4, 4 \leftrightarrow 5, 4 \leftrightarrow 8\}$ respectively.

□

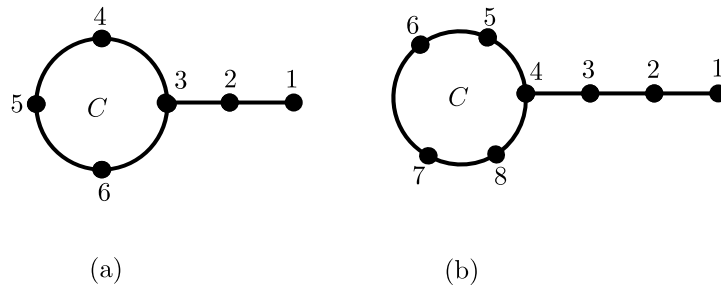


Figure 2.14: The subdivided lasso for (a) 3 particles, (b) 4 particles.

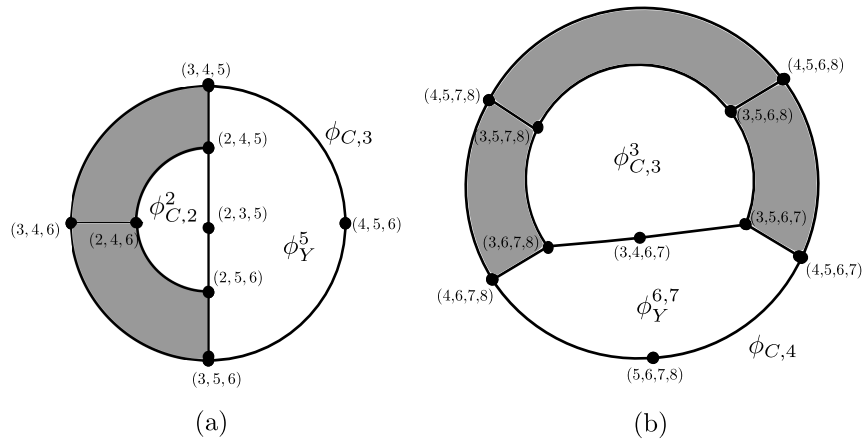


Figure 2.15: Subgraphs of the configurations spaces for the lasso graphs with (a) 3 particles: $\phi_{C,3} = \phi_{C,2}^2 + \phi_Y^5$, (b) 4 particles: $\phi_{C,4} = \phi_{C,3}^3 + \phi_Y^{6,7}$.

By repeated application of Lemma 2.4.1 we see that $\phi_{C,n}$ can be expressed as a sum of an AB-phase and the Y-phases corresponding to different positions of $n - 2$ particles. For example in the case of the graphs from figure 2.14(a) and 2.14(b) we get

$$\begin{aligned}\phi_{C,3} &= \phi_Y^5 + \phi_{C,2}^2 = \phi_Y^5 + \phi_Y^1 + \phi_{C,1}^{1,2}, \\ \phi_{C,4} &= \phi_Y^{6,7} + \phi_{C,3}^3 = \phi_Y^{6,7} + \phi_{C,3}^1 = \phi_Y^{6,7} + \phi_Y^{1,6} + \phi_Y^{1,2} + \phi_{C,1}^{1,2,3}.\end{aligned}$$

Aharonov-Bohm phases Assume now that we have n particles on Γ . Let C be a cycle of Γ and e_1 and e_2 two sufficiently subdivided edges attached to C (see figure 2.16(a)). We denote by $\phi_{C,1}^{k_1,k_2}$ the AB-phase corresponding to the situation where one particle goes around the cycle C while k_1 particles are in the edge e_1 and k_2 particles are in the edge e_2 , $k_1 + k_2 = n - 1$. For each distribution (k_1, k_2) of the $n - 1$ particles between the edges e_1 and e_2 we get a (possibly) different AB-cycle and AB-phase in $\mathcal{D}^n(\Gamma)$. We want to know how they are related. To this end notice that

$$\phi_{C,2}^{k_1,k_2} = \phi_{C,1}^{k_1+1,k_2} + \phi_{Y_1}^{k_1,k_2}, \quad \phi_{C,2}^{k_1,k_2} = \phi_{C,1}^{k_1,k_2+1} + \phi_{Y_2}^{k_1,k_2}, \quad (2.4.1)$$

and hence

$$\phi_{C,1}^{k_1+1,k_2} - \phi_{C,1}^{k_1,k_2+1} = \phi_{Y_2}^{k_1,k_2} - \phi_{Y_1}^{k_1,k_2}. \quad (2.4.2)$$

The relations between different AB-phases for a fixed cycle C of Γ are therefore encoded in the 2-particle phases ϕ_Y , albeit these phases can depend on the positions of the remaining $n - 2$ particles.

A spanning set of $H_1((D)^n(\Gamma))$ is given by the following (see section 2.7 for proof):

1. All 2-particle cycles corresponding to the exchange of two particles on the Y subgraph while $n - 2$ particles are at vertices not belonging to the considered Y -graph. In general the phases ϕ_Y depend on the position of the remaining $n - 2$ particles.
2. The set of $\beta_1(\Gamma)$ AB-cycles, where $\beta_1(\Gamma)$ is the number of the independent cycles of Γ .

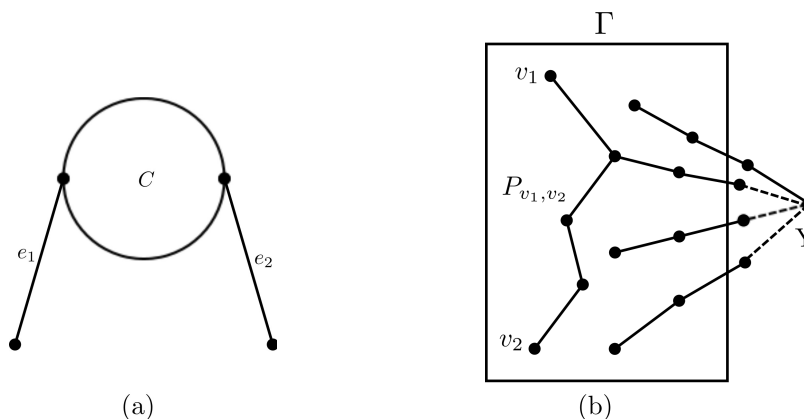


Figure 2.16: (a) The relation between AB-phases, (b) the stabilization of the first homology group.

Theorem 2.4.2. *For a 2-connected graph Γ the first homology group stabilizes with respect to the number of particles, i.e. $H_1(\mathcal{D}^n(\Gamma)) = H_1(\mathcal{D}^2(\Gamma))$.*

Proof. Using our spanning set it is enough to show that phases on the Y-cycles do not depend on the position of the remaining $n - 2$ particles. Notice that if any pair of the vertices not belonging to the chosen Y-graph is connected by a path then clearly the corresponding Y-phases have this property. Since the graph Γ is 2-connected it remains at least 1-connected after removal of a vertex. Removing the central vertex of the Y (see figure 2.16(b)), the theorem follows. \square

2.5 n -particle statistics on 1-connected graphs

By Theorem 2.4.2, in order to fully characterize the first homology group of $\mathcal{D}^n(\Gamma)$ for an arbitrary graph Γ we are left to calculate $H_1(\mathcal{D}^n(\Gamma))$ for graphs which are 1-connected but not 2-connected. This is achieved by considering n -particle star and fan graphs.

2.5.1 Star graphs

In the following we consider a particular family of 1-connected graphs, namely the star graphs S_E with E edges (see figure 2.17(a)). Our aim is to provide a formula for the dimension of the first homology group, β_n^E , of the n -particle configuration space $\mathcal{D}^n(S_E)$. Let us recall that a graph Γ is 1-connected iff after deletion of one vertex it splits into at least two connected components.

Star graph with non-subdivided edges It turns out that the computation of β_n^E can be reduced to the case of n particles on a star graph with non-subdivided edges, so we consider this case first. Let \bar{S}_E denote the star graph with $E + 1$ vertices and E edges each connecting the central vertex to a single vertex of valency 1; such a star graph is not sufficiently subdivided for $n > 2$ particles. As there are no pairs of disjoint edges (every edge contains the central vertex), there are no contractible cycles. Therefore, the n -particle configuration space, $\mathcal{D}^n(\bar{S}_E)$ is a graph, i.e. a one-dimensional cell complex. The number of independent cycles in $\mathcal{D}^n(\bar{S}_E)$, denoted here and in what follows by γ_n^E , is given by the first Betti number, $E_n - V_n + 1$, where E_n and V_n are the number of edges and vertices in $\mathcal{D}^n(S_E)$. It is easy to see that $V_n = \binom{E+1}{n}$ and $E_n = E \cdot \binom{E-1}{n-1}$. Hence

$$\gamma_n^E = E \binom{E-1}{n-1} - \binom{E+1}{n} + 1. \quad (2.5.1)$$

Y-graph The simplest case of a sufficiently subdivided star graph is a Y-graph where each arm has $n - 1$ segments. As there are no cycles on the Y-graph itself, cycles in the n -particle configuration space are generated by two-particle exchanges on the non-subdivided subgraph \bar{Y} comprised of the three segments adjacent to the central vertex. A basis of independent cycles is obtained by taking all possible configurations of the $n - 2$ particles amongst the three arms of the Y-graph. As configurations which differ by shifting particles within the arms of the Y produce homotopic cycles, the number of distinct configurations is the number of partitions of $n - 2$ indistinguishable particles amongst three distinguishable boxes, or $\binom{(n-2)+(3-1)}{n-2} = \binom{n}{n-2}$. Therefore,

$$\beta_n^3 = \binom{n}{n-2} \gamma_2^3 = \frac{n(n-1)}{2}. \quad (2.5.2)$$

Star graph with five arms For star graphs with more than three arms, it is necessary to take account of relations between cycles involving two or more moving particles. With this in mind, we introduce the following terminology: an (n, m) -cycle is a cycle of n particles on which m particles move and $(n - m)$ particles remain fixed.

The general case is well illustrated by considering the star graph with $E = 5$ arms. As above, we suppose that each arm of S_5 has $(n - 1)$ segments, and is therefore sufficiently subdivided to accommodate n particles. Let \bar{S}_5 denote the non-subdivided subgraph consisting of the five segments adjacent to the central vertex. As there are no cycles on S_5 , a spanning set for the first homology group of the n -particle configuration space is provided by two-particle cycles on the Y 's contained in \bar{S}_5 . The number of independent two-particle cycles on \bar{S}_5 is given by γ_5^2 . For each of these, we can distribute the remaining $(n - 2)$ particles among the five edges of S_5 (cycles which differ by shifting particles within an edge are homotopic). Therefore, we obtain a spanning set consisting of $\beta''_n{}^5$ $(n, 2)$ -cycles, where

$$\beta''_n{}^5 := \binom{n+2}{4} \gamma_2^5.$$

The preceding discussion of non-subdivided star graphs reveals that there are relations among the cycles in the spanning set. In particular, a subset of the $(n, 2)$ -cycles can be replaced by a smaller number of $(n, 3)$ -cycles.

To see this, consider first the case of $n = 3$ particles on the non-subdivided star graph \bar{S}_5 . By definition, the number of independent $(3, 3)$ -cycles is γ_3^5 . However, the number of $(3, 2)$ -cycles on \bar{S}_5 is larger; it is given by $\binom{5}{1} \gamma_2^4$, where the first factor represents the number of positions of the fixed particle, and the second factor represents the number of independent $(2, 2)$ -cycles on the remaining four edges of \bar{S}_5 . It is easily checked that $\gamma_3^5 - \binom{5}{1} \gamma_2^4 = -3$, so that there are three relations amongst the $(3, 2)$ -cycles on \bar{S}_5 .

We return to the case of n particles. For each $(3, 3)$ -cycle on \bar{S}_5 , there are $\binom{n+1}{4}$ $(n, 3)$ -cycles on S_5 ; the factor $\binom{n+1}{4}$ is the number of ways to distribute the $n - 3$ fixed particles on the five edges of S_5 outside of \bar{S}_5 . Calculating the number of $(n, 2)$ -cycles on S_5 obtained from $(3, 2)$ -cycles on \bar{S}_5 requires a bit more care. The reasoning underlying the preceding count of $(n, 3)$ cycles would suggest that the number of such $(n, 2)$ -cycles is given by $\binom{n+1}{4} \binom{5}{1} \gamma_2^4$. However, this expression introduces some double counting. In particular, $(n, 2)$ -cycles for which two of the fixed particles lie in \bar{S}_5 are counted twice, as each of these two fixed particles is separately regarded as the fixed particle in a $(3, 2)$ -cycle on \bar{S}_5 . The correct expression is obtained by subtracting the number of doubly counted cycles; this is given by $\binom{n}{4} \binom{5}{2} \gamma_2^3$. Thus we may replace this subset of $(n, 2)$ -cycles by the $(n, 3)$ -cycles to which they are related to obtain a smaller spanning set with $\beta'_n{}^5$ elements, where

$$\beta'_n{}^5 = \beta''_n{}^5 + \binom{n+1}{4} \gamma_3^5 - \left(\binom{n+1}{4} \binom{5}{1} \gamma_2^4 - \binom{n}{4} \binom{5}{2} \gamma_2^3 \right).$$

Finally, we must account for relations among the $(n, 3)$ -cycles. Consider first the case of just four particles on \bar{S}_5 . The number of independent $(4, 4)$ -cycles is γ_4^5 . The number of $(4, 3)$ -cycles is $\binom{5}{1} \gamma_3^4$, where the first factor represents the number of positions of the fixed particle, and the second factor represents the number of independent $(3, 3)$ -cycles on the remaining four edges of \bar{S}_5 . For each $(4, 4)$ -cycle on \bar{S}_5 , there are $\binom{n}{4}$ $(n, 4)$ cycles on S_5 . Similarly, for each $(4, 3)$ -cycle on \bar{S}_5 , there are $\binom{n}{4}$ $(n, 3)$ -cycles on S_5 (there is no over-counting, as there are no five-particle cycles on \bar{S}_5). Replacing this subset of $(n, 3)$ -cycles by the $(n, 4)$ -cycles to which they are related, we get a smaller spanning set of β_n^5 elements, where

$$\beta_n^5 = \beta'_n{}^5 + \binom{n}{4} \left(\gamma_4^5 - \binom{5}{1} \gamma_3^4 \right) = 6 \binom{n+2}{4} - 4 \binom{n+1}{4} + \binom{n}{4}.$$

As there are no five-particle cycles on \bar{S}_5 , there are no additional relations, and the resulting spanning set constitutes a basis.

n particles on a star graph with E arms The formula in the general case of E edges is obtained following a similar argument. We start with a spanning set

of $\binom{n+E-3}{E-1} \gamma_2^E$ $(n, 2)$ -cycles on S_E . We then replace a subset of $(n, 2)$ -cycles by a smaller number of $(n, 3)$ -cycles, then replace a subset of these $(n, 3)$ -cycles by a smaller number of $(n, 4)$ -cycles, and so on, proceeding to $(n, E-1)$ -cycles, thereby obtaining a basis. The number of elements in the basis is given by

$$\beta_n^E = \sum_{m=2}^{E-1} \left(\binom{n-m+E-1}{E-1} \gamma_m^E + \sum_{j=1}^{E-m} (-1)^j \binom{n-m-j+E}{E-1} \binom{E}{j} \gamma_{m-1}^{E-j} \right). \quad (2.5.3)$$

The outer m -sum is taken over (n, m) -cycles. The m th term is the difference between the number of (n, m) -cycles and the number of $(n, m-1)$ -cycles to which they are related. The inclusion-exclusion sum over j compensates for over-counting $(n, m-1)$ -cycles with j fixed particles in \bar{S}_E .

It turns out to be convenient to rearrange the sums in (2.5.3) to obtain the following equivalent expression:

$$\beta_n^E = \sum_{k=2}^{E-1} \binom{n-k+E-1}{E-1} \alpha_k^E \quad (2.5.4)$$

where

$$\alpha_k^E = \sum_{i=0}^{k-2} (-1)^i \binom{E}{i} \cdot \gamma_{k-i}^{E-i}. \quad (2.5.5)$$

This is because the coefficients α_k^E turn out to have a simple expression. First, straightforward manipulation yields

$$\alpha_k^E = \gamma_k^E - \sum_{i=1}^{k-2} \binom{E}{i} \alpha_{k-i}^{E-i}. \quad (2.5.6)$$

We then have the following:

Lemma 2.5.1. *The coefficients $\alpha_k^E = (-1)^k \binom{E-1}{k}$.*

Proof. We proceed by induction. Direct calculations give $\alpha_2 = \binom{E-1}{2}$. Assume that $\alpha_i^E = (-1)^i \binom{E-1}{i}$ for $i \in \{2, \dots, k-1\}$ and $k \leq E$. Using this assumption and (2.5.6)

$$\alpha_k = \gamma_k^E - (-1)^k \sum_{i=1}^{k-2} (-1)^i \binom{E}{i} \binom{E-i-1}{k-i}.$$

Making use of the identity $\binom{r}{k} = (-1)^k \binom{k-r-1}{k}$ and Vandermonde's convolution $\sum_{i=0}^k \binom{E}{i} \binom{k-E}{k-i} = 1$, we get

$$\begin{aligned} (-1)^k \sum_{i=1}^{k-2} (-1)^i \binom{E}{i} \binom{E-i-1}{k-i} &= \sum_{i=1}^{k-2} \binom{E}{i} \binom{k-E}{k-i} \\ &= 1 - (-1)^k \binom{E-1}{k} + (E-k) \binom{E}{k-1} - \binom{E}{k}. \end{aligned}$$

Using (2.5.1) for γ_k^E , we get

$$\alpha_k = (-1)^k \binom{E-1}{k} + E \binom{E-1}{k-1} - \binom{E+1}{k} - (E-k) \binom{E}{k-1} + \binom{E}{k}.$$

Expanding $\binom{E+1}{k} = \binom{E}{k} + \binom{E}{k-1}$ and straightforward manipulations show

$$\alpha_k = (-1)^k \binom{E-1}{k},$$

which completes the argument. \square

By Lemma 2.5.1

$$\begin{aligned} \beta_n^E &= \sum_{k=2}^{E-1} \binom{n-k+E-1}{E-1} \cdot \alpha_k = \sum_{k=2}^{E-1} (-1)^k \binom{E-1}{k} \binom{n-k+E-1}{E-1} \\ &= \sum_{k=2}^{E-1} (-1)^k \binom{E-1}{k} \binom{n-k+E-1}{n-k} = (-1)^n \sum_{k=2}^{E-1} \binom{E-1}{k} \binom{-E}{n-k}. \end{aligned}$$

By Vandermonde's convolution

$$\sum_{k=0}^{E-1} \binom{E-1}{k} \binom{-E}{n-k} = \sum_{k=0}^n \binom{E-1}{k} \binom{-E}{n-k} = \binom{-1}{n} = (-1)^n.$$

Therefore

$$\beta_n^E = 1 - \binom{n+E-1}{E-1} + \binom{n+E-2}{E-1} (E-1).$$

Notice that $\binom{n+E-1}{E-1} = \binom{n+E-2}{E-1} + \binom{n+E-2}{E-2}$ and thus

$$\beta_n^E = \binom{n+E-2}{E-1} (E-2) - \binom{n+E-2}{E-2} + 1. \quad (2.5.7)$$

Note finally that in contrast with 2-connected graphs, formula (2.5.7) indicates a strong dependence of the quantum statistics on the number of particles, n .

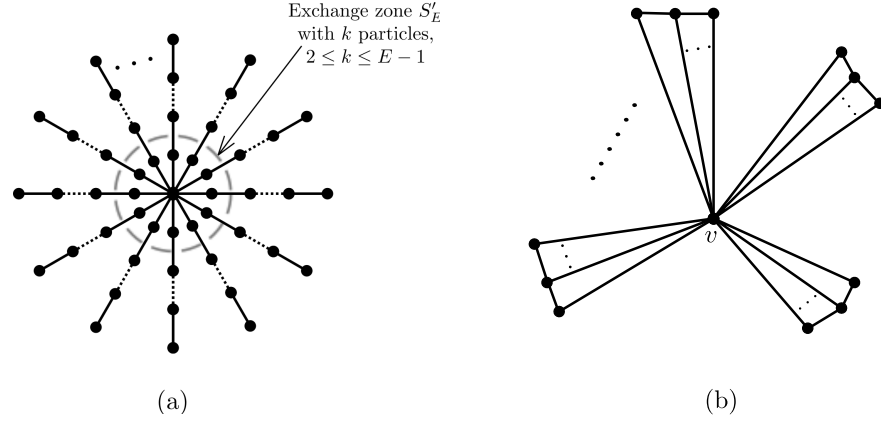


Figure 2.17: (a) The star graph with E arms and n particles. Each arm has n vertices. The exchange zone S'_E can accommodate $2, 3, \dots, E - 1$ particles. (b) The fan graph F .

2.5.2 The fan graphs

Following the argument presented in section 2.3.4 in order to treat a one-vertex cut v we need to count the number of the independent Y-phases which are lost due to the removal of v . As in Section 2.3.4, let $\mu = \mu(v)$ denote the number of connected components following the deletion of v , and denote these components by $\Gamma_1, \dots, \Gamma_\mu$. For Y-cycles with edges in three distinct components, the number of independent phases, β_n^μ , is given by the expression (2.5.7) for star graphs,

$$\beta_n^\mu = \binom{n + \mu - 2}{\mu - 1} (\mu - 2) - \binom{n + \mu - 2}{\mu - 2} + 1. \quad (2.5.8)$$

We must also determine the number of independent Y-cycles with two edges in the same component Γ_i , denoted $\gamma_n(v)$.

Let us first consider a simple example, namely the graphs shown in figures 2.18(a) and 2.18(b). Assume there are three particles. We calculate $\gamma_3(v)$ as follows. The Y subgraphs we are interested in are denoted by dashed lines and are Y_1 and Y_2 respectively. Note that each of them contributes three phases corresponding to different positions of the third particle $\{\phi_{Y_1}^A, \phi_{Y_1}^B, \phi_{Y_1}^C, \phi_{Y_2}^A, \phi_{Y_2}^B, \phi_{Y_2}^C\}$. They are,

however, not independent. To see this, note that using Lemma 2.4.1 we can write

$$\begin{aligned}\phi_{c,3} &= \phi_{Y_1}^A + \phi_{Y_1}^B + \phi_{c,1}^{B,B'}, & \phi_{c,3} &= \phi_{Y_2}^A + \phi_{Y_2}^C + \phi_{c,1}^{C,C'}, \\ \phi_{c,2}^B &= \phi_{Y_1}^B + \phi_{c,1}^{B,B'}, & \phi_{c,2}^B &= \phi_{Y_2}^B + \phi_{c,1}^{B,C}, \\ \phi_{c,2}^C &= \phi_{Y_1}^C + \phi_{c,1}^{B,C}, & \phi_{c,2}^C &= \phi_{Y_2}^C + \phi_{c,1}^{C,C'}.\end{aligned}$$

The phase $\phi_{c,3}$ is not lost when v is cut. On the other hand, the five phases

$$\{\phi_{c,1}^{C,C'}, \phi_{c,1}^{B,B'}, \phi_{c,1}^{B,C}, \phi_{c,2}^B, \phi_{c,2}^C\}, \quad (2.5.9)$$

are lost. The knowledge of them and ϕ_c^3 determines all six ϕ_Y phases. Therefore, $\gamma_3(v)$ is the number of 1 and 2-particle exchanges on cycle c (which is 5) rather than the number of Y phases (which is 6).

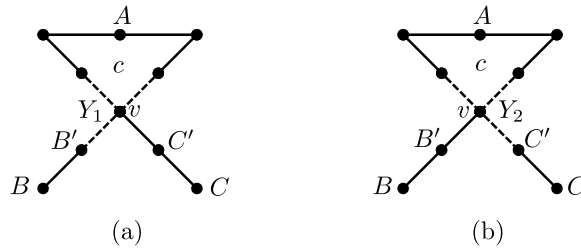


Figure 2.18: The Y subgraphs (a) Y_1 and (b) Y_2 .

For the general case, let ν_i denote the number of edges at v which belong to Γ_i . Since the Γ_i are connected, there exist $\nu_i - 1$ independent cycles in Γ_i which connect these edges. Denote these by $C_{i,1}, \dots, C_{i,\nu_i-1}$. Fan graphs (see Fig 2.17 (b)) provide the simplest realization. Using arguments similar to those in the above example, one can show that Y -cycles with two edges in the same component can be expressed in terms of two sets of cycles. The first set contains cycles which are wholly contained in just one of the connected components. These cycles are not lost when v is cut, and therefore do not contribute to $\gamma_n(v)$. The second type of cycle is characterised as follows: Consider a partition $\{n_i\}_{i=1}^\mu$ of the particles amongst the components Γ_i . For each partition, we can construct cycles where all of the particles in Γ_i – assuming Γ_i contains at least one particle, i.e. that $n_i > 0$ – are

taken to move once around $C_{i,j}$ while the other particles remain fixed. Excluding the cases in which all of the particles belong to a single component, the number of such cycles is given by the following sum over partitions $n_1 + \dots + n_\mu = n$:

$$\gamma_n(v) = \sum_{\substack{n_1, \dots, n_\mu=0 \\ n_1 + \dots + n_\mu = n}}^n \sum_{\substack{i=1 \\ 0 < n_i < n}}^\mu (\nu_i - 1).$$

Noting that

$$\sum_{\substack{i=1 \\ 0 < n_i < n}}^\mu = \sum_{i=1}^\mu - \sum_{\substack{i=1 \\ n_i=0}}^\mu - \sum_{\substack{i=1 \\ n_i=n}}^\mu$$

and $\sum_{i=1}^\mu (\nu_i - 1) = \nu - \mu$, we readily obtain

$$\gamma_n(v) = \left(\binom{n + \mu - 1}{n} - \binom{n + \mu - 2}{n} - 1 \right) (\nu - \mu) = \left(\binom{n + \mu - 2}{n - 1} - 1 \right) (\nu - \mu).$$

Hence the number of the phases lost when v is cut is given by

$$N_1(v, n) = \beta_n^\mu + \gamma_n(v) = \binom{n + \mu - 2}{\mu - 1} (\nu - 2) - \binom{n + \mu - 2}{\mu - 2} - (\nu - \mu - 1). \quad (2.5.10)$$

The final formula for $H_1(\mathcal{D}^n(\Gamma))$ By the repeated application of the one-vertex cuts the resulting components of Γ become finally 2-connected graphs. Let v_1, \dots, v_l be the set of cut vertices such that components $\Gamma_{v_i, k}$ are 2-connected. Making use of formula (2.3.8) we write

$$H_1(\mathcal{D}^n(\Gamma)) = \mathbb{Z}^{\beta(\Gamma) + N_1 + N_2 + N_3} \oplus \mathbb{Z}_2^{N'_3}, \quad (2.5.11)$$

where $N_1 = \sum_i N_1(v_i, n)$, the coefficients $N_1(v_i, n)$ are given by (2.5.10) and N_2, N_3, N'_3 are defined as in section 2.3.

2.6 Gauge potentials for 2-connected graphs

In this section we give a prescription for the n -particle topological gauge potential on $\mathcal{D}^n(\Gamma)$ in terms of the 2-particle topological gauge potential. For 2-connected

graphs all choices of n -particle topological gauge potentials on $\mathcal{D}^n(\Gamma)$ are realized by this prescription. The discussion is divided into three parts: i) separation of a 2-particle topological gauge potential into AB and quantum statistics components, ii) topological gauge potentials for 2-particles on a subdivided graph, iii) n -particle topological gauge potentials.

We start with some relevant background. Assume as previously that Γ is sufficiently subdivided. Recall that directed edges or 1-cells of $\mathcal{D}^n(\Gamma)$ are of the form $v_1 \times \dots \times v_{n-1} \times e$ up to permutations, where v_j are vertices of Γ and $e = j \rightarrow k$ is an edge of Γ whose endpoints are not $\{v_1, \dots, v_{n-1}\}$. For simplicity we will use the following notation

$$\{v_1, \dots, v_{n-1}, j \rightarrow k\} := v_1 \times \dots \times v_{n-1} \times e.$$

An n -particle gauge potential is a function $\Omega^{(n)}$ defined on the directed edges of $\mathcal{D}^n(\Gamma)$ with the values in \mathbb{R} modulo 2π such that

$$\Omega^{(n)}(\{v_1, \dots, v_{n-1}, k \rightarrow j\}) = -\Omega^{(n)}(\{v_1, \dots, v_{n-1}, j \rightarrow k\}). \quad (2.6.1)$$

In order to define Ω on linear combinations of directed edges we extend (2.6.1) by linearity.

For a given gauge potential, $\Omega^{(n)}$ the sum of its values calculated on the directed edges of an oriented cycle C will be called the flux of Ω through C and denoted $\Omega(C)$. Two gauge potentials $\Omega_1^{(n)}$ and $\Omega_2^{(n)}$ are called equivalent if for any oriented cycle C the fluxes $\Omega_1^{(n)}(C)$ and $\Omega_2^{(n)}(C)$ are equal modulo 2π .

The n -particle gauge potential $\Omega^{(n)}$ is called a *topological gauge potential* if for any contractible oriented cycle C in $\mathcal{D}^n(\Gamma)$ the flux $\Omega^{(n)}(C) = 0 \pmod{2\pi}$. It is thus clear that equivalence classes of topological gauge potentials are in 1-1 correspondence with the equivalence classes in $H_1(\mathcal{D}^n(\Gamma))$.

Pure Aharonov-Bohm and pure quantum statistics topological gauge potentials

Let Γ be a graph with V vertices. We say that a 2-particle gauge potential $\Omega_{AB}^{(2)}$ is a *pure Aharonov-Bohm gauge potential* if and only if

$$\Omega_{AB}^{(2)}(\{i, j \rightarrow k\}) = \omega^{(1)}(j \rightarrow k), \text{ for all distinct vertices } i, j, k \text{ of } \Gamma. \quad (2.6.2)$$

Here $\omega^{(1)}$ can be regarded as a gauge potential on Γ . Thus, for a pure AB gauge potential, the phase associated with one particle moving from j to k does not depend on where the other particle is. We say that a 2-particle gauge potential $\Omega_S^{(2)}$ is a *pure statistics gauge potential* if and only if

$$\sum_{\substack{i \\ i \neq j, k}} \Omega_S^{(2)}(\{i, j \rightarrow k\}) = 0, \text{ for all distinct vertices } j, k \text{ of } G. \quad (2.6.3)$$

That is, the phase associated with one particle moving from j to k averaged over all possible positions of the other particle is zero. It is clear that an arbitrary gauge potential $\Omega^{(2)}$ has a unique decomposition into a pure AB and pure statistics gauge potentials, i.e.

$$\Omega^{(2)} = \Omega_{AB}^{(2)} + \Omega_S^{(2)}, \quad (2.6.4)$$

where

$$\Omega_{AB}^{(2)}(\{i, j \rightarrow k\}) = \frac{1}{V-2} \sum_{\substack{p \\ p \neq j, k}} \Omega^{(2)}(\{p, j \rightarrow k\}), \quad \Omega_S^{(2)} = \Omega^{(2)} - \Omega_{AB}^{(2)}. \quad (2.6.5)$$

It is straightforward to verify that if $\Omega^{(2)}$ is a topological gauge potential, then so are $\Omega_{AB}^{(2)}$ and $\Omega_S^{(2)}$, and vice versa. Moreover, one can easily check that $\Omega_{AB}^{(2)}$ vanishes on any Y-cycle of $\mathcal{D}^2(\Gamma)$. Note, however, that for a given cycle C of Γ the AB-phase, $\phi_{C,1}^v$ considered in the previous sections is not $\Omega_{AB}^{(2)}(v \times C)$ but rather $\Omega^{(2)}(v \times C)$ as AB-phases can depend on the position of the stationary particle.

Gauge potential for a subdivided 2-particle graph Let $\bar{\Gamma}$ be a graph with vertices $\bar{V} = \{1, \dots, \bar{V}\}$. Let $\bar{\Omega}^{(2)}$ be a gauge potential on $\mathcal{D}^2(\bar{\Gamma})$.

We assume that $\bar{\Omega}^{(2)}$ is topological, that is, for every pair of disjoint edges of $\bar{\Gamma}$, $i \leftrightarrow k$ and $j \leftrightarrow l$ we have

$$\bar{\Omega}^{(2)}(i, j \rightarrow l) + \bar{\Omega}^{(2)}(l, i \rightarrow k) + \bar{\Omega}^{(2)}(k, l \rightarrow j) + \bar{\Omega}^{(2)}(j, k \rightarrow i) = 0. \quad (2.6.6)$$

Assume we add a vertex to $\bar{\Gamma}$ by subdividing an edge. Let p and q denote the vertices of this edge, and denote the new graph by Γ and the added vertex by a . Since subdividing an edge does not change the topology of a graph, it is clear that

we can find a gauge potential, $\Omega^{(2)}$, on $\mathcal{D}^2(\Gamma)$ that is, in some sense, equivalent to $\bar{\Omega}^{(2)}$.

For the sake of completeness, we first give a precise definition of what it means for gauge potentials on $\mathcal{D}^2(\Gamma)$ and $\mathcal{D}^2(\bar{\Gamma})$ to be equivalent. Given a path \bar{P} on $\mathcal{D}^2(\bar{\Gamma})$, we can construct a path P on $\mathcal{D}^2(\Gamma)$ by making the replacements

$$\begin{aligned} \{i, p \rightarrow q\} &\mapsto \{i, p \rightarrow a \rightarrow q\}, \\ \{i, q \rightarrow p\} &\mapsto \{i, q \rightarrow a \rightarrow p\}. \end{aligned} \quad (2.6.7)$$

Similarly, given a path P on $\mathcal{D}^2(\Gamma)$ we can construct a path \bar{P} on $\mathcal{D}^2(\bar{\Gamma})$ by making the following substitutions:

$$\begin{aligned} \{i, p \rightarrow a \rightarrow p\} &\mapsto \{i, p\}, \\ \{i, p \rightarrow a \rightarrow q\} &\mapsto \{i, p \rightarrow q\}, \\ \{i, q \rightarrow a \rightarrow p\} &\mapsto \{i, q \rightarrow p\}, \\ \{i, q \rightarrow a \rightarrow q\} &\mapsto \{i, q\}. \end{aligned} \quad (2.6.8)$$

We say that $\Omega^{(2)}$ and $\bar{\Omega}^{(2)}$ are equivalent if

$$\Omega^{(2)}(P) = \bar{\Omega}^{(2)}(\bar{P}) \quad (2.6.9)$$

whenever P and \bar{P} are related as above.

Next we give an explicit prescription for $\Omega^{(2)}$. For edges in $\mathcal{D}^2(\Gamma)$ that do not involve vertices on the subdivided edge, we take $\Omega^{(2)}$ to coincide with $\bar{\Omega}^{(2)}$. That is, for i, j, k all distinct from p, a, q , we take

$$\Omega^{(2)}(\{i, j \rightarrow k\}) = \bar{\Omega}^{(2)}(\{i, j \rightarrow k\}). \quad (2.6.10)$$

As p and q are not adjacent on Γ , we take

$$\Omega^{(2)}(\{i, p \rightarrow q\}) = 0. \quad (2.6.11)$$

For edges on $\mathcal{D}^2(\Gamma)$ involving the subdivided segments $p \rightarrow a$ and $a \rightarrow q$, we require that $\Omega^{(2)}(\{i, p \rightarrow a\})$ and $\Omega^{(2)}(\{i, a \rightarrow q\})$ add up to give the phase

$\bar{\Omega}^{(2)}(i, p \rightarrow q)$ on the original edge. The partitioning of the original phase between the subdivided segments amounts to a choice of gauge. For definiteness, we will take the phases on the two halves of the subdivided edge to be the same, so that

$$\Omega^{(2)}(\{i, p \rightarrow a\}) = \Omega^{(2)}(\{i, a \rightarrow q\}) = \frac{1}{2}\bar{\Omega}^{(2)}(\{i, p \rightarrow q\}). \quad (2.6.12)$$

It remains to determine $\Omega^{(2)}$ for edges of $C_2(G)$ on which the stationary particle sits at the new vertex a . This follows from requiring that $\Omega^{(2)}$ satisfy the relations

$$\begin{aligned} \Omega^{(2)}(\{a, i \rightarrow j\}) + \Omega^{(2)}(\{j, a \rightarrow p\}) + \Omega^{(2)}(\{p, j \rightarrow i\}) + \Omega^{(2)}(\{i, p \rightarrow a\}) &= 0, \\ \Omega^{(2)}(\{a, i \rightarrow j\}) + \Omega^{(2)}(\{j, a \rightarrow q\}) + \Omega^{(2)}(\{q, j \rightarrow i\}) + \Omega^{(2)}(\{i, q \rightarrow a\}) &= 0. \end{aligned} \quad (2.6.13)$$

From (2.6.12) and the antisymmetry property $\Omega^{(2)}(\{i, j \rightarrow k\}) = -\Omega^{(2)}(\{i, k \rightarrow j\})$, along with the relations (2.6.6) satisfied by $\bar{\Omega}^{(2)}$, it follows that these conditions are equivalent, and both are satisfied by taking

$$\Omega^{(2)}(a, i \rightarrow j) = \frac{1}{2}(\bar{\Omega}^{(2)}(p, i \rightarrow j) + \bar{\Omega}^{(2)}(q, i \rightarrow j)). \quad (2.6.14)$$

Finally, when i or j coincide with one of the vertices p or q the expression should be

$$\Omega^{(2)}(\{a, q \rightarrow j\}) = (\bar{\Omega}^{(2)}(\{p, q \rightarrow j\}) + \frac{1}{2}\bar{\Omega}^{(2)}(\{j, q \rightarrow p\})). \quad (2.6.15)$$

It is then straightforward to verify that $\Omega^{(2)}(P) = \bar{\Omega}^{(2)}(\bar{P})$ whenever P and \bar{P} are related as in (2.6.7) and (2.6.8) and that $\Omega^{(2)}$ is a topological gauge potential.

Construction of n -particle topological gauge potential Let $\bar{\Omega}^{(2)}$ be a gauge potential on $\mathcal{D}^2(\bar{\Gamma})$. By repeatedly applying the procedure from the previous paragraph, we can construct an equivalent gauge potential $\Omega^{(2)}$ on $\mathcal{D}^2(\Gamma)$, where Γ is a sufficiently subdivided version of $\bar{\Gamma}$, in which $n - 2$ vertices are added to each edge of $\bar{\Gamma}$. We resolve $\Omega^{(2)}$ into its AB and statistics components $\Omega_{AB}^{(2)}$ and $\Omega_S^{(2)}$, as in (2.6.4). Suppose the pure AB component is described by the gauge potential $\omega^{(1)}$

on Γ . We define the n -particle gauge potential, $\Omega^{(n)}$, on $\mathcal{D}^n(\Gamma)$ as follows. Given $(n+1)$ vertices of Γ , denoted $\{v_1, \dots, v_{n-1}, i, j\}$, with $i \sim j$, we take

$$\Omega^{(n)}(\{v_1, \dots, v_{n-1}, i \rightarrow j\}) = \omega^{(1)}(i \rightarrow j) + \sum_{r=1}^{n-1} \Omega_S^{(2)}(\{v_r, i \rightarrow j\}). \quad (2.6.16)$$

That is, the phase associated with the one-particle move $i \rightarrow j$ is the sum of the AB-phase $\omega^{(1)}(i, j)$ and the two-particle statistics phases $\Omega_S^{(2)}(\{v_r, i \rightarrow j\})$ summed over the positions of the other particles.

Given that $\Omega^{(2)}$ is a topological gauge potential, let us verify that $\Omega^{(n)}$ is a topological gauge potential. Let $i \rightarrow k$ and $j \rightarrow l$ be distinct edges of Γ , and let $\{v_1, \dots, v_{n-2}\}$ denote $(n-2)$ vertices of Γ that are distinct from i, j, k, l . We need to verify if

$$\begin{aligned} & \Omega^{(n)}(\{v_1, \dots, v_{n-2}, i, j \rightarrow l\}) + \Omega^{(n)}(\{v_1, \dots, v_{n-2}, l, i \rightarrow k\}) + \\ & + \Omega^{(n)}(\{v_1, \dots, v_{n-2}, k, l \rightarrow j\}) + \Omega^{(n)}(\{v_1, \dots, v_{n-2}, j, k \rightarrow i\}) = 0. \end{aligned}$$

Using (2.6.16) it reduces to

$$\begin{aligned} & \omega^{(1)}(i \rightarrow k) + \omega^{(1)}(k \rightarrow i) + \omega^{(1)}(j \rightarrow l) + \omega^{(1)}(l \rightarrow k) + \\ & + \left(\sum_{r=1}^{n-2} \Omega_S^{(2)}(\{v_r, j \rightarrow l\}) + \Omega_S^{(2)}(\{i, j \rightarrow l\}) \right) + \left(\sum_{r=1}^{n-2} \Omega_S^{(2)}(\{v_r, i \rightarrow k\}) + \Omega_S^{(2)}(\{l, i \rightarrow k\}) \right) + \\ & + \left(\sum_{r=1}^{n-2} \Omega_S^{(2)}(\{v_r, l \rightarrow j\}) + \Omega_S^{(2)}(\{k, l \rightarrow j\}) \right) + \left(\sum_{r=1}^{n-2} \Omega_S^{(2)}(\{v_r, k \rightarrow i\}) + \Omega_S^{(2)}(\{j, k \rightarrow i\}) \right). \end{aligned}$$

Next, using the antisymmetry property $\Omega_S^{(2)}(\{v_r, i \rightarrow k\}) = -\Omega_S^{(2)}(\{v_r, k \rightarrow i\})$ and the fact that $\Omega_S^{(2)}$ is a topological gauge potential we get

$$\begin{aligned} & \sum_{r=1}^{n-2} \left(\Omega_S^{(2)}(\{v_r, j \rightarrow l\}) + \Omega_S^{(2)}(\{v_r, l \rightarrow j\}) \right) + \left(\Omega_S^{(2)}(\{v_r, i \rightarrow k\}) + \Omega_S^{(2)}(\{v_r, k \rightarrow i\}) \right) + \\ & + \Omega_S^{(2)}(\{i, j \rightarrow l\}) + \Omega_S^{(2)}(\{l, i \rightarrow k\}) + \Omega_S^{(2)}(\{k, l \rightarrow j\}) + \Omega_S^{(2)}(\{j, k \rightarrow i\}) = 0. \end{aligned}$$

Therefore, the gauge potential defined by (2.6.16) is topological. Equivalence classes of n -particle topological gauge potentials are essentially elements of the

first homology group $H_1(\mathcal{D}^2(\Gamma))$. By Theorem 2.4.2 the equivalence classes in $H_1(\mathcal{D}^n(\Gamma))$ are in 1-1 correspondence with equivalence classes in $H_1(\mathcal{D}^2(\Gamma))$. Hence, for 2-connected graphs all choices of n -particle topological gauge potential on $\mathcal{D}^n(\Gamma)$ can be realized by (2.6.16). Finally, note that, as explained in [26], having an n -particle topological gauge potential one can easily construct a tight-binding Hamiltonian which supports quantum statistics represented by it (see [26] for more details).

2.7 Morse theory argument

We present an argument which shows the n -particle cycles given in sections 2.3.1 and 2.4.1 form an over-complete spanning set of the first homology group $H_1(\mathcal{D}^n(\Gamma))$. The argument follows the characterization of the fundamental group using discrete Morse theory by Farley and Sabalka [19–21] or alternatively the characterization of the discrete Morse function for the n -particle graph [43]. Here, however, we present the central idea in a way that does not assume a familiarity with discrete Morse theory in order to remain accessible. For a rigorous proof we refer to the articles cited above.

Given a sufficiently subdivided graph Γ we identify some maximal spanning subtree T in Γ ; T is obtained by omitting exactly $\beta_1(\Gamma)$ of the edges in Γ such that T remains connected but contains no loops. The tree can then be drawn in the plane to fix an orientation. A single vertex of degree 1 in T is identified as the root and the vertices of T are labeled $1, 2, \dots, |V|$ starting with 1 for the root and labeling each vertex in turn traveling from the root around the boundary of T clockwise, see figure 2.19.

To characterize a spanning set of n -particle cycles for the first homology group we fix a root configuration $\mathbf{x}_0 = \{1, 2, \dots, n\}$ where the particles are lined up as close to the root as possible, see figure 2.20(a). The tree T is used to establish a set of contractable paths between n -particle configurations on the graph (a discrete vector field). Given an n -particle configuration $\mathbf{x} = \{v_1, \dots, v_n\}$ on the graph a

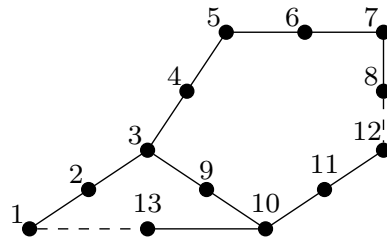


Figure 2.19: A sufficiently subdivided graph for 3 particles, edges in a maximal spanning tree are shown with solid lines and edges omitted to obtain the tree are shown with dashed lines. Vertices are labeled following the boundary of the tree clockwise from the root vertex 1.

path from \mathbf{x} to \mathbf{x}_0 is a sequence of one-particle moves, where a single particle hops to an adjacent vacant vertex with the remaining $n - 1$ particles remaining fixed. This is a 1-cell $\{v_1, \dots, v_{n-1}, u \rightarrow v\}$ where u and v are the locations of the moving particle. The labeling of the vertices in the tree provides a discrete vector field on the configuration space. A particle moves according to the vector field if $n + 1 \rightarrow n$, i.e. the particle moves towards the root along the tree. This allows a particle to move through a non-trivial vertex (a vertex of degree ≥ 3) if the particle is coming from the direction clockwise from the direction of the root. To define a flow that takes any configuration back to \mathbf{x}_0 we also define a set of priorities at the non-trivial vertices that avoids n -particle paths crossing. A particle may also move onto a non-trivial vertex u according to the vector field if the 1-cell $\{v_1, \dots, v_{n-1}, u \rightarrow v\}$ does not contain a vertex v_j with $v < v_j < u$; i.e. moving into a nontrivial vertex particles give way (yield) to the right. So a particle can only move into the nontrivial vertex if there are no particles on branches of the graph between the branch the particle is on and the root direction clockwise from the root. With this set of priorities it is clear that a path (sequence of 1-cells) exists that takes any configuration \mathbf{x} to \mathbf{x}_0 using only 1-cells in the discrete vector field. Equivalently by reversing the direction of edges in 1-cells we can move particles from the reference configuration \mathbf{x}_0 to any configuration \mathbf{x} against the flow. As n -particle paths following this discrete flow do not cross these paths are contractible; equivalently, the phase around closed loops combining paths following and against the discrete flow is zero. Note, we will

describe paths either in the direction of the flow or against it as according to the vector field.

It remains to find a spanning set for the cycles that use 1-cells not in the discrete vector field (that is, cells that are neither in the direction of the flow or against it). We see now that there are only two types of 1-cells that are excluded; those where the edge $u \leftrightarrow v$ is one of the $\beta_1(\Gamma)$ edges omitted from Γ to construct T , and those where a particle moves through a non-trivial vertex out of order - without giving way to the right.

We first consider a 1-cell $c_{u \rightarrow v} = \{v_1, \dots, v_{n-1}, u \rightarrow v\}$ where $u \leftrightarrow v$ is an omitted edge. Such a 1-cell is naturally associated with a cycle where the particles move from \mathbf{x}_0 to $\{v_1, \dots, v_{n-1}, u\}$ against the flow, then follow $c_{u \rightarrow v}$ and finally move back from $\{v_1, \dots, v_{n-1}, v\}$ to \mathbf{x}_0 following the flow. These n -particle cycles are typically the AB-cycles where one particle moves around a loop in Γ with the other particles at a given configuration. We saw in section 2.3.1 that while the phase associated with an AB-cycle can depend on the position of the other particles, these phases can be parameterized by only $\beta_1(\Gamma)$ independent parameters; one parameter for those cycles using each omitted edge.

We now consider, instead, cycles that include a 1-cell $c = \{v_1, \dots, v_{n-1}, u \rightarrow v\}$ where a particle moves out of order at a nontrivial vertex. Again each such 1-cell is naturally associated to a cycle C through \mathbf{x}_0 where the particle moves according to the vector field except when it uses the 1-cell c . Such a cycle is shown in figure 2.20.

Such a cycle can be broken down into a product of Y -cycles in which pairs of particles are exchanged using three arms of the tree connected to the nontrivial vertex v identified by $u, 1$ and some v_j where v_j is a vertex in c with $v < v_j < u$. Figure 2.21 shows a cycle homotopic to the cycle in figure 2.20 broken into the product of two Y -cycles; paths (a) through (c) and (d) through (e) respectively. Notice that moving according to the vector field one returns from the initial configuration in figure 2.21(a) to the root configuration in figure 2.20(a) and similarly one returns from the final configuration in figure 2.21(e) to the final configuration figure

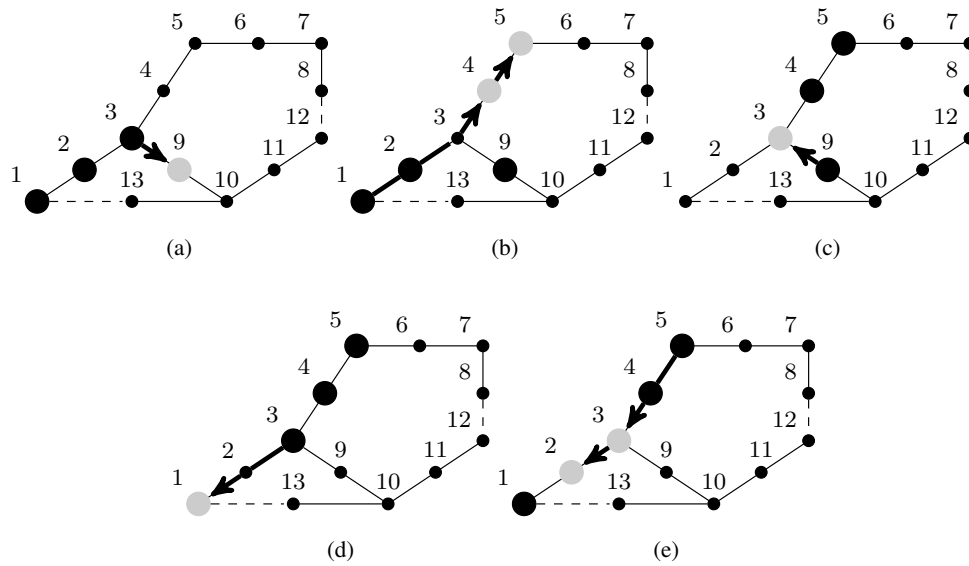


Figure 2.20: An exchange cycle starting from the root configuration $\{1, 2, 3\}$ and using a single 1-cell (c) that does not respect the flow at the non-trivial vertex 3. Large bold nodes indicate the initial positions of particles and light nodes their final positions. In paths (a),(b),(d) and (e) particles move according to the vector field.

2.21(d). Then by contracting adjacent 1-cells in the paths where the direction of the edge has been reversed it is straightforward to verify that the cycles in figures 2.20 and 2.21 are indeed homotopic.

Given a cycle C from x_0 associated with a 1-cell c that does not respect the ordering at a nontrivial vertex to obtain a factorization of C as a product of Y -cycles one need only start from c and follow C until it is necessary to move a third particle. Instead of moving the third particle close the path to make a Y -cycle, which requires moving only one of the two particles moved so far. Then retrace ones steps to rejoin C and move the third particle through the nontrivial vertex again close a Y -cycle and repeat. As any permutation can be written as the product of exchanges any such cycle C can be factored as a product of Y -cycles.

Finally, as any n -particle cycle can be written as a closed sequence of 1-cells and between 1-cells we can add contractable paths according to the vector field without changing the phase associated with a cycle, we see that the AB-cycles and the cycles associated with Y subgraphs centered at the nontrivial vertices form a

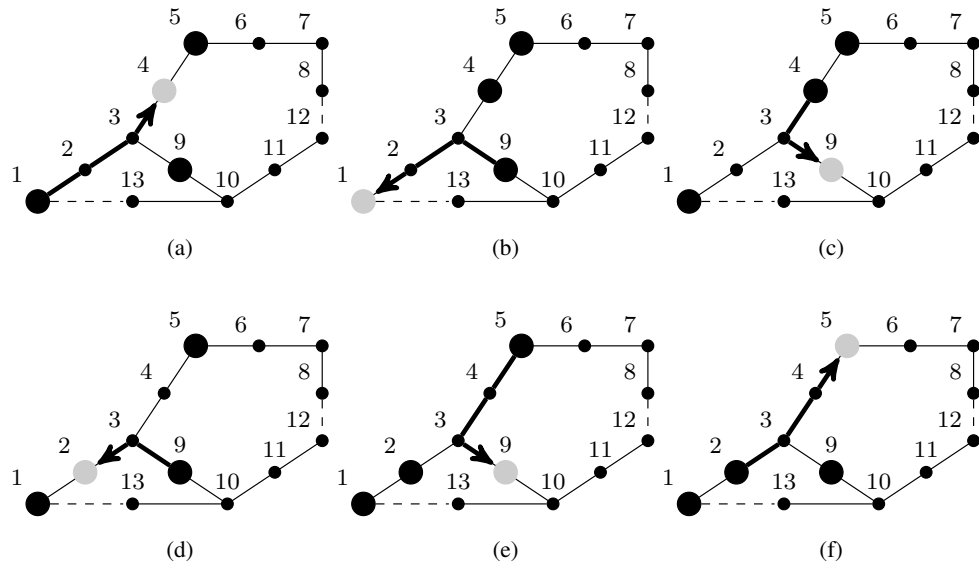


Figure 2.21: Examples of paths that form Y -cycles in the over-complete spanning set; large bold nodes indicate the initial positions of particles on the path and light nodes the final position a particle moves to. (a),(b) and (c) together form a Y -cycle, exchanging two particles at the non-trivial vertex 3, similarly (c),(d) and (e) also form a Y -cycle. Paths (a) through (e) together in order is a cycle homotopic to the exchange cycle starting from the root configuration shown in figure 2.20.

spanning set for the n -particle cycles. Clearly this spanning set will, in general, be over-complete as many relations between these cycles exist in a typical graph, in fact the full discrete Morse theory argument shows that all such relations are determined by critical 2-cells [19].

Chapter 3

Discrete Morse functions for graph configuration spaces

3.1 Introduction

In the last section of chapter 2 some ideas of discrete Morse theory has been already introduced. In this chapter we present an alternative application of discrete Morse theory for two-particle graph configuration spaces. In contrast to previous constructions, which are based on discrete Morse vector fields, our approach is through Morse functions, which have a nice physical interpretation as two-body potentials constructed from one-body potentials. We also give a brief introduction to discrete Morse theory.

Recently there has been significant progress in understanding topological properties of configuration spaces of many particles on metric graphs [21, 30]. This was enabled by the foundational development of discrete Morse theory by Forman during the late 1990's [18]. This theory reduces the calculation of homology groups to an essentially combinatorial problem, namely the construction of certain discrete Morse functions, or equivalently discrete gradient vector fields. Using this idea Farley and Sabalka [21] gave a recipe for the construction of such a discrete gradient vector field [21] on many-particle graphs and classified the first homology groups

for tree graphs. In 2011 Ko and Park [30] significantly extended these results to arbitrary graphs by incorporating graph-theoretic theorems concerning the decomposition of a graph into its two and three-connected components.

In this chapter we give an alternative application of discrete Morse theory for two-particle graph configuration spaces. In contrast to the construction given in [21], which is based on discrete Morse vector fields, our approach is through discrete Morse functions. Our main goal is to provide an intuitive way of constructing a discrete Morse function and hence a discrete Morse gradient vector field. The central object of the construction is the ‘trial Morse’ function. It may be understood as two-body potential constructed from one-body potential, a perspective which is perhaps more natural and intuitive from a physics point of view. Having a perfect Morse function¹ f_1 on a graph Γ we treat it as a one-body potential. The value of the trial Morse function at each point of a two-particle configuration space is the sum of the values of f_1 corresponding to the two particles positions in Γ . The trial Morse function is typically not a Morse function, i.e. it might not satisfy some of the relevant conditions. Nevertheless, we find that it is always possible to modify it and obtain a proper Morse function out of it. In fact, the trial Morse function is not ‘far’ from being a Morse function and the number of cells at which it needs fixing is relatively small. Remarkably, this simple idea leads to similar results as those obtained in [21]. We demonstrate it in Section 3.4 by calculating two simple examples. We find that in both cases the trial Morse function has small defects which can be easily removed and a proper Morse function is obtained. The corresponding discrete Morse vector field is equivalent to the one stemming from the Farley and Sabalka method [21]. As is shown in Section 3.6, it is always possible to get rid of defects of the trial Morse function. The argument is rather technical. However, since the problem is of a certain combinatorial complexity we believe it cannot be easily simplified. We describe in details how the final result, i.e set of discrete Morse functions along with rules for identifying the critical cells and constructing the boundary map of the associated Morse complex, is built in stages

¹For the definition of a perfect Morse function see section 3.2.1.

from this simple idea. Our main purpose is hence to present an approach which we believe is conceptually simple and physically natural. It would be interesting to check if the presented constructions can give any simplification in understanding the results of [30] but we do not pursue this here.

The chapter is organized as follows. In section 3.2 we give a brief introduction to discrete Morse theory. Then in sections 3.3 and 3.4, for two examples we present a definition of a ‘trial’ Morse function \tilde{f}_2 for two-particle graph configuration space. We notice that the trial Morse function typically does not satisfy the conditions required of a Morse function according to Forman’s theory. Nevertheless, we show in Section 3.6 that with small modifications, which we explicitly identify, the trial Morse function can be transformed into a proper Morse function f_2 . In theorem 3.6.1 we give an explicit definition of the function f_2 and theorem 3.6.2 specifies its critical cells. Since the number of critical cells and hence the size of the associated Morse complex is small compared with the size of configuration space the calculation of homology groups are greatly simplified. The technical details of the proofs are given in the section 3.8. In section 3.5 we discuss more specifically how the techniques of discrete Morse theory apply to the problem of quantum statistics on graphs.

3.2 Morse theory in the nutshell

In this section we briefly present both classical and discrete Morse theories. We focus on the similarities between them and illustrate the ideas by several simple examples.

3.2.1 Classical Morse theory

The concept of classical Morse theory is essentially very similar to its discrete counterpart. Since the former is better known we have found it beneficial to first discuss the classical version. A good reference is the monograph by Milnor [37]. Classical

Morse theory is a useful tool to describe topological properties of compact manifolds. Having such a manifold M we say that a smooth function $f : M \rightarrow \mathbb{R}$ is a Morse function if its Hessian matrix at every critical point is nondegenerate, i.e.,

$$df(x) = 0 \Rightarrow \det \left(\frac{\partial^2 f}{\partial x_i \partial x_j} \right) (x) \neq 0. \quad (3.2.1)$$

It can be shown that if M is compact then f has a finite number of isolated critical points [37]. The classical Morse theory is based on the following two facts:

1. Let $M_c = \{x \in M : f(x) \leq c\}$ denote a sub level set of f . Then M_c is homotopy equivalent to $M_{c'}$ if there is no critical value² between the interval (c, c') .
2. The change in topology when M_c goes through a critical value is determined by the index (i.e., the number of negative eigenvalues) of the Hessian matrix at the associated critical point.

The central point of classical Morse theory are the so-called Morse inequalities, which relate the Betti numbers $\beta_k = \dim H_k(M)$, i.e. the dimensions of k -homology groups [25], to the numbers m_k of critical points of index k , i.e.,

$$\sum_k m_k t^k - \sum_k \beta_k t^k = (1 + t) \sum_k q_k t^k, \quad (3.2.2)$$

where $q_k \geq 0$ and t is an arbitrary real number. In particular (3.2.2) implies that $\beta_k \leq m_k$. The function f is called a perfect Morse function iff $\beta_k = m_k$ for every k . Since there is no general prescription it is typically hard to find a perfect Morse function for a given manifold M . In fact a perfect Morse function may even not exist [9]. However, even if f is not perfect we can still encode the topological properties of M in a quite small cell complex. Namely it follows from Morse theory that given a Morse function f , one can show that M is homotopic to a cell complex with m_k k -cells, and the gluing maps can be constructed in terms of the gradient paths of f . We will not discuss this as it is far more complicated than in the discrete case.

²A critical value of f is the value of f at one of its critical points.

3.2.2 Discrete Morse function

In this section we discuss the concept of discrete Morse functions for cell complexes as introduced by Forman [18]. Let $\alpha^{(p)} \in X$ denote a p -cell. A discrete Morse function on a regular cell complex X is a function f which assigns larger values to higher-dimensional cells with ‘local’ exceptions.

Definition 3.2.1. A function $f : X \rightarrow \mathbb{R}$ is a discrete Morse function iff for every $\alpha^{(p)} \in X$ we have

$$\#\{\beta^{(p+1)} \supset \alpha : f(\beta) \leq f(\alpha)\} \leq 1, \quad (3.2.3)$$

$$\#\{\beta^{(p-1)} \subset \alpha : f(\beta) \geq f(\alpha)\} \leq 1. \quad (3.2.4)$$

In other words, definition 3.2.1 states that for any p -cell $\alpha^{(p)}$, there can be at most one $(p+1)$ -cell $\beta^{(p+1)}$ containing $\alpha^{(p)}$ for which $f(\beta^{(p+1)})$ is less than or equal to $f(\alpha^{(p)})$. Similarly, there can be at most one $(p-1)$ -cell $\beta^{(p-1)}$ contained in $\alpha^{(p)}$ for which $f(\beta^{(p-1)})$ is greater than or equal to $f(\alpha^{(p)})$. Examples of a Morse function and a non-Morse function are shown in figure 3.2. The most important part of discrete Morse theory is the definition of a critical cell:

Definition 3.2.2. A cell $\alpha^{(p)}$ is critical iff

$$\#\{\beta^{(p+1)} \supset \alpha : f(\beta) \leq f(\alpha)\} = 0, \text{ and} \quad (3.2.5)$$

$$\#\{\beta^{(p-1)} \subset \alpha : f(\beta) \geq f(\alpha)\} = 0. \quad (3.2.6)$$

That is, α is critical if $f(\alpha)$ is greater than the value of f on all of the faces of α , and $f(\alpha)$ is greater than the value of f on all cells containing α as a face. From definitions 3.2.1 and 3.2.2, we get that a cell α is noncritical iff either

1. \exists unique $\tau^{(p+1)} \supset \alpha$ with $f(\tau) \leq f(\alpha)$, or
2. \exists unique $\beta^{(p-1)} \subset \alpha$ with $f(\beta) \geq f(\alpha)$.

It is quite important to understand that these two conditions cannot be simultaneously fulfilled, as we now explain. Let us assume on the contrary that both conditions (i) and (ii) hold. We have the following sequence of cells:

$$\tau^{(p+1)} \supset \alpha^{(p)} \supset \beta^{(p-1)}. \quad (3.2.7)$$

Since $\alpha^{(p)}$ is regular there is necessarily an $\tilde{\alpha}^{(p)}$ such that $\tau^{(p+1)} \supset \tilde{\alpha}^{(p)} \supset \beta^{(p-1)}$ (see figures 3.1(a),(b) for an intuitive explanation). Since $f(\tau) \leq f(\alpha)$, by definition 3.2.1 we have

$$f(\tilde{\alpha}) < f(\tau). \quad (3.2.8)$$

We also know that $f(\beta) \geq f(\alpha)$ which, once again by definition 3.2.1, implies $f(\beta) < f(\tilde{\alpha})$. Summing up we get

$$f(\alpha) \leq f(\beta) < f(\tilde{\alpha}) < f(\tau) \leq f(\alpha), \quad (3.2.9)$$

which is a contradiction.

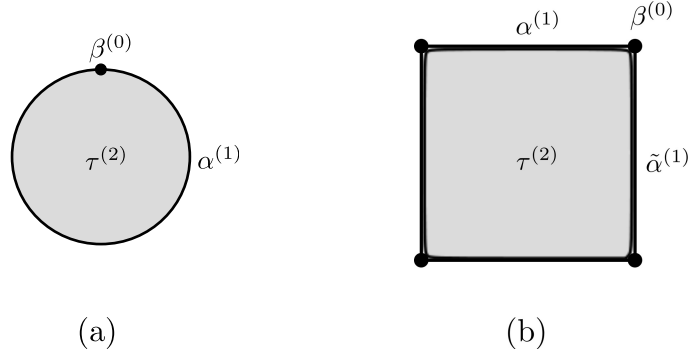


Figure 3.1: Examples of (a) an irregular cell complex. $\alpha^{(1)}$ is an irregular 1 - cell and $\beta^{(0)}$ is an irregular face of $\alpha^{(1)}$. (b) A regular cell complex with $\tau^{(2)} \supset \alpha^{(1)} \supset \beta^{(0)}$.

Following the path of classical Morse theory we define next the level sub-complex $K(c)$ by

$$K(c) = \cup_{f(\alpha) \leq c} \cup_{\beta \subseteq \alpha} \beta. \quad (3.2.10)$$

That is, $K(c)$ is the sub-complex containing all cells on which f is less or equal to c , together with their faces³. Notice that by definition (3.2.1) a Morse function does not have to be a bijection. However, we have the following [18]:

Lemma 3.2.3. *For any Morse function f_1 , there exist another Morse function f_2 which is 1-1 (injective) and which has the same critical cells as f_1 .*

³Notice that the value of f on some of these faces might be bigger than c .

The process of attaching cells is accompanied by two important lemmas which describe the change in homotopy type of level sub-complexes when critical or non-critical cells are attached. Since, from lemma 3.2.3, we can assume that a given Morse function is 1-1, we can always choose the intervals $[a, b]$ below so that $f^{-1}([a, b])$ contains exactly one cell.

Lemma 3.2.4. [18] *If there are no critical cells α with $f(\alpha) \in [a, b]$, then $K(b)$ is homotopy equivalent to $K(a)$.*

Lemma 3.2.5. [18] *If there is a single critical cell $\alpha^{(p)}$ with $f(\alpha) \in [a, b]$, then $K(b)$ is homotopy equivalent to*

$$K(b) = K(a) \cup \alpha \tag{3.2.11}$$

and $\partial\alpha \subset K(a)$.

The above two lemmas lead to the following conclusion:

Theorem 3.2.6. [18] *Let X be a cell complex and $f : X \rightarrow \mathbb{R}$ be a Morse function. Then X is homotopy equivalent to a cell complex with exactly one cell of dimension p for each critical cell $\alpha^{(p)}$*

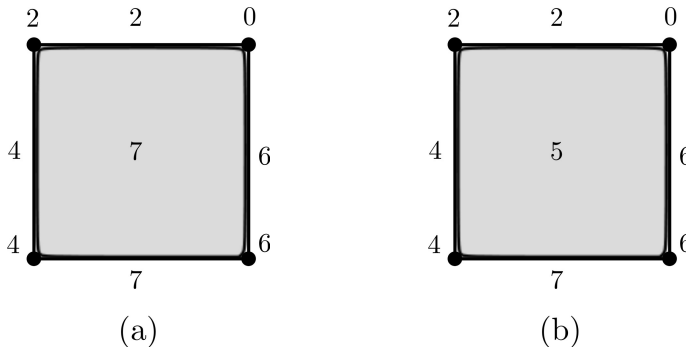


Figure 3.2: Examples of (a) a Morse function, and (b) a non-Morse function, since the 2-cell has value 5 and there are two 1-cells in its boundary with higher values assigned (6, 7).

3.2.3 Discrete Morse vector field

From theorem 3.2.6 it follows that a given cell complex is homotopy equivalent to a cell complex containing only its critical cells, the so-called Morse complex. The

construction of the Morse complex, in particular its boundary map (as well as the proof of theorem 3.2.6), depends crucially on the concept of a discrete vector field, which we define next. We know from definition 3.2.1 that the noncritical cells can be paired. If a p -cell is noncritical, then it is paired with either the unique noncritical $(p + 1)$ -cell on which f takes an equal or smaller value, or the unique noncritical $(p - 1)$ -cell on which f takes an equal or larger value. In order to indicate this pairing we draw an arrow from the $(p - 1)$ -cell to the p -cell in the first case or from the p -cell to the $(p + 1)$ -cell in the second case (see figure 3.3). Repeating this for all cells we get the so-called discrete gradient vector field of the Morse function. It also follows from section 3.2.2 that for every cell α exactly one of the following is true:

1. α is the tail of one arrow,
2. α is the head of one arrow,
3. α is neither the tail nor the head of an arrow.

Of course α is critical iff it is neither the tail nor the head of an arrow. Assume now that we are given a collection of arrows on some cell complex satisfying the above three conditions. The question we would like to address is whether it is a gradient vector field of some Morse function. In order to answer this question we need to be more precise. We define

Definition 3.2.7. *A discrete vector field V on a cell complex X is a collection of pairs $\{\alpha^{(p)} \subset \beta^{(p+1)}\}$ of cells such that each cell is in at most one pair of V .*

Having a vector field it is natural to consider its ‘integral lines’. We define the V - path as a sequence of cells

$$\alpha_0^{(p)}, \beta_0^{(p+1)}, \alpha_1^{(p)}, \beta_1^{(p+1)}, \dots, \alpha_k^{(p)}, \beta_k^{(p+1)} \quad (3.2.12)$$

such that $\{\alpha_i^{(p)} \subset \beta_i^{(p+1)}\} \in V$ and $\beta_i^{(p+1)} \supset \alpha_{i+1}^{(p)}$. Assume now that V is a gradient vector field of a discrete Morse function f and consider a V - path (3.2.12). Then

of course we have

$$f(\alpha_0^{(p)}) \geq f(\beta_0^{(p+1)}) > f(\alpha_1^{(p)}) \geq f(\beta_1^{(p+1)}) > \dots > f(\alpha_k^{(p)}) \geq f(\beta_k^{(p+1)}) \quad (3.2.13)$$

This implies that if V is a gradient vector field of the Morse function then f decreases along any V -path which in particular means that there are no closed V -paths. It happens that the converse is also true, namely a discrete vector field V is a gradient vector field of some Morse function iff there are no closed V -paths [18].

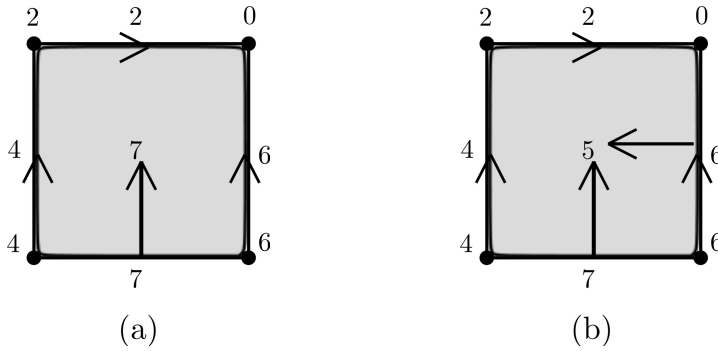


Figure 3.3: Examples of (a) a correct and (b) an incorrect discrete gradient vector fields; the 2-cell is the head of two arrows and the 1-cell is the head and tail of one arrow.

3.2.4 The Morse complex

Up to now we have learned how to reduce the number of cells of the original cell complex to the critical ones. However, it is still not clear how these cells are ‘glued’ together, i.e. what is the boundary map between the critical cells? The following result relates the concept of critical cells with discrete gradient vector fields [18].

Theorem 3.2.8. *Assume that orientation has been chosen for each cell in the cell complex X . Then for any critical $(p + 1)$ -cell β we have*

$$\tilde{\partial}\beta = \sum_{\text{critical } \alpha^{(p)}} c_{\beta,\alpha} \alpha, \quad (3.2.14)$$

where $\tilde{\partial}$ is the boundary map in the cell complex consisting of the critical cells, whose existence is guaranteed by theorem 3.2.6, and

$$c_{\beta,\alpha} = \sum_{\gamma \in P(\beta,\alpha)} m(\gamma), \quad (3.2.15)$$

where $P(\beta, \alpha)$ is the set of all V - paths from the boundary of β to cells whose boundary contains α and $m(\gamma) = \pm 1$, depending on whether the orientation induced from β to α through γ agrees with the one chosen for α .

The collection of critical cells together with the boundary map $\tilde{\partial}$ is called the Morse complex of the function f and we will denote it by $M(f)$. Examples of the computation of boundary maps for Morse complexes will be given in section 3.4.

3.3 A perfect Morse function on Γ and its discrete vector field.

In this section we present a construction of a perfect discrete Morse function on a 1 - particle graph. It is defined analogously as in the classical case, i.e. the number of critical cells in each dimension is equal to the corresponding dimension of the homology group. The existence of such a function will be used in section 3.4 to construct a ‘good’ but not necessarily perfect Morse function on a 2-particle graph.

Let $\Gamma = (V, E)$ be a graph with $v = |V|$ vertices and $e = |E|$ edges. In the following we assume that Γ is connected and simple. Let T be a spanning tree of Γ , i.e. T is a connected spanning subgraph of Γ such that $V(T) = V(\Gamma)$ and for any pair of vertices $v_i \neq v_j$ there is exactly one path in T joining v_i with v_j . We naturally have $|E(\Gamma)| - |E(T)| \geq 0$. The Euler characteristic of Γ treated as a cell complex is given by

$$\chi(\Gamma) = v - e = \dim H_0(\Gamma) - \dim H_1(\Gamma) = b_0 - b_1. \quad (3.3.1)$$

Since Γ is connected, $H_0(\Gamma) = \mathbb{Z}$. Hence we get

$$b_0 = 1, \quad (3.3.2)$$

$$b_1 = e - v + 1. \quad (3.3.3)$$

On the other hand it is well known that $b_1 = |E(\Gamma)| - |E(T)|$. Summing up from the topological point of view Γ is homotopy equivalent to a wedge sum of b_1 circles.

Our goal is to construct a perfect Morse function f_1 on Γ , i.e. the one with exactly b_1 critical 1 - cells and one critical 0 - cell. To this end we choose a vertex v_1 of valency one in T (it always exists) and travel through the tree anticlockwise from it labeling vertices by v_k . The value of f on the vertex v_k is $f_1(k) = 2k - 2$ and the value of f_1 on the edge $(i, j) \in T$ is $f_1((i, j)) = \max(f_1(i), f_1(j))$. The last step is to define f_1 on the deleted edges $(i, j) \in E(\Gamma) \setminus E(T)$. We choose $f_1((i, j)) = \max(f_1(i), f_1(j)) + 2$, where v_i, v_j are the boundary vertices of (i, j) . This way we obtain that all vertices besides v_1 and all edges of T are not critical cells of f_1 . The critical 1 - cells are exactly the deleted edges. The following example clarifies this idea (see figure 3.4).

Example 3.3.1. Consider the graph Γ shown in figure 3.4(a). Its spanning tree is denoted by solid lines and the deleted edges by dashed lines. For each vertex and edge the corresponding value of a perfect discrete Morse function f_1 is explicitly written. Notice that according to definition 3.2.2 we have exactly one critical 0 - cell (denoted by a square) and four critical 1 - cells which are deleted edges. The discrete vector field for f_1 is represented by arrows. The contraction of Γ along this field yields the contraction of T to a single point and hence the Morse complex $M(f_1)$ is the wedge sum of four circles (see figure 3.4(b))

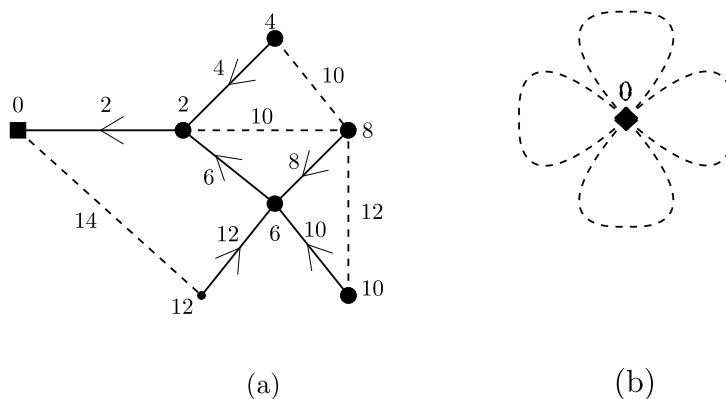


Figure 3.4: (a) The perfect discrete Morse function f_1 on the graph Γ and its discrete gradient vector field. (b) The Morse complex $M(f_1)$.

3.4 The main examples

In this section we present a method of construction of a ‘good’ Morse function on the two particle configuration space $\mathcal{D}^2(\Gamma_i)$ for two different graphs Γ_i shown in figures 3.5(a) and 3.7(a). We also demonstrate how to use the tools described in section 3.2 in order to derive a Morse complex and compute the first homology group. We begin with a graph Γ_1 which we will refer to as lasso (see figure 3.5(a)). The spanning tree of Γ_1 is denoted in black in figure 3.5(a). In figure 3.5(b) we see an example of the perfect Morse function f_1 on Γ_1 together with its gradient vector field. They were constructed according to the procedure explained in section 3.3. The Morse complex of Γ_1 consists of one 0-cell (the vertex 1) and one 1-cell (the edge (3, 4)).



Figure 3.5: (a) One particle on lasso, (b) The perfect discrete Morse function f_1

The two particle configuration space $\mathcal{D}^2(\Gamma_1)$ is shown in figure 3.6(a). Notice that $\mathcal{D}^2(\Gamma_1)$ consists of one 2 - cell $(3, 4) \times (1, 2)^4$, six 0 - cells and eight 1 - cells. In order to define the Morse function f_2 on $\mathcal{D}^2(\Gamma_1)$ we need to specify its value for each of these cells. We begin with a trial function \tilde{f}_2 which is completely determined once we know the perfect Morse function on Γ_1 . To this end we treat f_1 as a kind of ‘potential energy’ of one particle. The function \tilde{f}_2 is simply the sum of the energies of both particles, i.e. the value of \tilde{f}_2 on a cell corresponding to a particular position of two particles on Γ_1 is the sum of the values of f_1 corresponding to this position.

⁴This notation should be understood as the Cartesian product of edges (3, 4) and (1, 2), hence a square.

To be more precise we have for

$$\begin{aligned}
 0 - \text{ cells : } \quad & \tilde{f}_2(i \times j) = f_1(i) + f_1(j), \\
 1 - \text{ cells : } \quad & \tilde{f}_2(i \times (j, k)) = f_1(i) + f_1((j, k)), \\
 2 - \text{ cells : } \quad & \tilde{f}_2((i, j) \times (k, l)) = f_1((i, j)) + f_1((k, l)). \quad (3.4.1)
 \end{aligned}$$

In figure 3.6(b) we can see $\mathcal{D}^2(\Gamma_1)$ together with \tilde{f}_2 . Observe that \tilde{f}_2 is not a Morse function since the value of $\tilde{f}_2((3, 4))$ is the same as the value of \tilde{f}_2 on edges $4 \times (2, 3)$ and $3 \times (2, 4)$ which are adjacent to the vertex $(3, 4)$. The rule that 0 - cell can be the face of at most one 1 - cell with smaller or equal value of \tilde{f}_2 is violated. In order to have Morse function f_2 on $\mathcal{D}^2(\Gamma_1)$ we introduce one modification, namely

$$f_2(3 \times (2, 4)) = \tilde{f}_2(3 \times (2, 4)) + 1, \quad (3.4.2)$$

and f_2 is \tilde{f}_2 on the other cells.

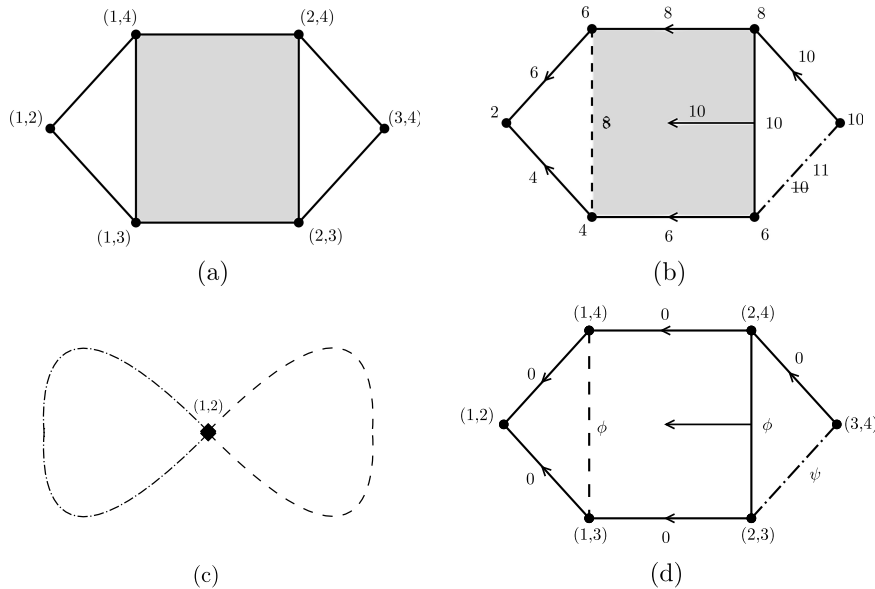


Figure 3.6: (a) The two particles on lasso, $\mathcal{D}^2(\Gamma_1)$, (b) the discrete Morse function and its gradient vector field (c) the Morse complex (d) the topological gauge potential Ω

Notice that the choice we made is not unique. We could have changed $\tilde{f}_2(4 \times (2, 3))$ in a similar way and leave $\tilde{f}_2(3 \times (2, 4))$ untouched. After the modification (3.4.2) we construct the corresponding discrete vector field for f_2 . The Morse complex

Table 3.1: The critical cells of \tilde{f}_2 and the vertices and edges causing \tilde{f}_2 to not be a Morse function.

Critical cells of the trial Morse function \tilde{f}_2		\tilde{f}_2 is not Morse function because		
0 - cells	1×2	vertex	edges	value
1 - cells	$1 \times (4, 5), 2 \times (1, 3)$	(3, 4)	$3 \times (2, 4), 4 \times (2, 3)$	$\tilde{f}_2 = 10$
2 - cells	$(1, 3) \times (4, 5)$	(3, 5)	$5 \times (2, 3), 3 \times (2, 5)$	$\tilde{f}_2 = 12$
		(4, 5)	$5 \times (2, 4), 4 \times (2, 5)$	$\tilde{f}_2 = 14$

of f_2 consists of one critical 0-cell (vertex (1, 2)) and two critical 1 - cells (edges $3 \times (2, 4)$ and $1 \times (3, 4)$). Observe that there are two different mechanisms responsible for criticality of these 1 - cells. The cell $1 \times (3, 4)$ is critical due to the definition of trial Morse function \tilde{f}_2 and $3 \times (2, 4)$ has been chosen to be critical in order to make \tilde{f}_2 the well defined Morse function f_2 . We will see later that these are in fact the only two ways giving rise to the critical cells. Notice finally that function f_2 is in fact a perfect Morse function and the Morse inequalities for it are equalities.

We will now consider a more difficult example. The one particle configuration space, i.e. graph Γ_2 together with the perfect Morse function and its gradient vector field are shown in figure 3.7(a) and 3.7(b).

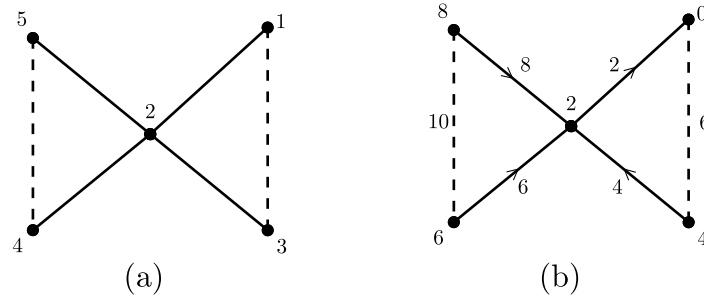


Figure 3.7: (a) One particle on bow-tie (b) Perfect discrete Morse function

The construction of two particle configuration space is a bit more elaborate than in the lasso case and the result is shown in figure 3.8(a). Using rules given in (3.4.1) we obtain the trial Morse function \tilde{f}_2 which is shown in figure 3.8(b). The critical cells of \tilde{f}_2 and the cells causing \tilde{f}_2 to not be a Morse function are given in table 3.1.

In figure 3.8(b) we have chosen 1 - cells: $3 \times (2, 4)$, $3 \times (2, 5)$ and $4 \times (2, 5)$ to

Table 3.2: The boundary of c_2 .

boundary of c_2	path	critical 1 - cells	orientation
$1 \times (4, 5)$	\emptyset	$1 \times (4, 5)$	+
$5 \times (1, 3)$	$5 \times (1, 3), (2, 5) \times (1, 3), 2 \times (1, 3).$ $5 \times (1, 3), (2, 5) \times (1, 3), 3 \times (2, 5).$	$2 \times (1, 3)$ $3 \times (2, 5)$	- -
$3 \times (4, 5)$	$3 \times (4, 5), (4, 5) \times (2, 3), 2 \times (4, 5),$ $(1, 2) \times (4, 5), 1 \times (4, 5).$	$1 \times (4, 5)$	-
$4 \times (1, 3)$	$4 \times (1, 3), (1, 3) \times (2, 4), 2 \times (1, 3).$ $4 \times (1, 3), (1, 3) \times (2, 4), 3 \times (2, 4).$	$2 \times (1, 3)$ $3 \times (2, 4)$	+ +

be critical, although we should emphasize that it is one choice out of eight possible ones. We will now determine the first homology group of the Morse complex $M(f_2)$ and hence $H_1(\mathcal{D}^2(\Gamma_2))$. The Morse complex $M(f_2)$ is the sum of $M_0(f_2)$ consisting of one 0-cell (vertex 1×2), $M_1(f_2)$ which consists of five critical 1-cells and $M_2(f_2)$ which is one critical 2-cell $c_2 = (1, 3) \times (4, 5)$.

$$M_2(f_2) \xrightarrow{\tilde{\partial}_2} M_1(f_2) \xrightarrow{\tilde{\partial}_1} M_0(f_2).$$

The first homology is given by

$$H_1(M(f_2)) = H_1(\mathcal{D}^2(\Gamma_2)) = \frac{\text{Ker}\tilde{\partial}_1}{\text{Im}\tilde{\partial}_2}. \quad (3.4.3)$$

It is easy to see that $\tilde{\partial}_1 c_1 = 0$ for any $c_1 \in M_1(f_2)$ and hence $\text{Ker}\tilde{\partial}_1 = \mathbb{Z}^5$. What is left is to find $\tilde{\partial}_2 c_2$ which is a linear combination of critical 1-cells from $M_1(f_2)$. According to formula (3.2.14) we take the boundary of c_2 in $C_2(\Gamma_2)$ and consider all paths starting from it and ending at the 2-cells containing critical 1-cells (see table 3.2). Eventually taking into account orientation we get

$$\tilde{\partial}_2(c_2) = 1 \times (4, 5) - 3 \times (2, 5) - 2 \times (1, 3) - 1 \times (4, 5) + \quad (3.4.4)$$

$$+ 3 \times (2, 4) + 2 \times (1, 3) = -3 \times (2, 5) + 3 \times (2, 4). \quad (3.4.5)$$

Hence,

$$H_1(\mathcal{D}^2(\Gamma_2)) = \frac{\text{Ker}\tilde{\partial}_1}{\text{Im}\tilde{\partial}_2} = \mathbb{Z}^4. \quad (3.4.6)$$

The Morse complex $M(f_2)$ is shown explicitly in figure 3.8(c). It is worth mentioning that in this example f_2 is not a perfect Morse function.

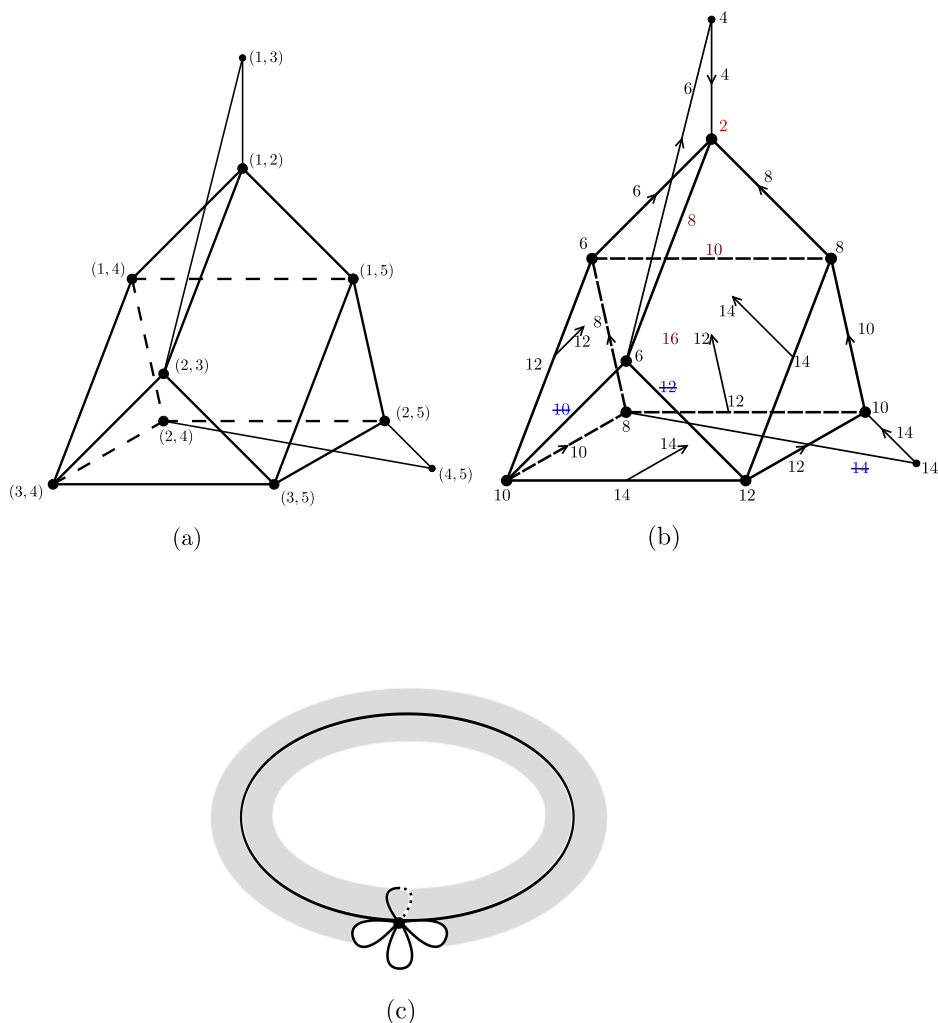


Figure 3.8: (a) Two particles on bow-tie (b) the discrete Morse function and its gradient vector field, (c) the Morse complex $M(f_2)$.

3.5 Discrete Morse theory and topological gauge potentials

In this section we describe more specifically how the techniques of discrete Morse theory apply to the problem of quantum statistics on graphs. A more general discussion of the model can be found in [26]. Here we describe a particular representative example, highlighting the usefulness of discrete Morse theory.

Let Γ be a graph shown in figure 3.5(a). The Hilbert space associated to Γ is

$\mathcal{H} = \mathbb{C}^4$ and is spanned by the vertices of Γ . The dynamics is given by Schrödinger equation where the Hamiltonian H is a hermitian matrix, such that $H_{jk} = 0$ if j is not adjacent to k in Γ . As discussed in [26] this corresponds to the so-called tight binding model of one-particle dynamics on Γ . One can add to the model an additional ingredient, namely whenever the particle hops between adjacent vertices of Γ the wavefunction gains an additional phase factor. This can be incorporated to the Hamiltonian by introducing a gauge potential. It is an antisymmetric real matrix Ω such that each $\Omega_{jk} \in [0, 2\pi[$ and $\Omega_{jk} = 0$ if j is not adjacent to k in Γ . The modified Hamiltonian is then $H_{jk}^\Omega = H_{jk}e^{i\Omega_{jk}}$. The flux of Ω through any cycle of Γ is the sum of values of Ω on the directed edges of the cycle. It can be given a physical interpretation in terms of the Aharonov-Bohm phase.

In order to describe in a similar manner the dynamics of two indistinguishable particles on Γ we follow the procedure given in [26]. The structure of the Hilbert space and the corresponding tight binding Hamiltonian are encoded in $\mathcal{D}^2(\Gamma)$. Namely, we have $\mathcal{H}_2 = \mathbb{C}^6$ and is spanned by the vertices of $\mathcal{D}^2(\Gamma)$. The Hamiltonian is given by a hermitian matrix, such that $H_{j,k \rightarrow l} = 0$ if k is not adjacent to l in Γ . The notation $j, k \rightarrow l$ describes two vertices (j, k) and (j, l) connected by an edge in $\mathcal{D}^2(\Gamma)$. The additional assumption which we add in this case stems from the topological structure of $\mathcal{D}^2(\Gamma)$ and is reflected in the condition on the gauge potential. Namely, since the 2-cell $c_2 = (1, 2) \times (3, 4)$ is contractible we require that the flux through its boundary vanishes, i.e.

$$\Omega(\partial c_2) = \Omega_{1,3 \rightarrow 4} + \Omega_{4,1 \rightarrow 2} + \Omega_{2,4 \rightarrow 3} + \Omega_{3,2 \rightarrow 1} = 0 \pmod{2\pi}. \quad (3.5.1)$$

Our goal is to find the parametrization of all gauge potentials satisfying (3.5.1), up to a so-called trivial gauge, i.e. up to addition of Ω' such that $\Omega'(c) = 0 \pmod{2\pi}$, for any cycle c . To this end we use discrete Morse theory. We first notice that the edges of $\mathcal{D}^2(\Gamma)$ which are heads of an arrow of the discrete Morse vector field form a tree. Without loss of generality we can put $\Omega_{j,k \rightarrow l} = 0$ whenever $j \times (k, l)$ is a head of an arrow. Next, on the edges corresponding to the critical 1-cells we put arbitrary phases $\Omega_{1,3 \rightarrow 4} = \phi$ and $\Omega_{3,2 \rightarrow 4} = \psi$. Notice that since f_2 is a perfect Morse

function these phases are independent. The only remaining edge is $2 \times (3, 4)$ which is a tail of an arrow. In order to decide what phase should be put on it we follow the gradient path of the discrete Morse vector field which leads to edge $1 \times (3, 4)$. Hence $\Omega_{2,3 \rightarrow 4} = \phi$. The effect of our construction is the topological gauge potential Ω which is given by two independent parameters (see figure 3.6(d)) and satisfies (3.5.1). The described reasoning can be *mutatis mutandis* applied to any graph Γ , albeit the phases on edges corresponding to the critical cells are not independent if f_2 is not a perfect Morse function. Finally notice, that in the considered example, the phase ϕ can be interpreted as an Aharonov-Bohm phase and ψ as the exchange phase. The latter gives rise to anyon statistics.

3.6 General consideration for two particles

In this section we investigate the first Homology group $H_1(C_2(\Gamma))$ by means of discrete Morse theory. In section 3.4 the idea of a trial Morse function was introduced. Let us recall here that the trial Morse function is defined in two steps. The first one is to define a perfect Morse function on Γ . To this end one chooses a spanning tree T in Γ . The vertices of Γ are labeled by $1, 2, \dots, |V|$ according to the procedure described in section 3.3. The perfect Morse function f_1 on Γ is then given by its value on the vertices and edges of Γ , i.e.

$$f_1(i) = 2i - 2, \quad (3.6.1)$$

$$f_1((j, k)) = \max(f_1(j), f_1(k)), \quad (j, k) \in T, \quad (3.6.2)$$

$$f_1((j, k)) = \max(f_1(j), f_1(k)) + 2, \quad (j, k) \in \Gamma \setminus T \quad (3.6.3)$$

When f_1 is specified the trial Morse function on $\mathcal{D}^2(\Gamma)$ is given by the formula

$$\begin{aligned} 0 - \text{cells} : \quad & \tilde{f}_2(i \times j) = f_1(i) + f_1(j), \\ 1 - \text{cells} : \quad & \tilde{f}_2(i \times (j, k)) = f_1(i) + f_1((j, k)), \\ 2 - \text{cells} : \quad & \tilde{f}_2((i, j) \times (k, l)) = f_1((i, j)) + f_1((k, l)). \end{aligned} \quad (3.6.4)$$

Let us emphasize that the trial Morse function is typically not a Morse function, i.e., the conditions of definition 3.2.1 might not be satisfied. Nevertheless, we will show that it is always possible to modify the function \tilde{f}_2 and obtain a Morse function f_2 out of it. In fact the function \tilde{f}_2 is not 'far' from being a Morse function and, as we will see, the number of cells at which it needs fixing is relatively small. In the next paragraphs we localize the obstructions causing \tilde{f}_2 to not be a Morse function and explain how to overcome them.

The cell complex $\mathcal{D}^2(\Gamma)$ consists of 2, 1, and 0-cells which we will denote by α , β and κ respectively. For all these cells we have to verify the conditions of definition 3.2.1. Notice that checking these conditions for any cell involves looking at its higher and lower dimensional neighbours. In case of 2-cell α we have only the former ones, i.e., the 1-cells β in the boundary of α . For the 1-cell β both 2-cells α and 0-cells κ are present. Finally for the 0-cell κ we have only 1-cells β .

Our strategy is the following. We begin with the trial Morse function \tilde{f}_2 and go over all 2-cells checking the conditions of definition 3.2.1. The outcome of this step is a new trial Morse function \bar{f}_2 which has no defects on 2-cells. Next we consider all 1-cells and verify the conditions of definition 3.2.1 for \bar{f}_2 . It happens that they are satisfied. Finally we go over all 0-cells. The result of this three-steps procedure is a well defined Morse function f_2 . Below we present more detailed discussion. The proofs of all statements are in section 3.8.

1. **Step 1** We start with a trial Morse function \tilde{f}_2 . We notice first that for any edge $e \in T$ there is a unique vertex v in its boundary such that $f_1(e) = f_1(v)$. In other words every vertex v , different from $v = 1$, specifies exactly one edge $e \in T$ which we will denote by $e(v)$. Next we divide the set of 2-cells into three disjoint classes. The first one contains 2-cells $\alpha = e_i \times e_j$, where both $e_i, e_j \notin T$. The second one contains 2-cells $\alpha = e_i \times e(v)$, where $e(v) \in T$ and $e_i \notin T$, and the last one contains 2-cells $\alpha = e(u) \times e(v)$, where both $e(u), e(v) \in T$. Now, since there are no 3-cells, we have only to check that

for each 2-cell α

$$\#\{\beta \subset \alpha : \tilde{f}_2(\beta) \geq \tilde{f}_2(\alpha)\} \leq 1 \quad (3.6.5)$$

The following results are proved in section 3.8

- (a) For the 2-cells $\alpha = e_i \times e_j$ where both $e_i, e_j \notin T$ the condition (3.6.5) is satisfied (see fact 2).
- (b) For the 2-cells $\alpha = e_i \times e(v)$ where $e_i \notin T$ and $e(v) \in T$ the condition (3.6.5) is satisfied (see fact 3).
- (c) For the 2-cells $\alpha = e(u) \times e(v)$ where both $e(u), e(v) \in T$ the condition (3.6.5) is not satisfied. There are exactly two 1-cells $\beta_1, \beta_2 \subset \alpha$ such that $\tilde{f}_2(\beta_1) = \tilde{f}_2(\alpha) = \tilde{f}_2(\beta_2)$. They are of the form $\beta_1 = u \times e(v)$ and $\beta_2 = v \times e(u)$. The function \tilde{f}_2 can be fixed in two ways (see fact 4). We put $\bar{f}_2(\alpha) = \tilde{f}_2(\alpha) + 1$ and either $\bar{f}_2(\beta_1) := \tilde{f}_2(\beta_1) + 1$ or $\bar{f}_2(\beta_2) := \tilde{f}_2(\beta_2) + 1$. In both cases $\{\beta_i, \alpha\}$ is the pair of noncritical cells.

The result of this step is a new trial Morse function \bar{f}_2 , which satisfies (3.6.5).

2. **Step 2** We divide the set of 1-cells into two disjoint classes. The first one contains 1-cells $\beta = v \times e$, where $e \notin T$ and the second one contains $\beta = v \times e(u)$, where $e(u) \in T$. For the 1-cells within each of this classes we introduce additional division with respect to condition $e(v) \cap e = \emptyset$ (or $e(v) \cap e(u) = \emptyset$). Notice that all 1-cells β which were modified in **Step 1** belong to the second class and satisfy $e(v) \cap e(u) = \emptyset$. Next we take a trial Morse function \bar{f}_2 and go over all 1-cells β checking for each of them if

$$\#\{\alpha \supset \beta : \bar{f}_2(\alpha) \leq \bar{f}_2(\beta)\} \leq 1, \quad (3.6.6)$$

$$\#\{\kappa \subset \beta : \bar{f}_2 \geq \bar{f}_2(\beta)\} \leq 1. \quad (3.6.7)$$

What we find out is

- (a) For the 1-cells $\beta = v \times e(u)$, where $e(u) \in T$ and $e(v) \cap e(u) \neq \emptyset$ the conditions (3.6.6, 3.6.7) are satisfied (see fact 5).

- (b) For the 1-cells $\beta = v \times e$, where $e \notin T$ and $e(v) \cap e \neq \emptyset$ the conditions (3.6.6, 3.6.7) are satisfied (see fact 6).
- (c) For the 1-cells $\beta = v \times e(u)$, where $e(u) \in T$ and $e(v) \cap e(u) = \emptyset$ the conditions (3.6.6, 3.6.7) are satisfied (see fact 7).
- (d) For the 1-cells $\beta = v \times e$, where $e \notin T$ and $e(v) \cap e = \emptyset$ the conditions (3.6.6, 3.6.7) are satisfied (see fact 8).

Summing up the trial Morse function \bar{f}_2 , obtained in **Step 1** satisfies both (3.6.5) and (3.6.6), (3.6.7). We switch now to the analysis of 0-cells.

3. **Step 3** We divide the set of 0-cells into four disjoint classes in the following way. We denote by $\tau(v) \neq v$ the vertex to which $e(v)$ is adjacent and call it the terminal vertex of $e(v)$. For any 0-cell $\kappa = v \times u$ we have that either

- (a) $e(v) \cap e(u) \neq \emptyset$ and the terminal vertex $\tau(v)$ of $e(v)$ is equal to u .
- (b) $e(v) \cap e(u) \neq \emptyset$ and the terminal vertex $\tau(u)$ of $e(u)$ is equal to the terminal vertex $\tau(v)$ of $e(v)$.
- (c) $e(v) \cap e(u) = \emptyset$.
- (d) $\kappa = 1 \times u$.

What is left is checking the following condition for any 0-cell κ :

$$\#\{\beta \supset \kappa : \bar{f}_2(\beta) \leq \bar{f}_2(\kappa)\} \leq 1 \quad (3.6.8)$$

We find out that

- (a) For the 0-cell $\kappa = u \times v$ belonging to 3a the condition (3.6.8) is satisfied (see fact 9).
- (b) For the 0-cell $\kappa = u \times v$ belonging to 3b the condition (3.6.8) is not satisfied. There are exactly two 1-cells $\beta_1, \beta_2 \supset \kappa$ such that $\bar{f}_2(\beta_1) = \bar{f}_2(\kappa) = \bar{f}_2(\beta_2)$. They are of the form $\beta_1 = u \times e(v)$ and $\beta_2 = v \times e(u)$. The function \bar{f}_2 can be fixed in two ways. We put $f_2(\beta_1) := \bar{f}_2(\beta_1) + 1$

or $f_2(\beta_2) := \bar{f}_2(\beta_2) + 1$ (see fact 10). Moreover, this change does not violate the Morse conditions at any 2-cell containing β_i .

- (c) For the 0-cell $\kappa = u \times v$ belonging to 3c the condition (3.6.8) is satisfied (see fact 11)
- (d) For the 0-cell $\kappa = u \times v$ belonging to 3d the condition (3.6.8) is satisfied (see fact 12)

As a result of the above procedure we obtain the Morse function f_2 . The following theorem summarizes the above described procedure.

Theorem 3.6.1. *Let f_1 be a perfect Morse function on a 1-particle graph Γ defined by (3.6.1). Define a trial Morse function \tilde{f}_2 on $\mathcal{D}^2(\Gamma)$ by $\tilde{f}_2(\alpha \times \beta) := f_1(\alpha) + f_1(\beta)$. A Morse function f_2 on $\mathcal{D}^2(\Gamma)$ is the modification of \tilde{f}_2 obtained in the following way:*

1. *For 2-cells of the form $\alpha = e(u) \times e(v)$ where both $e(u), e(v) \in T$, increment $\tilde{f}_2(\alpha)$ by 1 and increment either $\tilde{f}_2(u \times e(v))$ or $\tilde{f}_2(e(u) \times v)$ by 1 as well.*
2. *For 0-cells of the form $\kappa = u \times v$ where $\tau(e(u)) = \tau(e(v))$, increment either $\tilde{f}_2(u \times e(v))$ or $\tilde{f}_2(e(u) \times v)$ by 1.*

We can now ask the question which cells of $\mathcal{D}^2(\Gamma)$ are critical cells of f_2 . Careful consideration of the arguments given in facts 2-12 lead to the following conclusions:

Theorem 3.6.2. *The conditions for the critical cells of f_2 are*

- *The 0-cell is critical if and only if it is 1×2*
- *The 1-cell is critical if and only if*
 1. *It is $v \times e$ where $e \notin T$ and $e(v) \cap e \neq \emptyset$ or $v = 1$.*
 2. *Assume that $e(v) \cap e(u) \neq \emptyset$ and the terminal vertex $\tau(u)$ of $e(u)$ is equal to the terminal vertex $\tau(v)$ of $e(v)$. Then either the 1-cell $v \times e(u)$ or the 1-cell $u \times e(v)$ is critical, but not both.*

- *The 2-cell is critical if and only if it is $e_1 \times e_2$ where both $e_i \notin T$.*

These rules are related to those given by Farley and Sabalka in [21]. As pointed out by an anonymous referee the freedom in choosing noncritical 1-cells (see fact 3 in section 3.8) and critical 1-cells (see fact 9 in section 3.8) is also present in Farley and Sabalka's [21] construction. Moreover, a perfect Morse function on a 1-particle graph used in our construction stems from the labeling of the tree discussed in [21].

3.7 Summary

We have presented a description of topological properties of two-particle graph configuration spaces in terms of discrete Morse theory. Our approach is through discrete Morse functions, which may be regarded as two-particle potential energies. We proceeded by introducing a trial Morse function on the full two-particle cell complex, $\mathcal{D}^2(\Gamma)$, which is simply the sum of single-particle potentials on the one-particle cell complex, Γ . We showed that the trial Morse function is close to being a true Morse function provided that the single-particle potential is a perfect Morse function on Γ . Moreover, we give an explicit prescription for removing local defects. The fixing process is unique modulo the freedom described in facts 4 and 10. The construction was demonstrated by two examples. A future goal would be to see if these constructions can provide any simplification in understanding of the results of [30]. It will be also interesting to verify if the presented techniques can be extended to N -particle graphs and if they lead to analogous results as in [21]. The preliminary calculations indicate that the answer is positive, however small modifications of a perfect Morse function on a 1-particle graph are needed.

Finally, notice that using our analogy with the potential energy a trial Morse function is constructed as if particles do not interact. The modification of a trail Morse function can be hence viewed as introducing an interaction. On the other hand, in the considered graph setting, quantum statistics or anyons can be regarded as fermions which interact in some particular way. Remarkably, the modifications of a trial Morse function in particular these described in point 2 of theorem 3.6.1

correspond to situations when two particles come close together.

3.8 Proofs

In this section we give the proofs of the statements made in section 3.6. The following notation will be used. We denote by D_v all edges of Γ which are adjacent to v and belong to $\Gamma - T$. Similarly by T_v we denote all edges of Γ which are adjacent to v and belong to T , except one distinguished edge $e(v) \in T$, but not in T_v .

Fact 2. *Let $\alpha = e_1 \times e_2$ be a 2-cell such that both e_1 and e_2 do not belong to T . The condition (3.6.5) is satisfied and α is a critical cell.*

Proof. The two cell $e_1 \times e_2$ is shown in the figure 3.9, where $e_1 = (i, j)$ and $e_2 = (k, l)$ and $i > j, k > l$. The result follows immediately from this figure.

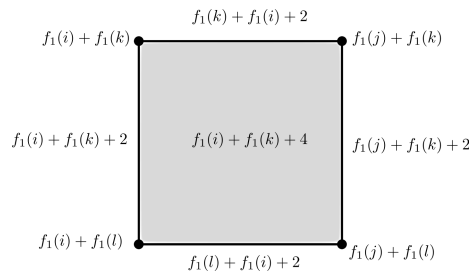


Figure 3.9: The critical cell $e_1 \times e_2$ where both e_1 and e_2 do not belong to T

Fact 3. *Let $\alpha = e \times e(v)$ be a 2-cell, where $e \notin T$ and $e(v) \in T$. Condition (3.6.5) is satisfied and α is a noncritical cell.*

Proof. We of course assume that $e(v) \cap e = \emptyset$. The 2-cell α is shown on figure 3.10, where we denoted $e(v) = (v, \tau(v))$ and $e = (j, k)$. The result follows immediately from this figure.

Fact 4. *Let $\alpha = e(u) \times e(v)$ be the 2-cells, where both $e(u), e(v) \in T$. Condition (3.6.5) is not satisfied. There are exactly two 1-cells $\beta_1, \beta_2 \subset \alpha$ such that $\tilde{f}_2(\beta_1) = \tilde{f}_2(\alpha) = \tilde{f}_2(\beta_2)$. They are of the form $\beta_1 = u \times e(v)$ and $\beta_2 = v \times e(u)$. The function \tilde{f}_2 can be fixed in two ways. We put $\bar{f}_2(\alpha) = \tilde{f}_2(\alpha) + 1$ and either $\bar{f}_2(\beta_1) := \tilde{f}_2(\beta_1) + 1$ or $\bar{f}_2(\beta_2) := \tilde{f}_2(\beta_2) + 1$.*

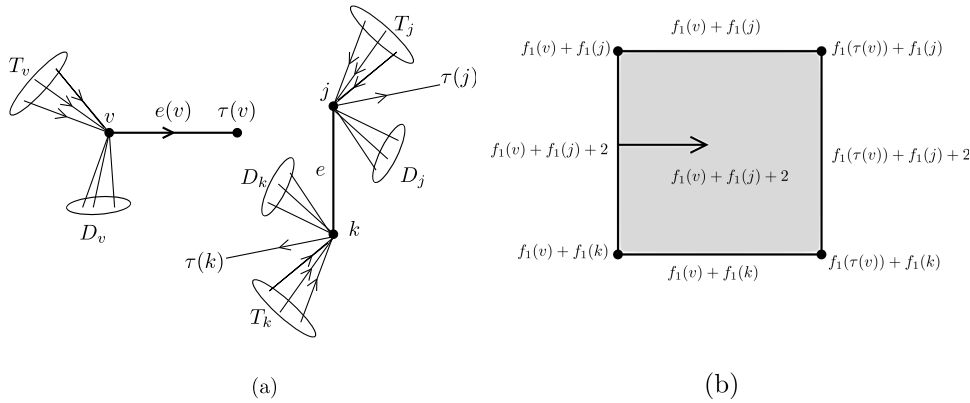


Figure 3.10: (a) $e(v) \cap e = \emptyset$ and $e \notin T$, (b) The noncritical cells $v \times e$ and $e(v) \times e$.

Proof. The 2-cell $e(v) \times e(u)$ when $e(v) \cap e(u) = \emptyset$ is presented in figure 3.11(a),(b). The trail Morse function \tilde{f}_2 requires fixing and two possibilities are shown on figure 3.11(c),(d). Notice that in both cases we get a pair of noncritical cells. Namely the 1-cell $v \times e(u)$ and 2-cell $e(v) \times e(u)$ for the situation presented in figure 3.11(c) and 1-cell $u \times e(v)$, 2-cell $e(v) \times e(u)$ for the situation presented in figure 3.11(d).

Fact 5. For the 1-cells $\beta = v \times e(u)$, where $e(u) \in T$ and $e(v) \cap e(u) \neq \emptyset$ the conditions (3.6.6, 3.6.7) are satisfied.

Proof. Let us first calculate $\bar{f}_2(\beta)$. To this end we have to check if β was modified in step 1. Notice that every 2-cell which has β in its boundary is one of the following forms:

1. $e(v) \times e(u)$
2. $e \times e(u)$ with $e \in D_v$
3. $e \times e(u)$ with $e \in T_v$

Case (1) is impossible since $e(v) \cap e(u) \neq \emptyset$. For any 2-cell belonging to (2) the value of \tilde{f}_2 was not modified on the boundary of $e \times e(u)$ (see fact 3). Finally, for 2-cells belonging to (3) the value of \tilde{f}_2 was modified on the boundary of $e \times e(u)$ but not on the cell β (see fact 3). Hence $\bar{f}_2(v \times e(u)) = \tilde{f}_2(v \times e(u)) = f_1(v) + f_1(e(u)) = f_1(v) + f_1(u)$. Let us now verify condition (3.6.7). The 1-cell β is adjacent to exactly two 0-cells, namely $v \times u$ and $v \times \tau(u)$. We have $\bar{f}_2(v \times u) =$

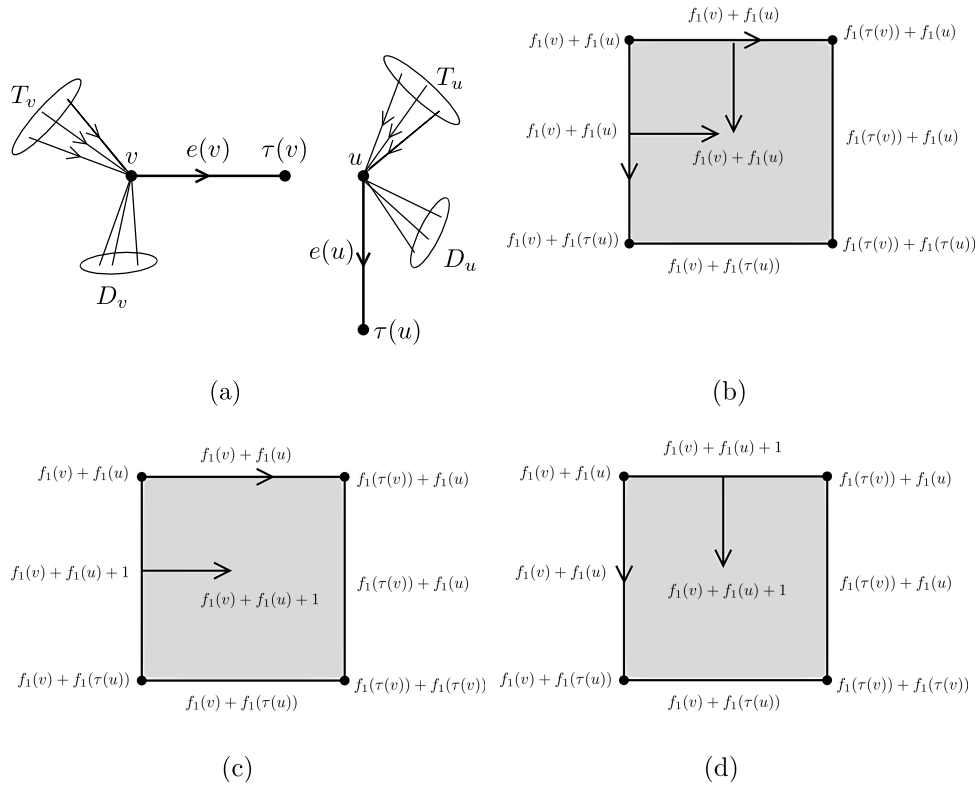


Figure 3.11: (a) Two edges of T with $e(v) \cap e(u) = \emptyset$, (b) The problem of 2-cell $e(v) \times e(u)$ (c),(d) two possible fixings of \tilde{f}_2

$\tilde{f}_2(v \times u) = f_1(v) + f_1(u)$ and $\tilde{f}_2(v \times \tau(u)) = \tilde{f}_2(v \times \tau(u)) = f_1(v) + f_1(\tau(u))$. Now since $f_1(\tau(u)) < f_1(u)$ condition (3.6.7) is satisfied. For condition (3.6.6) we have only to examine 2-cells of forms (2) and (3) (listed above). For 2-cells that belong to (2) we have $f_2(e \times e(u)) = f_1(e) + f_1(e(u)) > f_1(v) + f_1(u) + 2$ and for 2-cells that belong to (3) we have $f_2(e \times e(u)) = f_1(e) + f_1(e(u)) + 1 > f_1(v) + f_1(u) + 1$. Hence in both cases $\tilde{f}_2(e \times e(u)) > \tilde{f}_2(v \times e(u))$ and condition (3.6.6) is satisfied.

Fact 6. For the 1-cells $\beta = v \times e$, where $e \notin T$ and $e(v) \cap e \neq \emptyset$ conditions (3.6.6, 3.6.7) are satisfied.

Proof. Let us first calculate $\tilde{f}_2(\beta)$. To this end we have to check if β was modified in step 1. Notice that every 2-cell which has β in its boundary is one of the following forms:

1. $e(v) \times e$
2. $e_i \times e$ with $e_i \in D_v$

3. $e_i \times e$ with $e_i \in T_v$

Case (1) is impossible since $e(v) \cap e \neq \emptyset$. For any 2-cell belonging to (2) or (3) the value of \tilde{f}_2 was not modified on the boundary of $e_i \times e(u)$ (see fact 2 and 3). Hence $\bar{f}_2(v \times e) = \tilde{f}_2(v \times e) = f_1(v) + f_1(e)$. Let us now verify condition (3.6.7). To this end assume that $e = (j, k)$ with $j > k$. The 1-cell β is adjacent to exactly two 0-cells, namely $v \times j$ and $v \times k$. We have $\bar{f}_2(v \times j) = \tilde{f}_2(v \times j) = f_1(v) + f_1(j)$ and $\bar{f}_2(v \times k) = \tilde{f}_2(v \times k) = f_1(v) + f_1(k)$. Now since $f_1(e) = \max(f_1(j), f_1(k)) + 2$ condition (3.6.7) is satisfied. For condition (3.6.6) we have only to examine 2-cells of forms (2) and (3) (listed above). It is easy to see that in both cases $\bar{f}_2(e_i \times e) > \bar{f}_2(v \times e)$.

Fact 7. For the 1-cells $\beta = v \times e(u)$, where $e(u) \in T$ and $e(v) \cap e(u) = \emptyset$ conditions (3.6.6, 3.6.7) are satisfied.

Proof. Let us first calculate $\bar{f}_2(\beta)$. To this end we have to check if β was modified in step 1. Notice that every 2-cell which has β in its boundary is one of the following forms:

1. $e(v) \times e(u)$
2. $e \times e(u)$ with $e \in D_v$
3. $e \times e(u)$ with $e \in T_v$

For any 2-cell belonging to (2) the value of \tilde{f}_2 was not modified on the boundary of $e \times e(u)$ (see fact 3). For the 2-cells belonging to (3) the value of \tilde{f}_2 was modified on the boundary of $e \times e(u)$ but not on the cell β (see fact 3). Finally for the 2-cell $e(v) \times e(u)$ the value of \tilde{f}_2 was modified on the boundary of $e(v) \times e(u)$ and by fact 4 it might be the case that it was modified on β . Hence $\bar{f}_2(v \times e(u)) = \tilde{f}_2(v \times e(u)) = f_1(v) + f_1(e(u)) = f_1(v) + f_1(u)$ or $\bar{f}_2(v \times e(u)) = f_1(v) + f_1(u) + 1$. Let us now verify condition (3.6.7). The 1-cell β is adjacent to exactly two 0-cells, namely $v \times u$ and $v \times \tau(u)$. We have $\bar{f}_2(v \times u) = \tilde{f}_2(v \times u) = f_1(v) + f_1(u)$ and $\bar{f}_2(v \times \tau(u)) = \tilde{f}_2(v \times \tau(u)) = f_1(v) + f_1(\tau(u))$. Now since $f_1(\tau(u)) < f_1(u)$ condition (3.6.7)

is satisfied. For condition (3.6.6) we have to examine 2-cells from (1), (2) and (3) (listed above). In case when $\bar{f}_2(v \times e(u)) = f_1(v) + f_1(u)$ it is easy to see that $\bar{f}_2(e \times e(u)) > \bar{f}_2(v \times e(u))$ for $e \in D_v, T_v$ and $\bar{f}_2(e(v) \times e(u)) > \bar{f}_2(v \times e(u))$. For $\bar{f}_2(v \times e(u)) = f_1(v) + f_1(u) + 1$ we still have $\bar{f}_2(e \times e(u)) > \bar{f}_2(v \times e(u))$ for $e \in D_v, T_v$ and $\bar{f}_2(e(v) \times e(u)) = \bar{f}_2(v \times e(u))$. Hence condition (3.6.6) is satisfied in both cases.

Fact 8. For the 1-cells $\beta = v \times e$, where $e \notin T$ and $e(v) \cap e = \emptyset$ conditions (3.6.6, 3.6.7) are satisfied.

Proof. Let us first calculate $\bar{f}_2(\beta)$. To this end we have to check if β was modified in step 1. Notice that every 2-cell which has β in its boundary is one of the following forms:

1. $e(v) \times e$
2. $e_i \times e$ with $e_i \in D_v$
3. $e_i \times e$ with $e_i \in T_v$

For any 2-cell belonging to (1), (2) and (3) the value of \tilde{f}_2 was not modified on the boundary of an appropriate 2-cell (see fact 3 and 4). Hence $\bar{f}_2(v \times e) = \tilde{f}_2(v \times e) = f_1(v) + f_1(e)$. Let us now verify condition (3.6.7). To this end assume that $e = (j, k)$ with $j > k$. The 1-cell β is adjacent to exactly two 0-cells, namely $v \times j$ and $v \times k$. We have $\bar{f}_2(v \times j) = \tilde{f}_2(v \times j) = f_1(v) + f_1(j)$ and $\bar{f}_2(v \times k) = \tilde{f}_2(v \times k) = f_1(v) + f_1(k)$. Now since $f_1(e) = \max(f_1(j), f_1(k)) + 2$ condition (3.6.7) is satisfied. For condition (3.6.6) we have to examine 2-cells form (1), (2) and (3) (listed above). It is easy to see that $\bar{f}_2(e_i \times e) > \bar{f}_2(v \times e)$ for $e_i \in D_v, T_v$ and $\bar{f}_2(e(v) \times e) = \bar{f}_2(v \times e)$.

Fact 9. For the 0-cell $\kappa = u \times v$ such that $e(v) \cap e(u) \neq \emptyset$ with the terminal vertex $\tau(v)$ of $e(v)$ equal to u , condition (3.6.8) is satisfied.

Proof. The situation when $e(v) \cap e(u) \neq \emptyset$ and terminal vertex $\tau(v)$ of $e(v)$ is equal to u is presented in the figure 3.12. For the 0-cell $v \times u$ we have $\bar{f}_2 =$

$\tilde{f}_2(v \times u) = f_1(v) + f_1(u)$. Notice that there is exactly one edge $v \times e(u)$ for which $\bar{f}_2(v \times e(u)) = \bar{f}_2(v \times u)$. The function \bar{f}_2 on the other edges adjacent to $v \times u$ have a value greater than $\bar{f}_2(v \times u)$ and hence $v \times u$ and $v \times e(u)$ constitute a pair of noncritical cells.

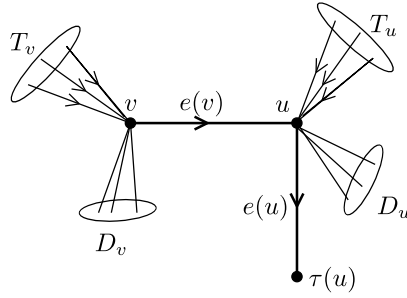


Figure 3.12: $e(v) \cap e(u) \neq \emptyset$ and $\tau(v) = u$

Fact 10. For the 0-cell $\kappa = u \times v$ such that $e(v) \cap e(u) \neq \emptyset$ with the terminal vertex $\tau(u)$ of $e(u)$ equal to the terminal vertex $\tau(v)$ of $e(v)$ condition (3.6.8) is not satisfied. There are exactly two 1-cells $\beta_1, \beta_2 \supset \kappa$ such that $\bar{f}_2(\beta_1) = \bar{f}_2(\kappa) = \bar{f}_2(\beta_2)$. They are of the form $\beta_1 = u \times e(v)$ and $\beta_2 = v \times e(u)$. The function \bar{f}_2 can be fixed in two ways. We put $f_2(\beta_1) := \bar{f}_2(\beta_1) + 1$ or $f_2(\beta_2) := \bar{f}_2(\beta_2) + 1$.

Proof. The situation when $e(v) \cap e(u) \neq \emptyset$ and terminal vertex $\tau(u)$ of $e(u)$ is equal to terminal vertex $\tau(v)$ of $e(v)$ is presented in the figure 3.13(a),(b). For the 0-cell $v \times u$ we have $\bar{f}_2(v \times u) = f_1(v) + f_1(u)$. There are two edges $v \times e(u)$ and $u \times e(v)$ such that $\bar{f}_2(v \times e(u)) = \bar{f}_2(v \times u) = \bar{f}_2(u \times e(v))$. It is easy to see that the value of \bar{f}_2 on the other edges adjacent to $v \times u$ is greater than $\bar{f}_2(v \times u)$. So the function \bar{f}_2 does not satisfy condition (3.6.8) and there are two possibilities 3.13(c),(d) to fix this problem. Either we put $\bar{f}_2(v \times e(u)) = \bar{f}_2(v \times u) + 1$ or $\bar{f}_2(u \times e(v)) = \bar{f}_2(v \times u) + 1$. They both yield that the vertex $v \times u$ is non-critical. Notice finally that by the definitions of f_1 and \tilde{f}_2 , increasing the value of $\bar{f}_2(\beta_i)$ by one does not influence 2-cells containing β_i in their boundary.

Fact 11. For the 0-cell $\kappa = u \times v$ such that $e(v) \cap e(u) = \emptyset$ condition (3.6.8) is satisfied.

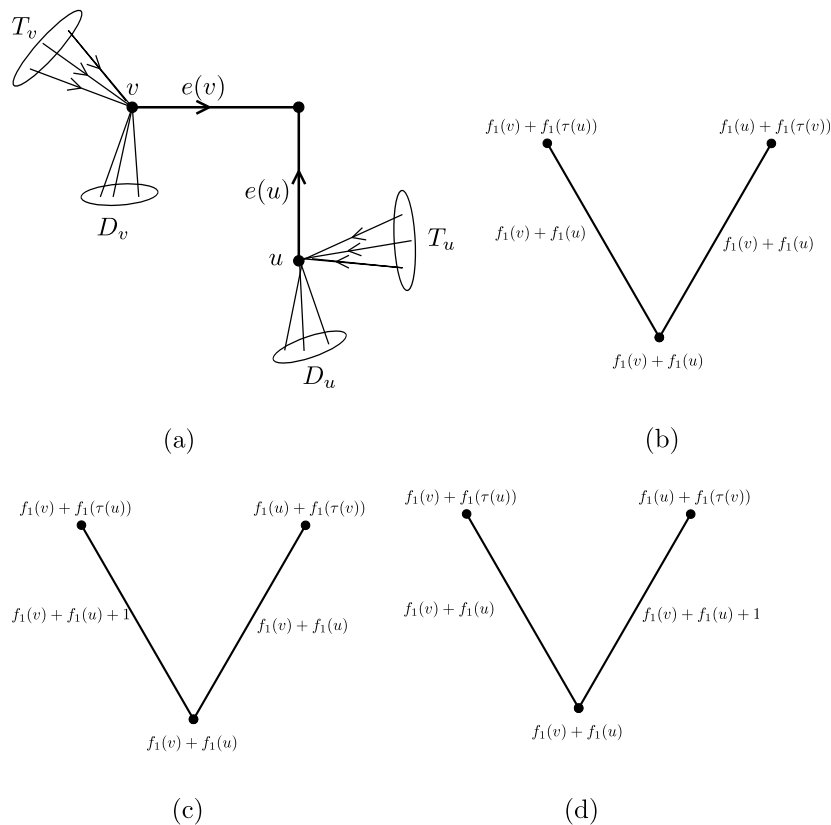


Figure 3.13: (a) Two edges of T with $e(v) \cap e(u) \neq \emptyset$, (b) The problem of 1-cells $v \times (u, \tau(u))$ and $u \times (v, \tau(v))$ (c),(d) The two possible fixings of \bar{f}_2

Proof. This is a direct consequence of the modification made for the 2-cell $\alpha = e(v) \times e(u)$ in step 1. Moreover, κ is noncritical.

Fact 12. For the 0-cell $\kappa = 1 \times u$ condition (3.6.8) is satisfied.

Proof. For the 0-cell $1 \times u$ we have $\bar{f}_2 = \tilde{f}_2(v \times u) = f_1(u)$. Notice that there is exactly one edge $1 \times e(u)$ for which $\bar{f}_2(1 \times e(u)) = \bar{f}_2(1 \times u)$. The function \bar{f}_2 on the other edges adjacent to $1 \times u$ have a value greater than $\bar{f}_2(1 \times u)$. Hence if $u \neq 2$ the 0-cell $1 \times u$ and the 1-cell $1 \times e(u)$ constitute a pair of noncritical cells. Otherwise κ is a critical 0-cell.

Chapter 4

Summary and outlook

In this thesis we developed a new set of ideas and methods which gave a full characterization of all possible abelian quantum statistics on graphs. Our approach enabled identification of the key topological determinants of the quantum statistics:

1. the connectivity of a graph,
2. the first homology group $H_1(C_n(\Gamma)) = \mathbb{Z}^{\beta_1} \oplus A$, where β_1 is the number of independent cycles in Γ and A determines quantum statistics
3. for 1-connected graphs number of anyon phases depends on the number of particles,
4. for 2-connected graphs quantum statistics stabilizes with respect to the number of particles $H_1(C_n(\Gamma)) = H_1(C_2(\Gamma))$,
5. for 3-connected non-planar graphs $A = \mathbb{Z}_2$, i.e. the usual bosonic/fermionic statistics is the only possibility whereas planar 3-connected graphs support one anyon phase, $A = \mathbb{Z}$. Thus, from the quantum statistics perspective, one can say that 3-connected graphs mimic \mathbb{R}^2 when they are planar and \mathbb{R}^3 when not.

It seems that the following problems can be approached using the methods developed in this thesis.

Problem 1. It was noticed by V. I. Arnold in the late 1960's [4, 5], and then generalized to some classes of manifolds, that the cohomology groups of the $C_n(\mathbb{R}^2)$ possess three basic properties:

1. finiteness: $H^i(C_n(\mathbb{R}^2))$ are finite except $H^0(C_n(\mathbb{R}^2)) = \mathbb{Z}$, $H^1(C_n(\mathbb{R}^2)) = \mathbb{Z}$ for $n \geq 2$; also $H^i(C_n(\mathbb{R}^2)) = 0$ for $i \geq n$,
2. recurrence: $H^i(C_{2n+1}(\mathbb{R}^2)) = H^i(C_{2n}(\mathbb{R}^2))$,
3. stabilization: $H^i(C_n(\mathbb{R}^2)) = H^i(C_{2i-2}(\mathbb{R}^2))$ for $n \geq 2i - 2$.

These raises the following questions in graph's context:

- what is the minimal connectivity of Γ that gives stabilization of $H_i(C_n(\mathbb{R}^2))$ for planar and non-planar graphs?,
- Is 'quantum statistics' components of $H_i(C_n(\Gamma))$ given by the torsion part of $H_i(C_n(\Gamma))$, for $i > 1$,
- what is the minimal connectivity of Γ for which 'quantum statistics' components of $H_i(C_n(\Gamma))$ up to the given i are the same as for \mathbb{R}^2 and \mathbb{R}^3 , i.e. when planar graphs mimic \mathbb{R}^2 up to $H_i(C_n(\mathbb{R}^2))$ and non-planar graphs mimic \mathbb{R}^3 up $H_i(C_n(\mathbb{R}^3))$ for given i .

Problem 2. The aim is to lay the foundations for the understanding of the influence of complex topology, which gives rise to generalized anyon statistics, on many-particle transport properties of complex networks. The principal attraction of quantum graphs is that they provide mathematically tractable models of complex physical systems. The fact that anyon statistics is present for many-particle graph configuration spaces gives at least *a priori* various possible applications of this model. Using graph models one can investigate topological signatures and effects of quantum statistics in many-particle generalizations of a single-particle transport on networks. This should provide models and variants of the quantum Hall effect extending to many-particle quantum systems the transport theory for networks developed by Avron (see for example [6–8]).

Problem 3. The importance of topology and geometry in quantum information theory is present on both foundational and application levels. Of course the Holy Grail in this area of research is still the construction of a quantum computer. One of the difficulties in building a many-qubit quantum computer is quantum decoherence. Physical systems typically remain in a coherent superposition of states for a very short time because generic interactions with the environment will decohere them, destroying the information encoded in quantum states. Recently, a new approach based on topology has been proposed to overcome some of the difficulties of this kind [28]. In simple words the idea is motivated by the fact that topological invariants are very robust. So if information is encoded in topology it is hard to destroy it as it is immune to a large class of perturbations. More precisely, topological quantum computing is based on the concept of anyons, and in particular, non-abelian anyons [28]. One of the most profound examples of these ideas is the celebrated Kitaev toric code, which is a realization of topological quantum error correcting code on a two-dimensional spin lattice [29]. The excitations for this model were proved to be of anyon type [29]. It is therefore natural to expect that the anyon statistics which are present on graph configuration spaces might be related to these ideas. One of the explicit tasks would be to construct a spin graph model for which excitations behave exactly like anyons corresponding to many-particle graph configuration spaces. It is also believed that the fractional Quantum Hall States are promising candidates for physical realization of topological computing [39]. So the study of transport properties described in the previous paragraphs is inevitably related to these concepts

Problem 4. The entanglement of integer and fractional Quantum Hall States has recently been studied by several authors (see for example [34, 42]). An interesting problem would be to calculate the entanglement of eigenstates of many-particle graph configuration spaces with the topological gauge potential supporting anyon quantum statistics. When the topological gauge potential vanishes the Hamiltonian of the system is a non-interacting fermionic Hamiltonian. When this Hamiltonian has a non-degenerate spectrum, its eigenstates are given in terms of Slater deter-

minants. Otherwise the topological gauge potential introduces an interaction to the system, so that eigenstates of Hamiltonian might be entangled. It seems interesting to understand how the degree of entanglement for these states is related to the topological invariants of the one-particle graph, e.g. its connectivity and planarity.

Bibliography

- [1] Abrams A 2000 Configuration spaces and braid groups of graphs. Ph.D. thesis, UC Berkley.
- [2] Aharonov Y and Bohm D 1959 Significance of Electromagnetic Potentials in the Quantum Theory Phys. Rev., 115, 485.
- [3] Aizenman M, Sims R, Warzel S 2006 Absolutely continuous spectra of quantum tree graphs with weak disorder Commun. Math. Phys. 264 371-389.
- [4] Arnold V I 1969 The cohomology ring of colored braids, Mat. Zametki 5 No 2 (1969), 227-231 (Russian) English transl. in Trans. Moscow Math. Soc. 21 1970, 3052.
- [5] Arnold V I 1970 On some topological invariants of algebraic functions, Trudy Moscov. Mat. Obshch. 21 1970, 27-46 (Russian), English transl. in Trans. Moscow Math. Soc. 21 1970, 30-52.
- [6] Avron J E, Bachmann S, Graf G M, Klich I 2008 Fredholm determinants and the statistics of charge transport, Commun. Math. Phys., 280, 807-829.
- [7] Avron J E, Elgart A, Graf G M, Sadun L 2004 Transport and Dissipation in Quantum Pumps, J. Stat. Phys. 116, 425-473.
- [8] Avron J E, Berger J 1999 Quantum Transport in Molecular Rings and Chains, Proc. Roy. Soc. Lond. A. 455, 2729-2750.
- [9] Ayala R, Fernandez-Ternero D, Vilches J A 2011 Perfect discrete Morse functions on 2-complexes. Pattern Recognition Letters, Available online 10.1016/j.patrec.2011.08.011.
- [10] Balachandran A P, Ercolessi E 1992 Statistics on Networks, Int. J. Mod. Phys. A 07, 4633.
- [11] Berkolaiko G, Kuchment P 2013 Introduction to Quantum Graphs, Mathematical Surveys and Monographs 186; AMS.

- [12] Berry M V and Robbins J M 2000 Quantum indistinguishability: spin-statistics without relativity or field theory? *Spin-Statistics Connection and Commutation Relations* p. 3-15.
- [13] Bohm A, Mostafazadeh A, Koizumi H, Niu Q, and Zwanziger J 2003 *The Geometric Phase in Quantum Systems*, Springer-Verlag, New York.
- [14] Bolte J, Kerner J 2013 Quantum graphs with singular two-particle interactions *J. Phys. A: Math. Theor.* 46 045206.
- [15] Chambers R G 1960 Shift of an electron interference pattern by enclosed magnetic flux, *Phys. Rev. Lett.* 5, 3.
- [16] Dirac P A M 1958 *Principles of Quantum Mechanics* Oxford University Press, Oxford.
- [17] Dowker, J S 1985 Remarks on non-standard statistics *J. Phys. A: Math. Gen.* 18 3521.
- [18] Forman R 1998 Morse Theory for Cell Complexes *Advances in Mathematics* 134, 90145.
- [19] Farley D, Sabalka L 2005 Discrete Morse theory and graph braid groups *Algebr. Geom. Topol.* 5 1075-1109.
- [20] Farley D, Sabalka L 2012 Presentations of graph braid groups *Forum Math.* 24 827-859.
- [21] Farley D, Sabalka L 2008 On the cohomology rings of tree braid groups *J. Pure Appl. Algebra* 212 53-71.
- [22] Fox R H, Neuwirth L 1962 The braid groups, *Math. Scand.* 10, 119-126.
- [23] de Gennes P G 1981 Champ critique d'une boucle supraconductrice ramefée. *C. R. Acad. Sci. Paris* 292 279?282.
- [24] Ghrist R 2007 Configuration spaces, braids and robotics. Notes from the IMS Program on Braids, Singapore.
- [25] Hatcher A 2002 *Algebraic Topology*, Cambridge University Press.
- [26] Harrison J M, Keating J P and Robbins J M 2011 Quantum statistics on graphs *Proc. R. Soc. A* 8 January vol. 467 no. 2125 212-23.
- [27] Holberg W 1992 The decomposition of graphs into k-connected components *Discrete Mathematics* vol 109, issues 13, 133145.

- [28] Kitaev A Y 2003 Fault-tolerant quantum computation by anyons, *Annals of Physics*, Volume 303, Issue 1, Pages 2-30.
- [29] Kitaev A Y 1997 Quantum error correction with imperfect gates, in *Proceedings of the Third International Conference on Quantum Communication and Measurement*, edited by O. Hirota, A. S. Holevo, and C. M. Caves (Plenum, New York).
- [30] Ko K H, Park H W 2011 Characteristics of graph braid groups. arXiv:1101.2648.
- [31] Kostykin V and Schrader R 1999 Kirchhoff's rule for quantum wires *J. Phys. A* 32, 595-630.
- [32] Kottos T and Smilansky U 1997 Quantum chaos on graphs *Phys. Rev. Lett.* 79 4794 4797.
- [33] Kuratowski K 1930 Sur le problème des courbes gauches en topologie, *Fund. Math.* 15: 271–283.
- [34] Laeuchli A M, Bergholtz E J, Suorsa J, Haque M 2010 Disentangling Entanglement Spectra of Fractional Quantum Hall States on Torus Geometries, *Phys. Rev. Lett.* 104, 156404.
- [35] Laidlaw M G G, DeWitt C M 1971 Feynman Functional Integrals for Systems of Indistinguishable Particles, *Phys. Rev D* 3, 1375-1378.
- [36] Leinaas J M, Myrheim J 1977 On the theory of identical particles. *Nuovo Cim.*37B, 1–23.
- [37] Milnor J 1963 *Classical Morse Theory*, Princeton University Press.
- [38] Nakahara M 1990 *Geometry, Topology, and Physics*, Hilger London.
- [39] . Nayak C, Simon S H, Stern A, Freedman M, Das Sarma S 2008 Non-Abelian Anyons and Topological Quantum Computation?, *Rev. Mod. Phys.* 80, 1083-1159.
- [40] Pauli W 1940 The connection between spin and statistics. *Phys. Rev.* 58, 716-722.
- [41] Prue P, Scrimshaw T 2009 Abrams's stable equivalence for graph braid groups. arXiv:0909.5511
- [42] Rodriguez I D, Sierra G 2009 Entanglement entropy of integer quantum Hall states, *Phys. Rev. B* 80, 153303.
- [43] Sawicki A 2012 Discrete Morse functions for graph configuration spaces *J. Phys. A: Math. Theor.* 45 505202.

- [44] Souriau, J M 1970 Structure des systmes dynamiques, Dunod, Paris.
- [45] Tutte W T 2001 Graph Theory, Cambridge Mathematical Library.
- [46] Wilczek, F (ed.) 1990 Fractional statistics and anyon superconductivity. Singapore, Singapore: World Scientific.